TESIS DEFENDIDA POR

Jorge Flores Troncoso

Y APROBADA POR EL SIGUIENTE COMITÉ

Dr. Jaime Sánchez García

Director del Comité

Dr. Hamid Jafarkhani

Miembro del Comité

Dr. Luis Armando Villaseñor González

Miembro del Comité

Dr. José Rosario Gallardo López

Miembro del Comité

Dr. Carlos Alberto Brizuela Rodríguez

Miembro del Comité

Dr. Roberto Conte Galván

Coordinador del Programa de Posgrado en Electrónica y Telecomunicaciones

---

Dr. David Hilario Covarrubias Rosales

Director de Estudios de Posgrado

23 de Agosto de 2010

THESIS DEFENDED BY

Jorge Flores Troncoso

AND APPROVED BY THE FOLLOWING COMMITTEE

Dr. Jaime Sánchez García

Committee Director

Dr. Hamid Jafarkhani

Committee Member

Dr. Luis Armando Villaseñor González

Committee Member

Dr. José Rosario Gallardo López

Committee Member

Dr. Carlos Alberto Brizuela Rodríguez

Committee Member

Dr. Roberto Conte Galván

Electronics and Telecommunication Graduate Program Coordinator

Dr. David Hilario Covarrubias Rosales

Graduate Studies Director

August 23, 2010

CENTRO DE INVESTIGACIÓN CIENTÍFICA Y DE EDUCACIÓN SUPERIOR DE ENSENADA

PROGRAMA DE POSGRADO EN CIENCIAS EN ELECTRÓNICA Y TELECOMUNICACIONES

CODIFICACIÓN PARA REDES INALÁMBRICAS DE SIGUIENTE GENERACIÓN

TESIS

que para cubrir parcialmente los requisitos necesarios para obtener el grado de

DOCTOR EN CIENCIAS

Presenta:

JORGE FLORES TRONCOSO

Ensenada, Baja California, México, Agosto de 2010

RESUMEN de la tesis de **JORGE FLORES TRONCOSO**, presentada como requisito parcial para la obtención del grado de DOCTOR EN CIENCIAS en ELECTRÓNICA Y TELECOMUNICACIONES con orientación en TELECOMUNICACIONES.
Ensenada, Baja California, Agosto de 2010.

CODIFICACIÓN PARA REDES INALÁMBRICAS DE SIGUIENTE GENERACIÓN

Resumen aprobado por:

Dr. Jaime Sánchez García

Director de Tesis

En los sistemas de comunicación inalámbrica de banda ancha de siguiente generación (4G), el desarrollo de la tecnología de múltiple entrada y múltiple salida (MIMO) junto con la multicanalización por división de frecuencias ortogonales (OFDM), ha sido reconocida como una de las técnicas más prometedoras para proveer un alto desempeño y una tasa de datos elevada operando sobre canales con desvanecimiento selectivo en frecuencia. Se ha demostrado que al usar un esquema de codificado eficiente sobre los dominios del espacio, tiempo y frecuencia en sistemas MIMO-OFDM, la transmisión sobre un canal inalámbrico es mucho más confiable y robusta.
En la primer parte de esta Tesis Doctoral, se proponen dos diseños de códigos de enrejado espacio-tiempo-frecuencia (STF) de tasa completa para sistemas MIMO-OFDM. El primer diseño se basa en rotación de constelaciones y es llamado código de enrejado super-ortogonal extendido espacio-tiempo-frecuencia (Ex-SOSTFTC). En el segundo diseño llamado código de enrejado cuasi-ortogonal espacio-tiempo-frecuencia (QOSTFTC), se combina de manera sistemática la partición de conjuntos y la estructura de diseños cuasi-ortogonales espacio-tiempo-frecuencia. Además de diversidad espacial, los códigos STF propuestos proveen diversidad multi-trayectoria y alcanzan una alta ganancia de codificado sobre canales selectivos en frecuencia.
En la segunda parte de la tesis se proponen dos códigos de enrejado diferenciales cuasi-ortogonales espacio-frecuencia (DQOSFTCs) para sistemas MIMO-OFDM, los cuales pueden codificar diferencialmente señales ya sea dentro de un símbolo OFDM o sobre dos símbolos OFDM adyacentes. Los DQOSFTCs se construyen sistemáticamente combinando códigos unitarios de enrejado espacio-frecuencia y la modulación diferencial sobre el dominio de la frecuencia (DF-QOSFTC) o sobre el dominio del tiempo (DT-QOSFTC). Los DT-QOSFTCs permiten suponer que el canal entre símbolos OFDM adyacentes varia lentamente. De igual manera, en los DF-QOSFTCs se supone que el canal entre portadoras adyacentes dentro de un mismo símbolo OFDM varia lentamente. Los DQOSFTCs son capaces de obtener un excelente desempeño con una ganancia de codificado alta, diversidad multi-trayectoria y un decodificado sencillo cuando la información del estado del canal no existe en el transmisor ni en el receptor.

Palabras Clave: MIMO-OFDM, codificado espacio-tiempo-frecuencia, codificado diferencial espacio-frecuencia.

ABSTRACT of the thesis presented by **JORGE FLORES TRONCOSO**, in partial fulfillment of the requirements for the degree of DOCTOR OF SCIENCES in ELECTRONIC AND TELECOMMUNICATIONS with orientation in TELECOMMUNICATIONS. Ensenada, Baja California, August 2010.

CODING FOR NEXT GENERATION WIRELESS NETWORKS

With the arrival of next generation (4G) broadband wireless communications, deploying the multiple-input multiple-output (MIMO) wireless technology together with orthogonal frequency division multiplexing (OFDM) has been recognized as one of the most promising techniques to support high performance and high-data-rate communications operating over frequency-selective fading channels. An efficient coding scheme over the space, time, and frequency domains provided by MIMO-OFDM has been shown to be a much more reliable and robust transmission technique over the hostile wireless channel.

The first part of this Doctoral thesis, proposes two full-rate space-time-frequency (STF) trellis code designs for MIMO-OFDM systems. The first code based on rotating constellations is called extended super-orthogonal STF trellis code (Ex-SOSTFTC). The second code, called Quasi-Orthogonal STF trellis codes (QOSTFTCs), combines set partitioning and the structure of quasi-orthogonal space-frequency designs in a systematic way. In addition to spatial diversity, the proposed codes provide multipath diversity and achieve high-coding gain over a frequency selective fading channel.

The second part of this thesis, presents the proposal of two differential quasi-orthogonal space-frequency trellis codes (DQOSFTCs) for MIMO-OFDM systems. These proposed differential schemes can differentially encode signals either within one OFDM symbol, or over two adjacent OFDM symbols. The DQOSFTCs are systematically constructed by combining unitary quasi-orthogonal space-frequency trellis codes and differential modulation over the frequency domain (DF-QOSFTC) or time domain (DT-QOSFTCs). Unlike other existing researches, where it is assumed that the channel remains constant over multiple OFDM symbols, the DT-QOSFTCs allows to assume a quasi-static channel during each OFDM symbol and a slow changing channel from a duration of one OFDM symbol to another. Similarly, the DF-QOSFTCs allows the constant channel assumption during adjacent subcarriers within one OFDM symbol, and a slow change from a subcarrier to next adjacent subcarrier. Besides multipath diversity, the DQOSFTCs achieve high-coding gain and simple decoding when the channel state information is not available at both the transmitter and the receiver.

Keywords: MIMO-OFDM, space-time-frequency coding, differential space-frequency coding.

This thesis is dedicated to my loving wife Mayela, and our children Jorge Eduardo, Sarai Guadalupe, Aaron Jair and Jimena Montserrat.

Acknowledgments

During the development of this thesis, I have been helped and supported by many very enjoyable and fascinating individuals. The completion of this study would not have been possible without their contributions. Now it is a pleasure to use this opportunity to express my gratitude for all of them.

Many thanks to my advisor, Dr. Jaime Sánchez García. His kindness, his guidance, his teachings and faith in me provided encouragement and invaluable support in the journey of my Doctoral education. His passion and excitement for research is very inspiring.

I thank the committee members, Dr. Luis A. Villaseñor, Dr. José R. Gallardo, Dr. Carlos A. Brizuela and PhD. Hamid Jafarkhani, who offered guidance, time and their valuable suggestions.

I am especially thankful to Professor Hamid Jafarkhani, it has been a pleasure to work with him and I feel very fortunate to have had him as a committee member. I thank him for his guidance, his teachings, his listening, his help, and patience to endure. He is a great source of motivation and encouragement.

I thank from the bottom of my heart to my dear wife, Mayela. I could not have completed this hard work without her support, encouragement, endless care and affection. She has always been there for me and provided unconditional love and support. My wife and our children are the reason why I made it so far. I thank them for sacrificing everything so I can follow my dream.

Thanks to CONACyT and the Universidad Autónoma de Zacatecas for providing me with financial means to finish my doctoral studies. Thanks to all professors and

support staff of CICESE research center, who offered me their support and help at any time. CICESE, thank you for trusting me.

I would like to thank my wonderful friends and colleagues, Leonel Soriano, Ramón Maldonado, Enrique Pacheco and Felipe Ayala, who have become dear and treasured friends. They are so generous and kind to share with me their views and experience, and gave me the feeling of being at home when at work. I would especially like to thank my friend and compadre, Eduardo González, for his invaluable moral support, time and help with my personal paperwork. It is my luck to meet all of you.

Contents

Page

Resumen **i**

Abstract **ii**

Dedicatory **iii**

Acknowledgments **iv**

Contents **vi**

List of Figures **viii**

List of Tables **xi**

I. Introduction **1**
- I.1 Problem Statement and Motivation . . . 3
- I.2 Contributions of this Thesis . . . 6
- I.3 Thesis Outline . . . 7

II. Background **10**
- II.1 Fading Channel Models . . . 11
  - II.1.1 Fading . . . 11
- II.2 MIMO . . . 15
  - II.2.1 Diversity Techniques . . . 16
  - II.2.2 Quasi-Orthogonal Space-Time Block Codes . . . 17
  - II.2.3 Super Orthogonal Space-Time Trellis Coding . . . 22
- II.3 MIMO-OFDM . . . 27
  - II.3.1 Basic Principles of OFDM . . . 27
  - II.3.2 MIMO-OFDM system . . . 30
  - II.3.3 Space-Frequency Coded OFDM . . . 35
  - II.3.4 Space-Time-Frequency Coded OFDM . . . 36

III. Space-Time-Frequency Trellis Coding **39**
- III.1 Introduction . . . 39
- III.2 System Model . . . 41
- III.3 Design Criteria . . . 45
- III.4 Extended Space-Time-Frequency Trellis Codes . . . 48
  - III.4.1 Codeword structure . . . 48
  - III.4.2 Set partitioning . . . 49

Contents (continuation)

Page

III.4.3 Design of Ex-SOSTFTCs 50
III.4.4 Decoding of Extended-STF Trellis Codes 53
III.5 Quasi-Orthogonal Space-Time-Frequency Trellis Codes 53
III.5.1 Codeword structure 54
III.5.2 Set partitioning 55
III.5.3 QOSTFTCs design 59
III.5.4 Decoding of QOSTF Trellis Codes 61
III.5.5 Diversity of QOSTFTCs 62
III.6 Simulation Results and Discussions 64
III.7 Chapter Summary 72

IV. Differential Quasi-Orthogonal Space-Frequency Trellis Codes 74
IV.1 Introduction 74
IV.2 System Description 79
IV.3 Differential encoding and subcarrier map 80
IV.3.1 Unitary quasi-orthogonal block codes 80
IV.3.2 Subcarrier assignment 83
IV.3.3 Differential encoding 84
IV.4 Differential QOSFTCs 87
IV.4.1 Codeword sets 88
IV.4.2 Design criteria 89
IV.4.3 Set partitioning 89
IV.4.4 Unitary Quasi-Orthogonal SF Trellis Codes 91
IV.4.5 Differential encoding of the QOSFTCs 94
IV.4.6 Decoding of DQOSFTCs 95
IV.5 Simulation results 98
IV.6 Chapter Summary 103

V. Conclusions and Future Works 105
V.1 Conclusions 105
V.2 Future works 111

References 114

A. Notation and Abbreviations 120

List of Figures

Figure		Page
1	Basic MIMO scheme.	15
2	Transforming a 3 dimensional design to a 2 dimensional block code design for quasi-static fading channels.	20
3	Set partition for BPSK.	25
4	Set partition for QPSK.	25
5	A four state code, $r = 1$ bit/s/Hz using BPSK or $r = 2$ bit/s/Hz using QPSK.	26
6	OFDM symbols sequence.	28
7	SISO-OFDM System Block Diagram.	28
8	A simplified MIMO-OFDM system.	30
9	Correlation of a subcarrier with adjacent ones by varying the number of paths.	33
10	Inter-subcarriers correlation by varying σ_{rms}, with $N = 64$, $L = 16$ and $T_s = 50\ ns$.	34
11	Inter-subcarriers correlation by varying N, with $\sigma_{\text{rms}} = 150\ ns$, $L = 16$ and $T_s = 50\ ns$.	35
12	Rate-1 Space-Frequency coding using the Alamouti scheme.	36
13	Rate-1 Space-Time-Frequency coding.	37
14	Transceiver model.	44
15	Set partition for QPSK using two transmit antennas.	50
16	A 16-state Ex-SOSTFTC at rate of 2 bits/s/Hz using QPSK.	51
17	Two typical paths differing in 2 transitions.	52
18	Set partitioning for BPSK.	56
19	Set partitioning pattern follows with $M = 2$.	56
20	Final set partitioning using QOSTBCs with QPSK.	59

List of Figures (continuation)

Figure		Page
21	2-state and 4-state QOSTFTCs at rate of 2 bits/s/Hz using QPSK.	60
22	A 16-state QOSTFTC at rate of 2 bits/s/Hz using QPSK.	61
23	Uniform power delay profile a) two-ray, b) four-ray channel model.	65
24	Power delay profile of a) six-ray COST207-TU, b) HiperLAN/2 indoor channel model C.	66
25	Performance of 2-state and 4-state Quasi-Orthogonal STF trellis codes, in a two-tap equal-power channel, where the delay spread between paths is 30 μs; at 2 bits/s/Hz with QPSK.	67
26	Performance of 16-state Extended Super-Orthogonal and 16-state Quasi-Orthogonal STF trellis codes, in a two-tap equal-power channel, where the delay spread between paths is 30 μs; at 2 bits/s/Hz with QPSK.	68
27	Performance of 2-state and 4-state Quasi-Orthogonal STF trellis codes, in a four-tap equal-power channel, where the delay spread between paths is 10 μs; at 2 bits/s/Hz with QPSK.	69
28	Performance of 16-state Extended Super-Orthogonal and 16-state Quasi-Orthogonal STF trellis codes, in a four-tap equal-power channel, where the delay spread between paths is 10 μs; at 2 bits/s/Hz with QPSK.	70
29	FER Performance for 6-ray COST207-TU channel model, where the rms delay spread is 1.1 μs; at 2 bits/s/Hz with QPSK.	70
30	FER Performance for ETSI/BRAN channel model C, where the rms delay spread is 150 ns; at 2 bits/s/Hz with QPSK.	71
31	Differential Space-Frequency transmitter.	80
32	Final partitioning of sets (a) $\boldsymbol{\mathcal{O}}$ with Φ_0, and (b) $\boldsymbol{\mathcal{P}}$ with Φ_1.	91
33	Partitioning for sets (a) O and (b) P, using QPSK.	92
34	QOSTFTCs using QPSK (a) 4-state, (b) 8-state.	93
35	16-state QOSTFTC using QPSK.	94
36	SER performance for the two-ray power delay profile, and R =2 b/s/Hz.	99
37	SER performance for the TU six-ray power delay profile, with a normalized Doppler frequency $f_{Dn} = 0.0025$, and R =2 b/s/Hz.	100

List of Figures (continuation)

Figure Page

38 SER performance for all 8-states trellis codes, under a TU six-ray power delay profile, with a normalized Doppler frequency of $f_{Dn} = 0.0025$, and R =2 b/s/Hz. 101

39 SER performance for all 8-states trellis codes, under a TU six-ray power delay profile, with a normalized Doppler frequency of $f_{Dn} = 0.0125$, and R =2 b/s/Hz. 102

List of Tables

Table Page

I Optimal rotation angles for QOSTBCs 22

II Example of a vertical expansion to construct a new subset. 57

III Partial set partitioning for QOSTBCs with QPSK. 58

Chapter I

Introduction

The ever-increasing demand for reliable high-data-rate communication over the wireless channel has lead to the development of efficient modulation and coding schemes. Modern wireless communications applications such as data transfer, real-time voice and video, or paging and messaging have different time delay, bit rate and error rate requirements. However, in a practical wireless channel there are many different paths in a transmit-receive link. These paths experience different loss and phase changes. As a result, at the receiver all received signals create a multipath fading channel. In general, the wireless channel suffers from time-varying impairments like multipath fading, interference, and noise.

Diversity techniques are effective methods to combat the fading in wireless channels (Jafarkhani, 2005). Diversity provides different replicas of the transmitted signal to the receiver. The main diversity methods are temporal diversity, frequency diversity, spatial diversity and polarization diversity. Time and frequency diversity suffer from a loss in bandwidth efficiency. However, by employing multiple antennas either at the transmitter or receiver, i.e. a Multiple-Input Multiple-Output (MIMO) system, spatial diversity not suffer of a bandwidth deficiency.

MIMO systems are able to achieve higher data rate and provide more reliable reception performance when compared with traditional single-antenna systems. A Space-

Time (ST) code is a bandwidth-efficient method that can improve the reliability of data transmission in MIMO systems (Alamouti, 1998). By coding a data sequence across different transmit antennas and time slots, ST coding can transmit multiple redundant copies of the data sequence through independent fading channels. Consequently, more reliable detection can be obtained at the receiver (Diggavi *et al.*, 2004). Moreover, by employing multiple antennas for both the transmitter and receiver, other goals can be achieved, as a substantial increase in capacity when compared with the single antenna systems (Foschini and Gans, 1998).

On the other hand, Orthogonal Frequency Division Multiplexing (OFDM) has been recognized as one efficient technique for transmitting data over frequency selective channels. OFDM is based on the principle of dividing a broadband frequency channel into a few narrowband subchannels, without complicated equalization filters. OFDM is utilized as a digital modulation scheme via an Inverse Fast Fourier Transform (IFFT). To avoid Inter Symbol Interference (ISI) due to channel delay spread, a guard interval called *cyclic prefix* (CP) is appended in the OFDM symbol.

Since the OFDM technique can transform a Frequency Selective Channel (FSC) into multiple flat fading sub-channels, a MIMO-OFDM scheme can exploit both spatial and frequency diversity without requiring the Channel State Information (CSI) at the transmitter. Currently, the combination of MIMO wireless technology with OFDM (MIMO-OFDM) is being used in 4G wireless networks (Glisic, 2007). MIMO-OFDM systems provide many degrees of freedom in space, time, and frequency. A few examples of MIMO-OFDM applications in modern wireless systems are: IEEE 802.11n, the 3rd Generation Partnership Project (3GPP), Long Term Evolution (LTE), and Worldwide Interoperability for Microwave Access (WiMAX) standards.

I.1 Problem Statement and Motivation

As mentioned, due to the huge demands for fast and reliable communications over wireless channels, future broadband communication systems should provide a low-complexity, higher data rate, and robust performance. To address these challenges, one promising solution is to design efficient coding schemes over the space, time, and frequency domains for MIMO-OFDM systems (Bölcskei, 2006). Recent advances in such coding techniques have helped to increase the throughput and reliability of the wireless communication systems over such fading channels.

Su *et al.* (2005) have shown that the Space-Time-Frequency (STF) coding schemes can achieve a maximum diversity gain equal to $M_t M_r L\mathcal{T}$, where M_t and M_r are respectively, the number of transmit and receive antennas, L is the number of propagation paths , and $\mathcal{T}$ is the rank of the channel temporal correlation matrix over MIMO-OFDM system. So far, a large number of papers have been focused on obtaining the space-time-frequency diversity and reducing the decoding complexity for STF trellis schemes. In order to achieve that diversity, the length of the shortest error event path (the minimum effective length) of the STF trellis schemes should be as large as possible. Also, the coding gain depends on the channel response and thus optimizing the coding gain is not viable (Lu and Wang, 2003). Furthermore, since the OFDM channel in the frequency domain is highly correlated and slowly varying, interleaving across frequency tones is a vital requirement that allows the code to exploit the available frequency diversity.

A system combining STTC with OFDM was first proposed in (Agrawal *et al.*, 1998), by adapting Tarokh's space-time codes (Tarokh *et al.*, 1998) to OFDM with multiple transmit antennas. However, these codes are not optimized for OFDM channels and

cannot benefit from the available frequency diversity.

In order to simplify the design and reduce the complexity of the code, the authors in (Gong and Letaief, 2003) proposed to concatenate Trellis Coded Modulation (TCM) with Space-Time Block Codes (STBCs). The spatial diversity is guaranteed by STBC while the frequency diversity is achieved by TCM. Similarly, by optimizing the effective lengths for traditional TCM and by employing a random interleaver, a STTC for OFDM systems was proposed by Lu and Wang (2003). In both codes the full diversity is achieved at the expense of a low coding rate. Liu *et al.* (2002) extended the signal constellation and proposed a full-diversity linear-constellation-precoded space-time block code (LCP-STBC) OFDM system at the cost of low power efficiency of the OFDM system.

To overcome these problems, coding schemes that incorporate super-orthogonal codes derived by Jafarkhani and Seshadri (2003) with OFDM transmission, the so-called super-orthogonal space-time-frequency trellis codes (SOSTFTCs), were introduced by Aksoy and Aygölü (2007). These codes were designed for a quasi-static (over two adjacent OFDM symbols) fading channel using QPSK constellations with 16, 32 and 64-state trellis structures. However, the shortcoming of these codes is the fact that, to achieve multipath diversity, the number of parallel transitions is avoided by increasing the number of trellis states, while providing a lower coding gain on frequency selective channels.

Recently, Quasi-Orthogonal Space-Frequency Block Codes (QOSFBCs) and Quasi-Orthogonal Space-Time-Frequency Block Codes (QOSTFBCs) for two transmit antennas have been proposed in (Fazel and Jafarkhani, 2008). By coding across the three dimensions (space, time and frequency), these codes provide rate-one and exploit all the spatial, multipath and temporal diversity gains available in the MIMO-OFDM channel,

while providing no additional coding gain.

As can be seen, all these proposals have several drawbacks such as not being optimized for MIMO-OFDM systems, having a low coding rate, a low power efficiency, and a low coding gain among others. This motivated us to design simple trellis coding schemes that enable us to obtain more than one source of diversity and achieve a good performance, while keeping a low number of trellis states and low decoding complexity.

Furthermore, as either the number of antennas or the number of multiple paths increases, there is a restrictive complexity of acquiring knowledge of the CSI for frequency-selective fading channels, since it requieres the estimation of an increased number of fading coefficients. Therefore, the issues of exploiting the available spatial, temporal and frequency diversities, if neither the transmitter nor the receiver know the CSI, have been recently addressed. A recursive technique to contend with unknown CSI is differential modulation. Differential unitary space-time modulation schemes for frequency flat channels were independently derived by Hughes (2000), and Hochwald and Sweldens (2000).

Another elegant differential modulations based on orthogonal designs and Quasi Orthogonal codes are proposed by Tarokh and Jafarkhani (2001), and Zhu and Jafarkhani (2005), respectively. The differential scheme derived by Liu and Giannakis (2003) is able to achieve multipath diversity for single-antenna OFDM transmission over FSCs. The noncoherent SF codes derived by Borgmann and Bölcskei (2005) achieve the maximum diversity order available in FSCs, but these have large code size, which exponentially increases the coding and decoding complexity. Moreover, an increase in rate leads to a loss in coding gain. In (Ma *et al.*, 2005) and (Himsoon *et al.*, 2006), grouping techniques of SF codes are exploited and the authors obtained a differential transmission rule incorporated with subcarrier allocation methods. However, these implementations

require constant channel frequency response (CFR) from group to group, which would lead to severe error floor in FSCs.

Differential SF trellis codes (DSFTCs) based on orthogonal ST block codes and unitary groups codes were presented in Hong *et al.* (2006). DSFTCs can achieve rate-one, spatial diversity, and a simple decoding complexity. But, although the DSFTCs increase the coding gain, the error floor is still significant.

The weaknesses of previous work also motivate us to design new schemes with good performance, full-rate and coding gain, able to exploit the diversity available in MIMO-OFDM channel without knowing the CSI at the receiver nor in the transmitter.

I.2 Contributions of this Thesis

In this dissertation we propose several coding techniques for transmission over frequency-selective fading channels and present analytical and simulation results for the coded MIMO-OFDM system under different propagation scenarios.

Assuming perfect channel state information at the receiver, first we propose two space-time-frequency trellis coding schemes with two transmit antennas operating over frequency-selective fading channels. Contributions of this proposal are two simple coding techniques which systematically combine orthogonal and quasi-orthogonal space-time block codes with trellis structures using rotated constellations. Our designs guarantee rate-one, multipath diversity with high-coding gain, low number of trellis states and low decoding complexity. To the best of our knowledge, there has been no previous work on STF trellis codes with parallel transitions in the trellis structure, such that the multipath diversity and coding gain can be achieved despite parallel transitions. Moreover, the STF trellis schemes proposed in this thesis are based on certain design

criteria for space-frequency (SF) trellis codes such that our designs do not need any knowledge of multipath and delay effects of the channel.

In the second part of this work, we propose systematic designs of rate-one differential quasi-orthogonal SF trellis codes, capable of exploiting both spatial and frequency diversity operating over frequency-selective fading channels with lack of CSI at the transmitter and at the receiver. We derive a general structure of full-diversity unitary quasi-orthogonal space-time block codes. Thus, we systematically design unitary quasi-orthogonal SF trellis codes. Then, by exploiting correlation either between adjacent subcarriers within one OFDM symbol, or between adjacent OFDM symbols, we propose differentially encoded, respectively, over the frequency domain, or over the time domain. In addition, we take advantage of orthogonality of the inner matrices of the differential schemes, by using a simple Maximum Likelihood (ML) decoder at the receiver without requiring CSI. The ML decoder is constituted by a differential decoder followed by a Viterbi decoder.

I.3 Thesis Outline

The organization of this thesis is as follows:

In Chapter II, we provide some background material which will be used in developing our main contributions and results. We begin with a brief description of fading channel models and related fading parameters. Then, we discuss diversity techniques for MIMO wireless communications. Also, a general overview on space-time coding is given. Finally, combination of MIMO technology with OFDM modulation will be described, and some example of space-frequency and space-time-frequency coding are illustrated.

In Chapter III, we propose space-time-frequency codes for two transmit antennas over frequency selective fading channels. First, the channel model and design criteria for which a STF code guarantees multipath diversity and high coding gain over a MIMO-OFDM system are discussed. Furthermore, in the first part of the Chapter, we propose a STF code called Extended Super-Orthogonal Space-Time-Frequency Trellis Code (Ex-SOSTFTC). Here, we consider the concept of rotated constellations and we avoid parallel transitions in the trellis structure. Then, we extend the Super-Orthogonal Space-Time Trellis Codes (SOSTTCs) originally designed for the frequency-flat fading case, to the frequency-selective fading channel. Afterwards, decoding of extended-STF trellis codes is shown. In the second part of the chapter, we propose a coding scheme called Quasi-Orthogonal Space-Time-Frequency Trellis Codes (QOSTFTCs), where we systematically combine a Quasi-Orthogonal Space-Time Block Code (QOSTBC) with a trellis code, operating over a frequency selective fading channel. In addition, in order to provide the maximum coding gain for the QOSTFTCs, we will describe a systematic method to do set partitioning. Then, we derive a decoding process for the QOSTFTCs, and then the diversity of QOSTFTCs is discussed. Finally, performance simulation results of the proposed Ex-SOSTFTC and QOSTFTCs will be presented and examined. We show that our designs are able to exploit the full diversity gains available in the MIMO-OFDM channel, and can achieve high coding gain, good performance, and low decoding complexity with a low number of states in the trellis. Both proposals get full symbol rate (one symbol per frequency tone per time slot). We show with analysis and numerical simulations that our designs of STF codes outperform the best existing space-time-frequency trellis codes in the literature.

In Chapter 4, we briefly review the concept of differential modulation. Focusing on broadband MIMO-OFDM channels, we propose two systematic design of rate-one

Differential Quasi-Orthogonal Space-Frequency Trellis Codes (DQOSFTCs). First, we consider the design of matrix rotation based on unitary quasi-orthogonal codes. Later on, we will derive a general structure of full-diversity unitary quasi-orthogonal space-time block codes. Then, in order to achieve a rate-one transmission, we will expand the matrix constellation by introducing unitary rotation matrices. Afterward, we perform set partitioning to constellation of matrices. As a result, we will be able of systematically design the unitary quasi-orthogonal SF trellis codes (QOSFTCs). With the goal of relaxing the assumption of a constant Channel Frequency Response (CFR) from adjacent groups of subcarriers, we will provide a subcarrier map method, which divides an OFDM symbol into several subcarriers groups. Consequently, the diversity advantage will be increased. Afterwards, we will design two differential encoding methods, the first one codified the QOSFTCs differentially over the frequency domain (DF-QOSFTC), and the second codified the QOSFTCs differentially over the time domain (DT-QOSFTC). Next, we will show a simple differential decoder, which will take advantage of orthogonality from the inner matrices into the QOSFTCs. Finally, we will perform numerical simulations for the differential codes proposed operating over several fading channels scenarios. Also, we will compare our designs with that of existing Differential Space-Frequency Trellis Codes (DSFTCs).

Finally, Chapter V contains some concluding remarks and discussion on future research ideas on this fascinating topic.

Chapter II

Background

These days, the requirements of Wideband (WB) transmission are growing and studies are focusing on the problem of multipath propagation delay affecting the transmission. In the case of narrowband (NB) transmission, the delay spread of the propagation channel is considerably smaller than the symbol period of the modulated signal; the channel transfer function exhibits no frequency dependence, so that the fading environment is frequency-flat. The problem of rapid phase variations due to Doppler spread had become insignificant for single-carrier WB systems, but with the advent of Orthogonal Frequency Division Multiplexing (OFDM) transmission for wireless mobile applications, this problem has again become apparent. OFDM is a special case of Frequency-Division Multiplexing (FDM). Unlike FDM, OFDM uses the spectrum much more efficiently by dividing the available spectrum into many orthogonal carriers, each one being modulated by a low-rate stream. This modulation technique creates frequency-flat sub-channels within a Frequency Selective Channel (FSC). On the other hand, Multiple-Input Multiple-Output (MIMO) systems apply multiple antennas at both transmitter and receiver sides of the transmission link. The term MIMO refers to the wireless channel which possesses multiple inputs, i.e., the transmit antennas, and multiple outputs, i.e., the receive antennas. Thus, a combination of OFDM and MIMO can be adopted as the basis for high data-rate systems.

In this chapter we review the basic concepts and provide some issues of Multiple-Input Multiple-Output-Orthogonal Frequency Division Multiplexing systems that are needed in the rest of the thesis.

II.1 Fading Channel Models

We start examining a few channel fading issues. Then, we will discuss the MIMO system model, and several definitions that are part of the MIMO systems. This will be followed by a brief study of Space-Time (ST) coding techniques for cases when the channel is flat, and it is known to the transmitter and unknown to the receiver. We conclude with a review on OFDM.

II.1.1 Fading

The rapid fluctuations of the amplitude, phases, or multipath delays of a radio signal during a short period of time, or short travel distance, is called small-scale fading, or simply *fading*. The fading is a superposition of a large number of independent scattered components, arriving at the receiver through different paths (multipaths). As a result, the multipath effect can cause:

- Rapid variations in signal amplitude over a short time interval or a small travel distance.
- Varying Doppler shifts on different multipaths, which produce random frequency modulation.
- Time dispersion caused by multipath propagation delays.

By the central limit theorem, the components of the received signal can be represented by an independent zero mean Gaussian process. Then, the envelope of the received signal r follows a Rayleigh distribution as (Jankirman, 2004)

$$f(r) = \frac{2r}{\Omega} e^{\left(-\frac{r^2}{\Omega}\right)} u(r) \tag{1}$$

where $\Omega = 2\sigma^2$ is the average receive power and $u(r)$ is the unit step function defined as

$$u(r) = \begin{cases} 1, & r \geq 0 \\ 0 & r < 0 \end{cases} \tag{2}$$

If Line-of-sight exists, multipaths still occurs because there are reflections from the ground or surround structures. In this case, the distribution of the received signal is Ricean given by (Jankirman, 2004)

$$f(r) = \frac{2r(K+1)}{\Omega} \exp\left(-K - \frac{(K+1)r^2}{\Omega}\right) I_0\left(2r\sqrt{\frac{K(K+1)}{\Omega}}\right) u(r) \tag{3}$$

where the factor K is the ratio of the power in the mean component of the channel to the power in the scattered component and I_0 is the modified Bessel function of the first kind and of zero-order. Note that in the absence of the direct path, $K = 0$ and $I_0(0) = 1$. As a result, the Ricean distribution reduces to a Rayleigh distribution.

Basically, the fading can be classified in three types:

- Time selective fading (Doppler spread)
- Frequency selective fading (Delay spread)
- Space selective fading (Angle spread)

In what follows, we examine the two first fading types.

Time selective fading

Doppler shift in frequency is due to mobility of either the transmitter or receiver (or both). Let v be the velocity of the moving object and ϕ be the relative angle between the moving object and the receiver, the Doppler shift of the received signal is given by (Jakes, 1974)

$$f_d = \frac{v f_c}{c} cos\phi \tag{4}$$

where c is the speed of light and f_c is the transmitted frequency. Due to different Doppler shifts on each of multipath components observed at receiver, a random frequency modulation is obtained. As a result, any transmitted frequency results in a range of received frequencies, namely a spectral broadening at the receiver.

Doppler spread measures that spectral widening and is defined as the range of frequencies whose received Doppler spectrum is not zero. If f_D is the maximum Doppler shift, the transmitted frequency f_c will be received with frequency components in the range $f_c - f_D$ to $f_c + f_D$.

The coherence time of the channel T_c is a measured of how fast the channel changes in time. T_c is defined as the time range for which the signal autocorrelation coefficient reduces to 0.7 (Rappaport, 2002), and it is calculated as

$$T_c \approx \frac{1}{\sqrt{2}\pi f_D} \tag{5}$$

We can see from (5), that the larger the coherent time (i.e. a small f_D), the slower the channel fluctuation over time domain. In a quasi-static fading channel model, all the fading coefficients are constant during the transmission of one data frame, and change from one frame to another.

Frequency selective fading

A mobile radio channel may be modeled as a linear filter with a time varying impulse response, where the the time delays among the different arriving impulses are due to transmitter/receiver motion in space. Consequently, a frequency selective fading is caused. Frequency selective fading is characterized by the coherence bandwidth B_c, which is a measure of how the channel changes with frequency. B_c is the frequency range for which the channel's autocorrelation coefficient reduces to 0.7, defined as (Rappaport, 2002)

$$B_c \approx \frac{1}{2\pi \cdot \sigma_{\mathrm{RMS}}} \tag{6}$$

where σ_{RMS} is the Root mean square delay spread of the channel. It can be concluded from (6) that the larger the coherence bandwidth (i.e. a small σ_{RMS}), the slower the channel fluctuation over frequency domain. It is referred to as *flat fading* channel or frequency non-selective fading channel when it has a coherence bandwidth much larger than the transmitted signal bandwidth. Such signal is a narrowband signal. If the channel experiences both frequency-flat channel and time-flat fading, then it is called a quasi-static flat fading channel. Moreover, if the coherence bandwidth of the channel is much smaller than the transmitted signal bandwidth, then the transmitted signal undergoes independent fades, such a channel is known as a frequency-selective channel, or *fast fading* over frequency domain. As we will see in a subsequent section, the OFDM technique converts a frequency-selective broadband channel into flat fading sub-channels.

II.2 MIMO

A Multiple-Input Multiple-Output (MIMO) system is equipped with M_t transmit antennas and M_r receive antennas in a communication link, which is shown in Figure 1.

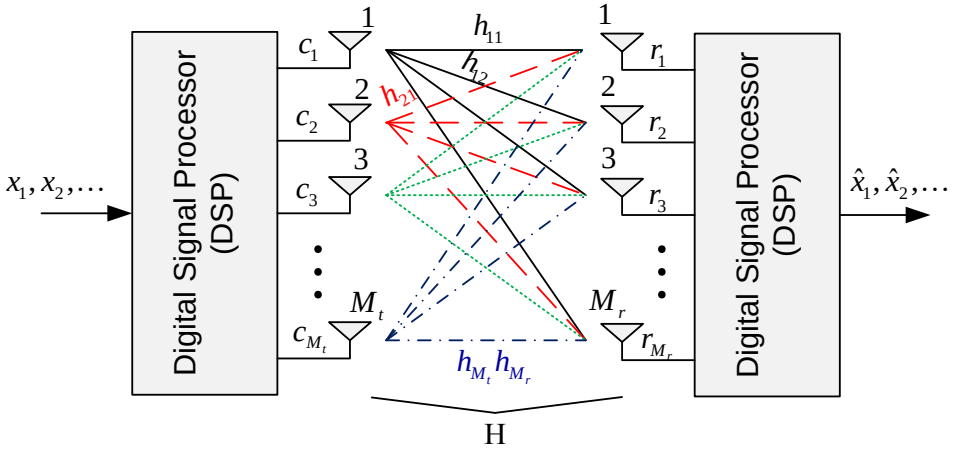

Figure 1. Basic MIMO scheme.

We pick up signals to be transmitted during T time slots from M_t transmit antennas in the matrix $\mathbf{C}$ as

$$\mathbf{C} = \begin{bmatrix} c_{1,1} & c_{1,2} & \cdots & c_{1,M_t} \\ c_{2,1} & c_{2,2} & \vdots & c_{2,M_t} \\ \vdots & \vdots & \ddots & \vdots \\ c_{T,1} & c_{T,2} & \cdots & c_{T,M_t} \end{bmatrix} \in \mathbb{C}^{T \times M_t}. \tag{7}$$

The total transmitted power at time slot t is given by

$$P = \|[c_{t,1}, c_{t,2}, \cdots, c_{t,M_t}]\|_F^2, \tag{8}$$

where $\|\cdot\|_F$ denotes the Frobenius norm. Since the transmitted energy is equally distributed to each transmit antenna, the transmitted symbol energy is

$$E_s = \frac{P}{M_t} \tag{9}$$

Since, the total received power per antena is equal to the total transmitted power, the Signal-to-Noise Ratio (SNR) can be written as

$$\gamma = \frac{E_s}{N_0}, \tag{10}$$

where N_0 is the noise power, i.e. the variance.

The channel matrix is given by

$$\mathbf{H} = \begin{bmatrix} h_{11} & h_{12} & \cdots & h_{1M_r} \\ h_{21} & h_{22} & \vdots & \vdots \\ \vdots & \vdots & \ddots & h_{M_t-1M_r} \\ h_{M_t1} & \cdots & h_{M_tM_r-1} & h_{M_tM_r} \end{bmatrix}, \tag{11}$$

where $h_{n,m}$ represents the channel coefficients from transmit antenna n to receive antenna m, which are modeled by using independent complex Gaussian random variables with zero mean and variance of $1/2$ per complex dimension. In the sequel, we assume that the channel is Rayleigh fading and quasi-static over T time slots. In coherent systems the channel coefficients are assumed to be perfectly known at the receiver.

Based on this model, the received signal vector $\mathbf{r}$ is given by the compact input-output relationship as follows (Jafarkhani, 2005)

$$\mathbf{r} = \mathbf{C} \cdot \mathbf{H} + \mathcal{N} \quad \in \mathbb{C}^{T \times M_r}, \tag{12}$$

where the components of $\mathcal{N}$, $\eta_{t,m}$, are Zero Mean Circularly Symmetrical Complex Gaussian (ZMCSCG) variables, with variance of 0.5 per dimension, i.e. $Var[\Re\{h_{n,m}\}] = Var[\Im\{h_{n,m}\}] = 0.5$, then $E[|h_{n,m}|^2] = 1$.

II.2.1 Diversity Techniques

The diversity is a technique used in MIMO systems to combat the channel impairments, which affect the transmitted signal intensities. It can be due to interference from other

users or other noise sources. The diversity provides different replicas of the transmitted signal to the receiver, which fades independently. Therefore, the received signals can be reliably decoded at the receiver. A definition of diversity gain is given by Jafarkhani (2005) in terms of the error probability P_e at a SNR equal to γ as

$$G_d = -\lim_{\gamma \to \infty} \frac{\log(P_e)}{\log(\gamma)}. \tag{13}$$

There are three basic diversity schemes in wireless communications, these are:

Time Diversity This technique consists in providing replicas of the transmitted signal across time by a combination of channel coding and time interleaving strategies. It is adequate for quasi-static channels.

Frequency Diversity In this case replicas of the signal are transmitted in the frequency domain. This is applicable in frequency non-selective fading channel.

Space Diversity It consists in providing replicas of the transmitted signal across different receive antennas, assuming that the antenna spacing is larger than the coherent distance to ensure independent fades among different antennas.

II.2.2 Quasi-Orthogonal Space-Time Block Codes

Recently, the joint design of MIMO and channel coding has been adopted for wireless communications. The Space-Time (ST) codes can achieve both diversity and coding gains. Space-time codes map the input information symbols into an encoded symbol vector/matrix called codeword. These symbols are transmitted simultaneously through multiple antennas. Because the encoded symbols are correlated in space and time, this coding scheme is named space-time coding.

Orthogonal Space-Time Block Codes (OSTBCs) provide full diversity transmission whit linear decoding complexity (Tarokh *et al.*, 1998). Tarokh *et al.* (1999a) has demonstrated that full-rate orthogonal designs with complex elements in its transmission matrix are impossible for more than two transmit antennas. The only example of a full-rate full-diversity complex space-time block code using orthogonal designs is the Alamouti code (Alamouti, 1998). We denote the Alamouti structure as $\boldsymbol{A}(x_1, x_2)$ for the indeterminate variables x_1 and x_2 by

$$\boldsymbol{A}(x_1, x_2) = \begin{pmatrix} x_1 & x_2 \\ -x_2^* & x_1^* \end{pmatrix} \tag{14}$$

By relaxing the separate decoding property to design full-rate codes, it is possible to design a new class of codes called Quasi-Orthogonal Space-Time Block Codes (QOSTBCs) where it is possible to decode independent symbol pairs (Jafarkhani, 2001; Tirkkonen *et al.*, 2000; Su and Xia, 2002).

The encoding for QOSTBCs is very similar to the encoding of OSTBCs. In order to transmit b bits per time slot, we need a constellation $\mathcal{A}$ containing $M = 2^b$ symbols. The constellation can be any real or complex constellation, for example Pulse Amplitude Modulation (PAM), Phase-Shift Keying (PSK), Quadrature Amplitude Modulation (QAM), and so on. As an example with M_t =4 transmit antennas, we use $4b$ input bits, then the complex symbols x_1, x_2, x_3, x_4 are picked up. A codeword matrix $\mathbf{C}_4(x_1, x_2, x_3, x_4)$ is given as (Jafarkhani, 2001)

$$\mathbf{C}_4 = \begin{pmatrix} \boldsymbol{A}(x_1, x_2) & \boldsymbol{A}(x_3, x_4) \\ -\boldsymbol{A}^*(x_3, x_4) & \boldsymbol{A}^*(x_1, x_2) \end{pmatrix} \tag{15}$$

Note that at time t, the four elements in the tth row of $\mathbf{C}_4$ are transmitted from the four transmit antennas, and these four symbols are transmitted in T =4 time slots.

As a result, $\mathbf{C}_4$ is a rate-one code.

Let $\widetilde{x}_i$ be the rotated symbols, $i = 1, 2, 3, 4$, and be ϕ the rotation parameter. By replacing either (x_3, x_4) with $(\widetilde{x}_3, \widetilde{x}_4)$ or (x_1, x_2) with $(\widetilde{x}_1, \widetilde{x}_2)$, it is possible to provide rate-one rotated-QOSTBCs with both full diversity and simple pairwise decoding (Tirkkonen, 2000; Su and Xia, 2002; Jafarkhani and Hassanpour, 2005; Wang and Xia, 2005; Sharma and Papadias, 2003). A rotated-QOSTBC for four transmit antennas $\mathbf{C}_4(x_1, x_2, x_3, x_4)$ is defined as

$$\mathbf{C}_4(x_1, x_2, \widetilde{x}_3, \widetilde{x}_4) = \begin{pmatrix} \boldsymbol{A}(x_1, x_2) & \boldsymbol{A}(\widetilde{x}_3, \widetilde{x}_4) \\ \boldsymbol{A}(\widetilde{x}_3, \widetilde{x}_4) & \boldsymbol{A}(x_1, x_2) \end{pmatrix} \tag{16}$$

where $\{x_1,\ x_2\}$ belong to constellation $\mathcal{A}$ and $\{\widetilde{x}_3,\ \widetilde{x}_4\}$ belong to the rotated constellation $e^{j\phi}\mathcal{A}$. Now, let us consider the following block diagonal QOSTBC structure derived by Fazel and Jafarkhani (2008)

$$\mathbf{C}_4(x_1, x_2, \widetilde{x}_3, \widetilde{x}_4) = \begin{pmatrix} \boldsymbol{A}(x_1 + \widetilde{x}_3,\ x_2 + \widetilde{x}_4) & 0 \\ 0 & \boldsymbol{A}(x_1 - \widetilde{x}_3,\ x_2 - \widetilde{x}_4) \end{pmatrix}. \tag{17}$$

The block-diagonal QOSTBC in Eq. (17) is equivalent to the QOSTBC in (16). Therefore the diversity conditions and code-gain structure properties are maintained.

Fazel and Jafarkhani (2008) introduced a novel 3-dimensional block code capable of achieving full diversity gains and rate-one, by coding across three dimensions: space, time and frequency. Figure 2 shows the transforming problem of a 3D code to an equivalent 2D code design in a quasi-static channel domain. This problem has been extensively studied in the STBCs literature.

Now, let us extend the structure (17), where $M_t = T = 2$, to design a QOSTBC for a multi-antenna system to $M_t' = KM_t = 2K$ equivalent transmit antennas. Let

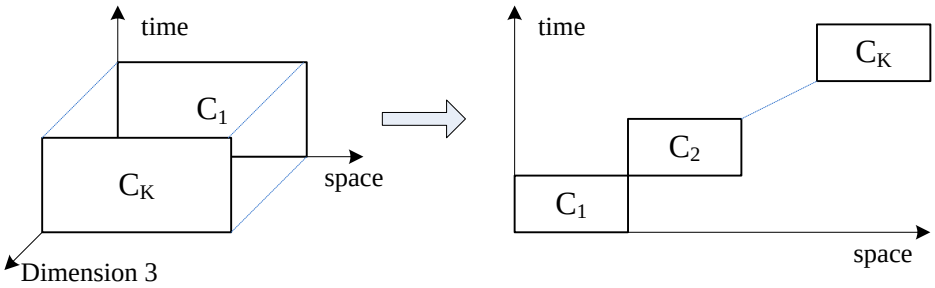

Figure 2. Transforming a 3 dimensional design to a 2 dimensional block code design for quasi-static fading channels.

$T' = TK = 2K$ be the time slots, and let $\{x_1, \ldots, x_{2K}\}$ be a block of $KM_t = 2K$ symbols, where $K = 2^r$ for some positive integer r, and $x_i \in \mathcal{A}$. Defining a new set of combined symbols $\{A_1, \ldots, A_{2K}\}$ as

$$[S_1 \; S_3 \; \ldots \; c_{2K-1}]^{\mathcal{T}} = \Phi\,[s_1 \; s_3 \; \ldots \; s_{2K-1}]^{\mathcal{T}} \tag{18a}$$

$$[S_2 \; S_4 \; \ldots \; S_{2K}]^{\mathcal{T}} = \Phi\,[s_2 \; s_4 \; \ldots \; S_{2K}]^{\mathcal{T}} \tag{18b}$$

where $\Phi = \mathbf{W}_K \; \mathrm{diag}(e^{j\phi_m})$, $m = 0, \ldots, K-1$ with $\phi_0 = 0$, and $\mathbf{W}_K \in \mathbb{C}^{K\times K}$ is a Hadamard matrix. A general class of QOSTBC's for the $2K$ transmit antennas, over a quasi-static flat channel is given by Fazel and Jafarkhani (2008) as

$$\mathbf{C}_{2K} = \frac{1}{\sqrt{2K}} \begin{pmatrix} \boldsymbol{A}(S_1, S_2) & 0 & \cdots & 0 \\ 0 & \boldsymbol{A}(S_3, S_4) & \cdots & 0 \\ \vdots & \vdots & \ddots & \vdots \\ 0 & 0 & \cdots & \boldsymbol{A}(S_{2K-1}, S_{2K}) \end{pmatrix} \in \mathbb{C}^{2K\times 2K} \tag{19}$$

In order to keep the average-transmit power constant, $\mathbf{C}_{2K}$ should satisfy the energy constraint

$$E\left[\sum_{i=1}^{KT}\sum_{j=1}^{KT} |S_{i,j}|^2\right] = KT = 2K \tag{20}$$

where $E\,[X]$ denotes the expected value of X.

Design criteria

As was discussed by Fazel and Jafarkhani (2008), $\mathbf{C}_{2K}$ can achieve full-diversity and rate one. Assuming that we have two distinct sets of symbols denoted by $\{x_1, x_2, \ldots, x_{2K}\}$ and $\{u_1, u_2, \ldots, u_{2K}\}$, where $x_i,\ u_i \in \mathcal{A},\ \forall\ i \in \{1, 2, \ldots, 2K\}$. Let us consider two distinct sets of combined symbols $S_1, S_2, \ldots, S_{2K}$ and $E_1, E_2, \ldots, E_{2K}$ corresponding to x_i's and u_i's respectively. Defining the set of pairwise combined symbol errors $\{D_1, D_2, \ldots, D_{2K}\}$, where $D_i = S_i - E_i$, $\forall\ i \in \{1, 2, \ldots, 2K\}$, it can be shown that

$$\begin{aligned}\det\left\{(\mathbf{C}_{2K} - \mathbf{E}_{2K})^H(\mathbf{C}_{2K} - \mathbf{E}_{2K})\right\} = \left(|D_1|^2 + |D_2|^2\right)^2 \left(|D_1|^2 + |D_2|^2\right)^2 \\ \ldots \left(|D_{2K-1}|^2 + |D_{2K}|^2\right)^2\end{aligned}. \tag{21}$$

Note that

$$\det\left\{(\mathbf{C}_{2K} - \mathbf{E}_{2K})^H(\mathbf{C}_{2K} - \mathbf{E}_{2K})\right\} \geq |D_1|^4|D_3|^4 \ldots |D_{2K-1}|^4. \tag{22}$$

With the equality happening when $\{D_2, D_4, \ldots, D_{2K}\} = 0$.

In order to chose the rotation angles $\{\phi_1, \phi_2, \ldots, \phi_{K-1}\}$ for the QOSTBC given by (19), considering all distinct sets of $\{x_1, \ldots, x_{2K}\}$ and $\{u_1, \ldots, u_{2K}\}$, the following two conditions must be satisfied (Fazel and Jafarkhani, 2008):

1. **Diversity**: In order to guarantee that the determinant in Eq. (21) does not vanish, the rotation angles are selected such that for $d_i = x_i - u_i,\ \forall x_i,\ u_i \in \mathcal{A}$,

$$|D_1| \ = \ |d_1 + e^{j\theta_1}d_2 + \cdots + e^{j\theta_{k-1}}d_K| \neq 0, \tag{23}$$

2. **Coding Gain**: To maximize the coding gain, the minimum value of Eq. (21) has to be maximized.

Table I. Optimal rotation angles obtained in (Fazel and Jafarkhani, 2008).

constellation	$M_t = 4$ ϕ_1	$M_t = 6$ ϕ_1, ϕ_2	$M_t = 8$ ϕ_1, ϕ_2, ϕ_3
BPSK	$\pi/2$	$\pi/4, 3\pi/4$	$\pi/4, \pi/2, 3\pi/4$
QPSK	$\pi/4$	0.4638, 0.9275	$\pi/8, \pi/4, 3\pi/8$

Optimal rotation angles

Observing that the minimum coding gain structure of the code in (17) is also the same as the minimum coding gain of the existing quasi-orthogonal codes. Then, the optimum rotation angles for this code, considering MPSK constellations, is π/M (for M even) and $\pi/2M$ (for M odd). Similarly, for a QAM constellation, the optimum rotation angle is $\pi/4$ (Jafarkhani, 2005). However, the optimal rotation angles are not unique. The Table I lists some of the optimal rotation angles for BPSK and QPSK constellations with 4, 6 and 8 transmit antennas (Fazel and Jafarkhani, 2008).

II.2.3 Super Orthogonal Space-Time Trellis Coding

Space-time codes provide an effective method to increase system capacity for wireless communications. Tarokh *et al.* (1998) first described the performance characteristics of space-time codes in terms of diversity gain and coding gain. As the diversity gain determines the asymptotic slope of Pairwise Error Probability (PEP) in logarithm domain, it is the most important factor in the design of space-time codes. Therefore, the design of the earliest space-time trellis codes has been focused primarily on implementing full diversity order, but non-optimal coding gain. The coding gain can be further increased by introducing the orthogonal design of space-time block codes into space-time trellis codes. In slow fading channel, the coding gain depends on the minimum determinant

of a full rank codeword distance matrix (Tarokh *et al.*, 1998). The codeword distance matrix is a Hermitian matrix. As a result, the optimal determinant will be obtained if the codeword distance matrix is also a diagonal matrix with equal eigenvalues.

Design of SOSTTC

Jafarkhani and Seshadri (2003) showed a systematic method to design the trellis codes for the quasi-static fading channel case, called Super-Orthogonal Space-Time Trellis Codes (SOSTTCs). In order to maximize the coding gain, STBCs are combined with a Trellis code. As a result, a new structure is obtained, which guarantees the full diversity with any given rate and number of states. In addition, the decoding complexity of SOSTTCs is smaller than that of Space-Time Trellis Codes (STTCs) derived by Tarokh *et al.* (1998).

The main idea behind SOSTTCs is to consider full-rate STBCs as modulation schemes for multiple transmit antennas. Then, STBC with specific symbol constellation are assigned to transitions originating from a trellis state. In order to achieve a desired rate of b bits/seg/Hz, one must have enough constituent orthogonal matrices. It is assumed that the matrix elements are from a M-PSK constellation and there must be enough constellation points to allow the transmission of $\log_2 \mathrm{M} = b$ bits/seg/Hz per channel use.

In general, for a STBC $\in \mathbb{C}^{T \times M_t}$, choosing a trellis branch emanating from a state is equivalent to transmitting TM_t symbols from M_t transmit antennas in T time intervals. The class of orthogonal transmission matrices for two transmit antennas is given by Jafarkhani and Seshadri (2003) as follows

$$\mathbf{C}(x_1, x_2, \theta) = \begin{pmatrix} x_1 & x_2 \\ -x_2^* & x_1^* \end{pmatrix} \begin{pmatrix} e^{j\theta} & 0 \\ 0 & 1 \end{pmatrix} = \begin{pmatrix} x_1 e^{j\theta} & x_2 \\ -x_2^* e^{j\theta} & x_1^* \end{pmatrix}. \tag{24}$$

At the first symbol interval, $x_1 e^{j\theta}$ and x_2 are the transmitted symbols from the first and second transmit antennas, respectively. The symbols $-x_2^* e^{j\theta}$ and x_1^* are transmitted from the first and second transmit antennas, at the second symbol interval, respectively. Note that for $\theta = 0$, Alamouti's code is obtained from equation (24).

By varying θ, multiple orthogonal block codes are constructed, and a super-orthogonal code is formed from the union of these codes to provide the necessary redundancy to achieve full rate. As a result of picking θ such that the resulting transmitted symbols are also from the same constellation, the constellation signals do not expand. Therefore, while the super-orthogonal code does not extend the constellation alphabet of the transmitted signals, it does expand the number of available orthogonal matrices. Another advantage of super-orthogonal codes lies in the fact that the codes are parameterized. Furthermore, the orthogonality of STBC building blocks makes it possible to reduce the complexity of the decoding process.

Following the definition of coding gain distance (CGD) derived by Jafarkhani and Seshadri (2003), the minimum of the determinant $\det(\mathbf{A_D})$ of the matrix $\mathbf{A_D} = \mathbf{D}^H\mathbf{D}$, where $\mathbf{D} = \mathbf{C} - \mathbf{E}$, over all possible pairs of distinct codewords $\mathbf{C}$ and $\mathbf{E}$, corresponds to the coding gain for a full diversity code.

$$\text{CGD} = \det(\mathbf{A_D}) = \prod_{i=1}^{M_t} \lambda_i, \qquad \lambda_i \text{ is the } i\text{th eigenvalue} \tag{25}$$

In order to perform set partitioning similar to the set partitioning procedure established by Ungerboeck (1982), the CGD is used instead of Euclidean distance. Jafarkhani and Seshadri (2003) showed that the coding gain of such a SOSTTC is dominated by

parallel transitions. The optimal set partitioning for BPSK, and QPSK are demonstrated by Jafarkhani and Seshadri (2003), and we illustrate these in Figs. 3 and 4, respectively. Note that the CGD is maximized at each level of partitioning. The numbers at leaves represent the indexes m of the MPSK symbols in a codeword.

For example, in the case of QPSK in Figure 4, the possible indexes are $m = (0, 1, 2, 3)$, whose complex points from the QPSK constellation are $(1, j, -1, -j)$, respectively.

The process of set partitioning is done to maximize the CGD at each level. Consequently, the coding gain of the resulting SOSTTC is also maximized.

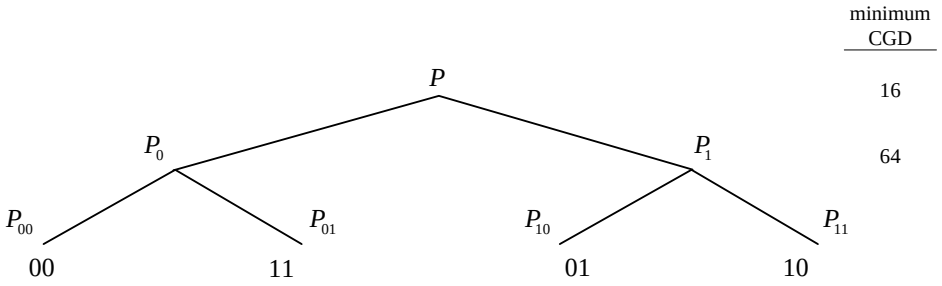

Figure 3. Set partition for BPSK.

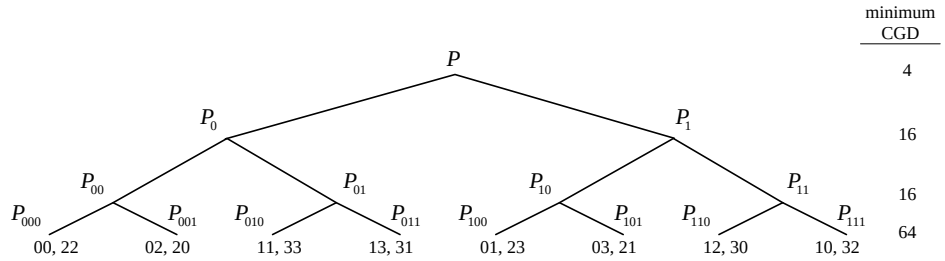

Figure 4. Set partition for QPSK.

Similar to general rules to design Multiple Trellis Coded Modulation (MTCM) schemes (Disvalar and Simon, 1988), a rule to maximize the coding gain is that all subsets should be used an equal number of times in the trellis. The design process key for the SOSTTCs is as follows: the adjacent states are usually assigned to different

constellation of STBCs. Similarly, we can assign the same STBC to branches that are merging into a state. Every pair of codewords diverging from (or merging into) a state achieves full diversity because the pair is from the same set of orthogonal codes (similar parameter θ). On the other hand, for codewords with different parameter θ, it is possible that they do not achieve full diversity. Since these codewords are assigned to different states, the resulting trellis code would provide full diversity despite the fact that a pair of codewords in a super-orthogonal code may not achieve full diversity (Jafarkhani and Seshadri, 2003).

To illustrate the design process, a four-state SOSTTC classic example is showed in Figure 5. For a set partitioning with BPSK, the rate of the code is one (1 bits/s/Hz). We use $C(x_1, x_2, 0)$ when departing from states zero and two, and use $C(x_1, x_2, \pi)$ when departing from states one and three. The minimum CGD of this code is 64. Similarly, for a QPSK constellation and the corresponding set partitioning, the result is a four-state SOSTTC at rate 2 bits/s/Hz, and the minimum CGD is equal to 16.

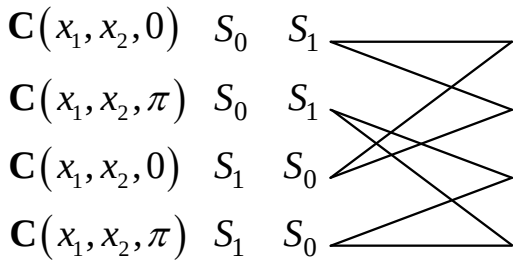

Figure 5. A four state code, $r = 1$ bit/s/Hz using BPSK or $r = 2$ bit/s/Hz using QPSK.

Note that there is a tradeoff between coding gain and the number of states. In addition, using different levels of the set partitioning to design SOSTTCs provides also a tradeoff between rate and coding gain. The code design can be extended to the case of more than two transmit antennas for not full-rate codes.

II.3 MIMO-OFDM

Recent developments in MIMO techniques promise a significant improvement in performance for Orthogonal Frequency Division Multiplexing (OFDM) systems. Broadband MIMO-OFDM systems with high bandwidth efficiencies are feasible for future Local Area Network (LAN) and Metropolitan Area Network (MAN) environments. In this section, we shall introduce a MIMO-OFDM basic concept and analyze its channel correlation properties.

II.3.1 Basic Principles of OFDM

OFDM is a modulation technique that is especially suited for transmitting high rate data in frequency selective channels. It divides the available broadband channel into N narrowband subchannels (called subcarriers or tones), that are transmitted in parallel, and easy equalized. Therefore, the symbol duration on each subcarrier becomes larger by a factor of N. OFDM separates the channels such that all carriers are orthogonal to one another, preventing interference between adjacent subcarriers. As a result, OFDM uses the spectrum much more efficiently than the conventional Frequency Division Multiple Access (FDMA). Currently, OFDM has been adopted in the IEEE802.11g and IEEE802.16e standards. OFDM is also being applied in IEEE802.20a, a standard operating at high-bandwidth connections to users moving at speeds up to 100 Km/h. OFDM symbol is generated according to spectrum required, the input data and modulation scheme to be used, commonly BPSK, QPSK or QAM.

An OFDM symbol is obtained by applying the Inverse Fast Fourier Transform (IFFT) to the the N data symbols to be transmitted. The IFFT provides a simple way to ensure subcarrier orthogonality. In order to remove the Inter Symbol

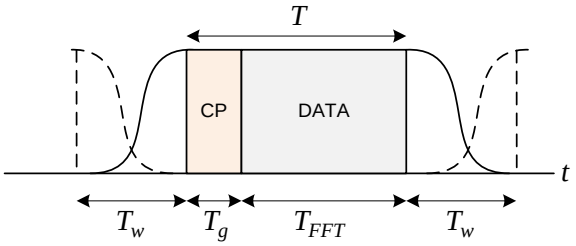

Figure 6. OFDM symbols sequence.

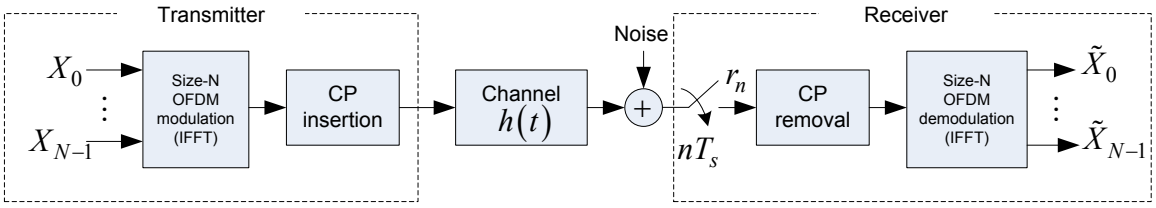

Figure 7. SISO-OFDM System Block Diagram.

Interference (ISI) which is caused by the multipath delay of the channel, it is necessary to add a guard interval to each OFDM symbol. The length of the guard interval should be equal to or greater than the delay spread of the multipath channel. This guard interval is also called cyclic prefix, and is built with the last N_{CP} samples of the OFDM symbol, and appended in front of the OFDM symbol. The cyclic prefix converts the convolution between the channel and the transmitted symbols to a circular convolution (i.e. this makes the transmitted OFDM symbols periodic), and avoid the Intercarrier Interference (ICI). The drawback of using a cyclic prefix is that it constitutes noise. As a result, there is a loss of signal-to-noise ratio, and reduced spectral efficiency. In order to reduce the out-of-band radiation due to discontinuities at the beginning or end of an OFDM symbol, a windowing is applied after cyclic prefix insertion. We can see in Figure 6 the sequence for a certain number of transmitted OFDM symbols. Figure 7 shows the block diagram of a OFDM system over a Single-Input Single-Output (SISO) channel.

Considering that in a N-tones OFDM system with a passband bandwidth B, the

complex symbols to be transmitted are denoted as $(X_{-N/2}, \ldots, X_{-1}, X_1, X_2, \ldots, X_{N/2})$. One N-tones OFDM symbol can be represented mathematically as (Jankirman, 2004)

$$s(t) = \begin{cases} \sum_{n=N/2,\ n\neq 0}^{N/2} X_n\ e^{j2\pi f_n t}, & \text{for } kT - T_w - T_g \leq t \leq kT + T_{FFT} + T_w; \\ 0 & \text{elsewhere,} \end{cases} \tag{26}$$

where f_n is the frequency of the nth subcarrier, $T_{FFT} = NT_s$ the duration of the total number of FFT-points, T_s the sampling rate, T_g the duration of the cyclic prefix, and T_w the duration of the windowing. We can replace $f_n = f_0 + n\Delta_n$, with f_0 as the center frequency (carrier) of the occupied frequency spectrum for $-N/2 \leq n \leq N/2$.

Applying the inverse operation to (26), we can demodulate the transmitted OFDM signal as:

$$x_n = \frac{1}{T_{FFT}} \int_{t=0}^{T_{FFT}} s(t) e^{-j2\pi f_n t} dt. \tag{27}$$

Since each bin of an IFFT corresponds to the amplitude and phase of a set of orthogonal sinusoids, the reverse process guarantees that the generated subcarriers are orthogonal. The orthogonality of complex signals among subcarriers is preserved by the spacing $\Delta_n = 1/T_{FFT}$, i.e.

$$\frac{1}{T_{FFT}} \int_{t=0}^{T_{FFT}} e^{-j\frac{2\pi}{T_{FFT}}(n-n')t} dt = \begin{cases} 1 & \text{for } n = n'; \\ 0 & \text{for } n \neq n'. \end{cases} \tag{28}$$

OFDM Issues

Although the OFDM modulation has several advantages over high data rate transmission, it presents also some inherent disadvantages. A major disadvantage is that the envelope is not constant, because the summation of sine waves. As a result, we have

large Peak-to-Average Power Ratio (PAPR). Theoretically, the difference of the PAPR between an OFDM system and a single carrier system is proportional to the number of tones. Large PAPR reduces the efficiency of the RF amplifiers, and results in non-linear distortion of the transmitted signal. Several techniques have been investigated to reduce the PAPR, such as clipping, windowing, peak phase shifting, coding, and so on. Due to subchannel's narrowband, OFDM is also sensitive to Doppler frequency and subcarrier offset. Because the subcarriers are closely spaced, the orthogonality among subchannels is destroyed by time variation over one OFDM symbol or subcarrier frequency offset. Consequently, there is Intercarrier Interference. If not compensated for, the ICI will result in an error floor, which increases with Doppler frequency.

II.3.2 MIMO-OFDM system

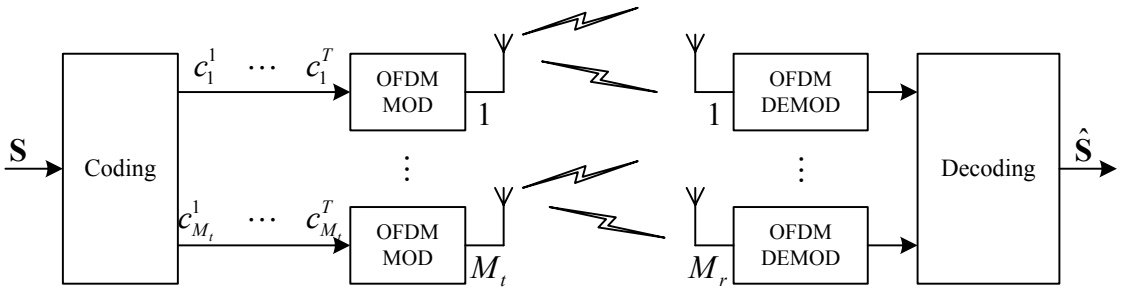

Figure 8. A simplified MIMO-OFDM system.

A MIMO-OFDM system consists of M_t transmit antennas, M_r receive antennas and a N-subcarrier OFDM modulator for each transmitting antenna, as shown in Figure 8. The incoming sequence $S = [s_1, s_2, \ldots, s_{N_s}]$ is encoding into a codeword $\boldsymbol{C} \in \mathbb{C}^{NT \times M_t}$, where s_i are modulated symbols using some modulation scheme such as QPSK. $\boldsymbol{C}$ will be transmitted through M_t transmit antennas in T OFDM symbols and it can be denoted as

$$\boldsymbol{C} = \begin{pmatrix} \mathbf{c}_1^1 & \cdots & \mathbf{c}_{M_t}^1 \\ \vdots & \ddots & \vdots \\ \mathbf{c}_1^T & \cdots & \mathbf{c}_{M_t}^T \end{pmatrix}, \tag{29}$$

where $\mathbf{c}_j^1, \mathbf{c}_j^2, \ldots, \mathbf{c}_j^T$ will be transmitted from the jth transmit antenna in OFDM symbols $1, 2, \ldots, T$, respectively. $\mathbf{c}_j^t$ is a N-length vector where $j = 1, 2, \ldots, M_t$ and $t = 1, 2, \ldots, T$.

A cyclic prefix is appended on each OFDM symbol, and the $\mathbf{c}_j^t$ will be transmitted from the jth transmit antenna at tth OFDM symbol duration. At the receiver, after removing cyclic prefix and performing FFT process, the received signal is decoding. It is possible to perform an optimal Maximum Likelihood (ML) detection if channel state information is available at the receiver.

MIMO-OFDM channel

In a MIMO-OFDM channel, the Channel Impulse Response (CIR) between the transmit antenna i and receive antenna j has L independent delay paths on each OFDM symbol and an arbitrary power delay profile. We can express the CIR as

$$h_{i,j}(t) = \sum_{l=0}^{L-1} \alpha_{i,j}(l)\delta(t - \tau_l) \tag{30}$$

where τ_l represents the l-th path delay and $\alpha_{i,j}(l)$ are the fading coefficients at delay τ_l. It is assumed that all channels have the same power-delay profile. Note that each $h_{i,j}(l)$ is a zero mean complex Gaussian random variable with variance $\frac{\sigma_l^2}{2}$ on each dimension. For normalization purposes, we assume that $\sum_{l=0}^{L-1} \sigma_l^2 = 1$ in each transmit-receive link.

With a proper cyclic prefix, a perfect sampling time, and tolerable leakage, the Channel Frequency Response (CFR), i.e. the fading coefficient for the n-th subcarrier between transmit antenna i and receive antenna j is expressed as

$$H_{i,j}(n) = \sum_{l=0}^{L-1} \alpha_{i,j}(l) e^{-j2\pi n \Delta_n \tau_l} \tag{31}$$

where Δ_n is the intersubcarrier spacing, $\tau_l = l\ T_s$ is the l-th path delay and $T_s = \dfrac{1}{N\Delta_n}$ is the sampling interval of the OFDM system.

Correlation properties

The channel path gains from neighboring subcarriers exhibit strong mutual correlations. The statistical characteristics of $H_{i,j}(n)$ by evaluating its mean, variance and auto-correlation have been extensively studied in literature. Assuming that the wireless propagation channel, established by a pair of transmit and receive antennas, has an uniform power channel model, $E\left[|\alpha_{ij}(l)|^2\right] = 1/L$, and using the known conditions, $E\left[\alpha_{ij}(l)\right] = 0$, and $E[\alpha_{ij}(l)\alpha^*_{i'j'}(l')] = 0$, $i \neq i'$, or $j \neq j'$, or $l \neq l'$, the statistical characteristics of channel were summarized by Liu and Chong (2004) as follows

$$E\left[H_{ij}(n)\right] = 0 \tag{32}$$

$$E\left[|H_{ij}(n)|^2\right] = 1 \tag{33}$$

$$\begin{aligned} R_{HH}(n, n+\Delta_n) &= E\left[H_{ij}(n) H^*_{ij}(n+\Delta_n)\right]. \\ &= \left(\frac{1}{L}\right) \frac{1 - e^{j2\pi L \Delta_n / N}}{1 - e^{j2\pi \Delta_n / N}} \end{aligned} \tag{34}$$

$i \in \{1, 2, \ldots, Mt\}$, $j \in \{1, 2, \ldots, Mr\}$, $n, \Delta_n \in \{0, 1, \ldots, N-1\}$. Note that the subcarriers are correlated, and the auto-correlation function $R_{HH}(\cdot)$ only depends on the difference of the subcarrier index Δ_n. The fade rate is slower at low number of paths and it is faster at higher number of paths, i.e., the larger the number of multipaths or time delay, the smaller the correlation between adjacent subcarriers. Therefore,

the sequence of fading coefficients along the subcarrier index Δ_n can be viewed as a wide-sense stationary narrowband complex Gaussian process. In other words, the fading channel that is established by all the consecutive subcarriers within one OFDM block can be viewed as a frequency-correlated fading channel, which is identical to the conventional time-correlated fading channel described by the well-known Jakes model (Jakes, 1974).

Figure 9 shows that for each subcarrier there are $L-1$ subcarriers that are uncorrelated with each other, and they are distributed uniformly among the N subcarriers within the interval N/L.

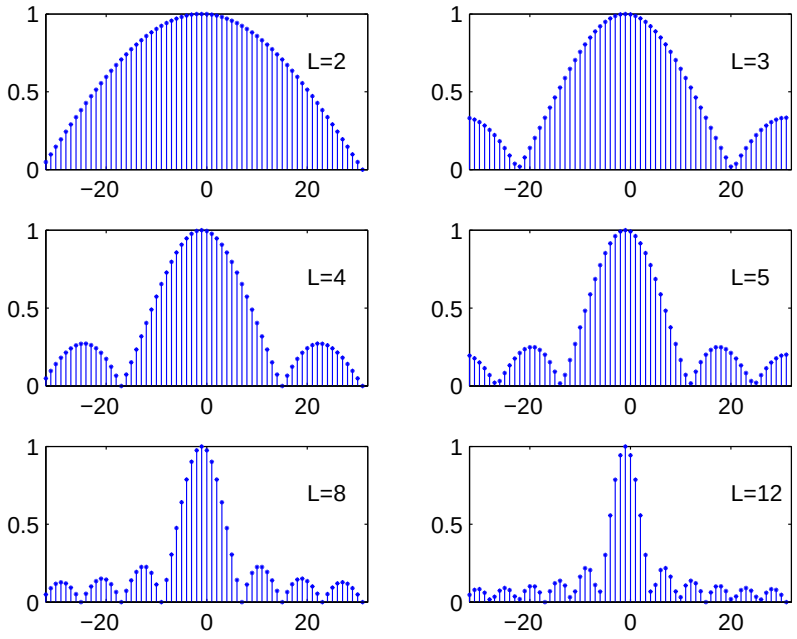

Figure 9. Correlation of a subcarrier with adjacent ones by varying the number of paths.

Currently, it is found that the channel follows an exponentially decaying power delay profile, and the average power on the lth channel tap satisfies

$$P_l = E\left[|\alpha_{ij}(l)|^2\right] = e^{-lT_s/\sigma_{\text{rms}}} \qquad 0 \le l \le L-1 \tag{35}$$

where T_s denotes the duration of a data symbol (sampling interval), σ_{rms} represents the average root-mean square delay spread, and $\sum_{l=0}^{L-1} P_l = 1$.

Liu and Jafarkhani (2007) quantify the frequency domain correlations using the exponential power delay, they showed that the correlation coefficient between two subcarriers can be calculated as

$$R_{HH}(n, n+\Delta_n) = \frac{\sum_{l=0}^{L-1} e^{\left(\frac{-T_s}{\sigma_{\text{rms}}} + \frac{j2\pi\Delta_n}{N}\right)l}}{\sum_{l=0}^{L-1} e^{\frac{-lT_s}{\sigma_{\text{rms}}}}} \tag{36}$$

where Δ_n denotes the distance between subcarriers in a OFDM symbol. Note that the key parameter in the frequency domain correlations is the root-mean square delay spread σ_{rms}.

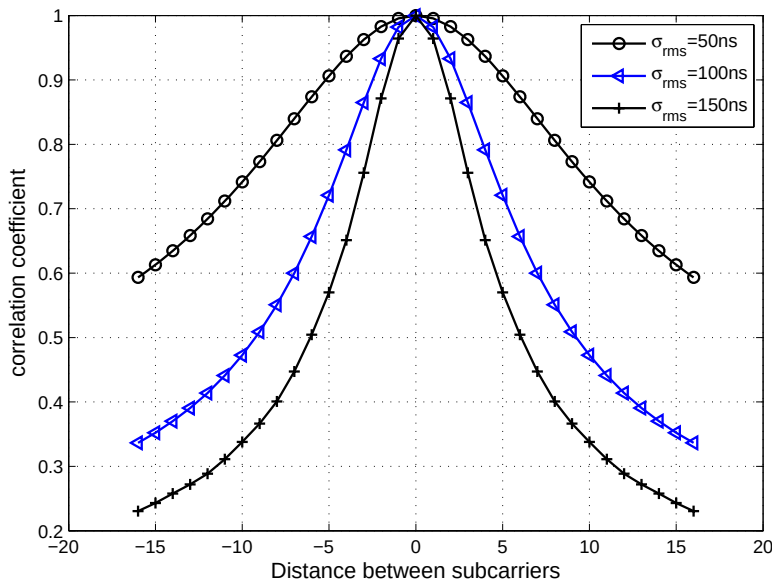

Figure 10. Inter-subcarriers correlation by varying σ_{rms}, with $N = 64$, $L = 16$ and $T_s = 50\ ns$.

Figure 10 shows that a smaller σ_{rms} will result in much stronger frequency domain correlations. Similarly, Figure 11 shows that when the number of OFDM tones N increases, the correlation between adjacent subcarriers becomes largest.

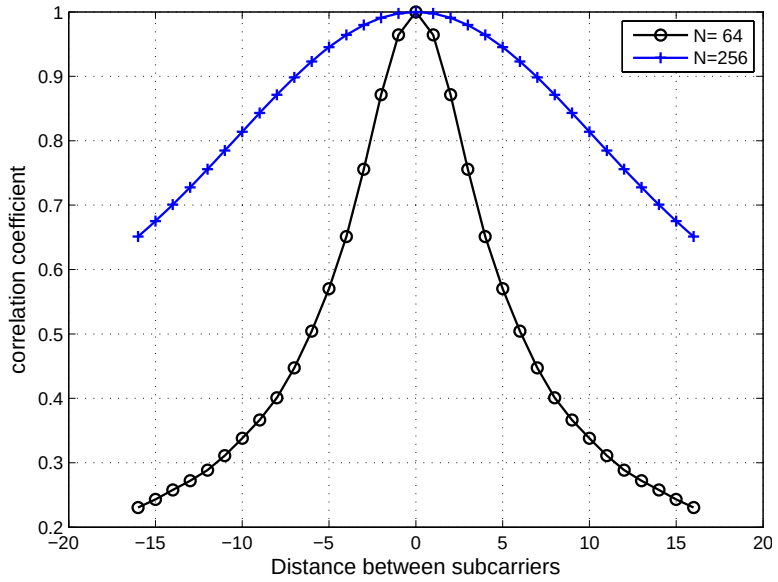

Figure 11. Inter-subcarriers correlation by varying N, with $\sigma_{\text{rms}} = 150\ ns$, $L = 16$ and $T_s = 50\ ns$.

Code rate in a MIMO-OFDM system

Let N_s be the total number of information symbols to be transmitted over NT channels, where N subcarriers are used in T times. The code rate of a coded MIMO-OFDM system can be defined as

$$R \triangleq \frac{N_s}{NT} \tag{37}$$

II.3.3 Space-Frequency Coded OFDM

A Space-Frequency (SF) coding scheme consists of coding across antennas and OFDM subcarriers. A simple way of realizing SF coding for two transmit antennas is achieved by applying the Alamouti code over two subcarriers in one OFDM symbol.

Figure 12 shows the example of Alamouti SF coding for two transmit antennas. At tth OFDM symbol duration, the two symbols to be transmitted s_1 and $-s_2^*$ are sent from subcarrier m and n at antenna 1, respectively. At the same time, s_2 and s_1^* are sent from subcarriers m and n of the OFDM symbol at antenna 2, respectively. How-

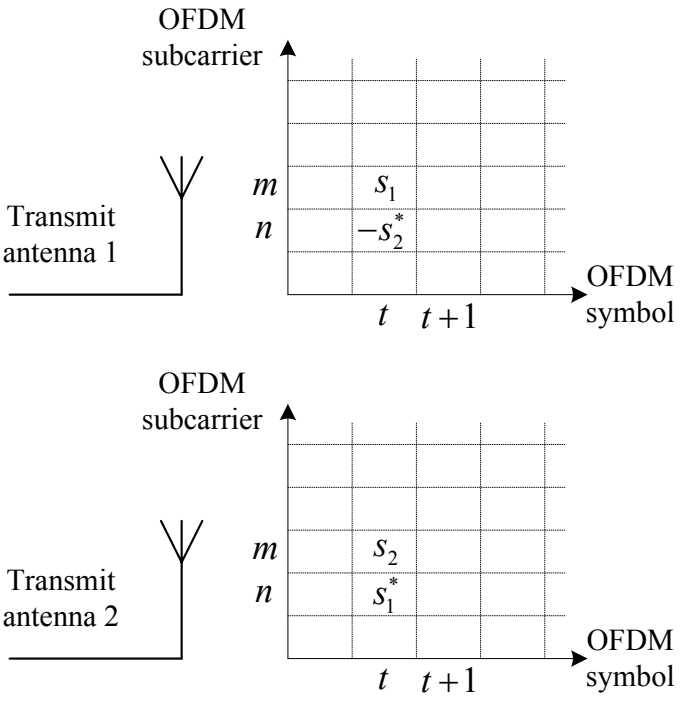

Figure 12. Rate-1 Space-Frequency coding using the Alamouti scheme.

ever, it has been shown that this SF coding approach can only achieve spatial diversity gain ($M_t M_r$), whereas the maximum diversity gain for SF coding in frequency-selective MIMO channels is $M_t M_r L$ (Liu *et al.*, 2002), where M_t is the number of transmit antennas, M_r is the number of receive antennas and L is the number of propagation paths.

II.3.4 Space-Time-Frequency Coded OFDM

In order to achieve a full diversity of $M_t M_r L\mathcal{T}$ (Lu *et al.*, 2002; Su *et al.*, 2005; Liu *et al.*, 2002) operating over MIMO-OFDM channels, where $\mathcal{T}$ is the number of independent fading blocks in the codewords. Space-Time-Frequency (STF) coding schemes spread coded symbols across different OFDM subcarriers, transmit antennas, and fading blocks.

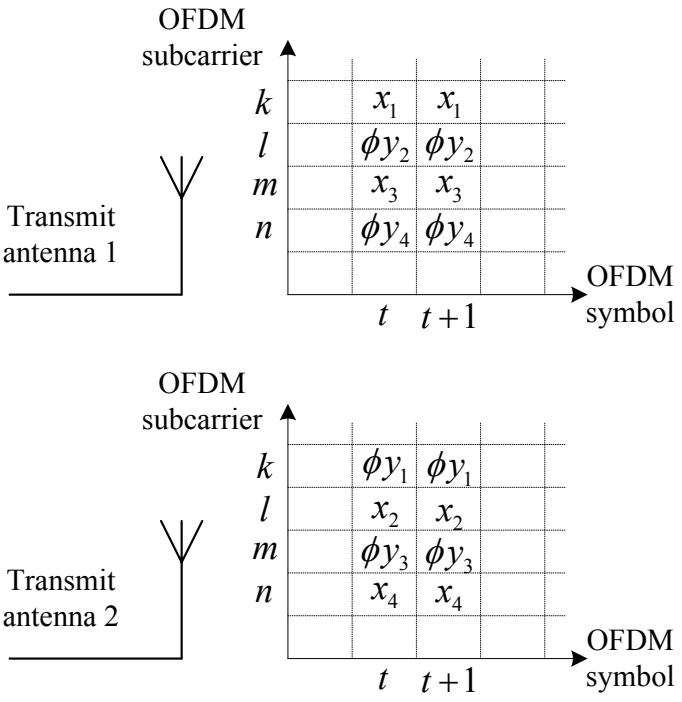

Figure 13. Rate-1 Space-Time-Frequency coding.

Figure 13 shows an example of the rate-1 STF coding structure for two transmit antennas (Zhang *et al.*, 2007). It can be seen that each layer of coded symbols are spread over space, time, and frequency dimensions. First, the vector containing the information symbols S is encoded using an algebraic rotation matrix Θ. Then, the resulting code vector $X = \Theta S$ is divided and expands on the different antennas and OFDM subcarriers. In Figure 13, the symbols to be transmitted are defined as

$$\begin{bmatrix} x_1 & x_2 & x_3 & x_4 \end{bmatrix}^T = \Theta \begin{bmatrix} s_1 & s_2 & s_3 & s_4 \end{bmatrix}^T \tag{38}$$

$$\begin{bmatrix} y_1 & y_2 & y_3 & y_4 \end{bmatrix}^T = \Theta \begin{bmatrix} s_5 & s_6 & s_7 & s_8 \end{bmatrix}^T \tag{39}$$

After interleaving the coded symbols x_i and y_i, a second layer is obtained by applying

a phase rotation ϕ to coded symbols y_i. As a result, the two layers of coded symbols can be sent as if they were transparent with each other.

Chapter III

Space-Time-Frequency Trellis Coding

III.1 Introduction

If we apply space-time codes to each subcarrier over a MIMO-OFDM system, then the frequency diversity and the correlation among different subcarriers would be ignored. As a result, the maximum possible diversity gain for the system could not be achieved. In order to achieve the maximum possible gain in such a system, one could transmit coding data over the three dimensions: space, time and frequency. Space-time-frequency coding schemes can achieve a maximum diversity gain equal to the product of the number of transmit antennas M_t, receive antennas M_r, the number of propagation paths L, and the rank of the channel temporal correlation matrix $\mathcal{T}$ ($M_t M_r L\mathcal{T}$), over a multiple-input multiple-output orthogonal frequency division multiplexing (MIMO-OFDM) system (Lu *et al.*, 2002; Su *et al.*, 2005; Liu *et al.*, 2002). There has been a lot of efforts in designing codes to obtain a high diversity for OFDM systems. This is achieved by designing space-time codes (Agrawal *et al.*, 1998; Lu and Wang, 2003), space-frequency codes (Gong and Letaief, 2003), and space-time frequency codes (Liu

et al., 2002; Aksoy and Aygölü, 2007). The code design method proposed by Su *et al.* (2005) can achieve full symbol rate and the maximum diversity order. The system derived by Agrawal *et al.* (1998) adapts the Tarokh's space-time codes to OFDM, and it becomes attractive for delay-sensitive applications. The authors in Gong and Letaief (2003) derived a coding scheme which guarantees both frequency and spatial diversity by concatenating Trellis Coded Modulation (TCM) with space-time block codes. Similarly, the scheme proposed by Lu and Wang (2003) optimizes the effective lengths for traditional TCM and employs a random interleaver to improve the system performance. In order to construct simplified designs for full-diversity group-STF trellis codes, Liu *et al.* (2002) incorporated subchannel grouping. The schemes derived by Aksoy and Aygölü (2007) can achieve a coding gain by combining super-orthogonal codes with 16, 32 and 64-state trellis structures, and OFDM. However, these proposals have several drawbacks such as not being optimized for MIMO-OFDM systems, having a low coding rate, a low power efficiency, and a low coding gain among others.

To overcome these problems, in this chapter we propose two new STF trellis coding schemes for two transmit antennas that improve the coding gain and guarantee multipath diversity in addition to spatial diversity. In order to achieve high coding gain, we incorporate in our first proposal the concept of rotated constellations shown by Zhu and Jafarkhani (2006), where the design of the original SOSTTCs from Jafarkhani and Seshadri (2003) was extended to improve their performance. However, the shortcoming of schemes derived by Zhu and Jafarkhani (2006) is that the large number of parallel transitions in their trellis structure restrict their performance in multipath channels. Hence, to achieve multipath diversity with an extended-SOSTTC, we avoided parallel transitions. We refer to the first proposal as Extended Super-Orthogonal Space-Time-Frequency Trellis Code (Ex-SOSTFTC).

Then, motivated by a need for Space-Time-Frequency trellis codes with good performance, low number of trellis states and low decoding complexity, we propose a second scheme called Quasi-Orthogonal Space-Time-Frequency Trellis Code (QOSTFTC), where we combine in a systematic way the Quasi-Orthogonal Space-Time-Frequency Block Code (QOSTFBC) derived by (Fazel and Jafarkhani, 2008) operating over a Frequency Selective Channel with two taps, with a trellis code. Although the block code from Fazel and Jafarkhani (2008) exploits the full diversity gains available in the MIMO-OFDM channel, it does not provide additional coding gain, as our proposed codes do for two transmit antennas.

Note that for this case ($L = 2$), the QOSTFBC is related to the QOSTBC with four transmit antennas proposed by Jafarkhani and Hassanpour (2005), with the difference that the QOSTFBC is implemented as a block diagonal quasi-orthogonal structure to take advantage of coding across the three dimensions (space, time and frequency).

To the best of our knowledge, there has been no previous work on Space-Time-Frequency trellis codes for two transmit antennas with parallel transitions in the trellis structure, such that both the multipath diversity and coding gain can be achieved despite parallel transitions. Furthermore, the STF trellis schemes proposed in this chapter are based on the design criteria for Space-Frequency trellis codes from Liu and Chong (2004) with appropriate arrangements, which do not need any knowledge of the channel state.

III.2 System Model

Consider a MIMO-OFDM system implemented with M_t transmit and M_r receive antennas. Each transmit antenna employs an OFDM modulator with N subcarriers. We

assume that the receiver has perfect channel knowledge while the transmitter does not know the channel. In addition, we assume no spatial fading correlation exists between antennas. In fact, if the distance among antennas is more than half the wavelength of the signal, it is frequently assumed that their path gains are independent of each other (Jafarkhani, 2005). We also assume that the CIR between the transmit antenna i and receive antenna j has L independent delay paths on each OFDM symbol and an arbitrary power delay profile, which can be expressed as

$$h_{i,j}(t) = \sum_{l=0}^{L-1} \alpha_{i,j}(l)\delta(t - \tau_l), \tag{40}$$

where τ_l represents the lth path delay and $\alpha_{i,j}(l)$ are the fading coefficients at delay τ_l. Furthermore we assume that all channels have the same power-delay profile. Note that each $\alpha_{i,j}(l)$ is a complex Gaussian random variable with zero mean and variance $\frac{\sigma_l^2}{2}$ on each dimension. For normalization purposes, we assume that $\sum_{l=0}^{L-1} \sigma_l^2 = 1$ in each transmit-receive link. In order to remove the Inter Symbol Interference (ISI) which is caused by the multipath delay of the channel, it is necessary to add a cyclic prefix to each OFDM symbol. With a proper cyclic prefix and a perfect sampling time, the CFR, i.e. the fading coefficient for the nth subcarrier between transmit antenna i and receive antenna j is given by

$$H_{i,j}(n) = \sum_{l=0}^{L-1} \alpha_{i,j}(l)e^{-j2\pi n\Delta_f \tau_l}, \tag{41}$$

where Δ_f is the intersubcarrier spacing, $\tau_l = l\ T_s$ is the lth path delay and $T_s = \frac{1}{N\Delta_f}$ is the sampling interval of the OFDM system. At the receiver, after matched filtering, removing the cyclic prefix and applying the fast Fourier transform (FFT), the signal at the nth subcarrier and antenna j is given by

$$r_j^t(n) = \sum_{i=1}^{M_t} c_i^t(n)H_{i,j}^t(n) + \mathcal{N}_j^t(n), \tag{42}$$

where $j = 1, \ldots, Mr$, and $N_j^t(n)$ is a circularly symmetric Gaussian noise term, with zero-mean and unit-variance at tth symbol period. $c_i^t(n)$ is the complex data transmitted in the tth OFDM symbol by the ith transmit antenna at the nth subcarrier, with $n = 0, \ldots, N-1$.

A general representation of a space-frequency codeword for M_t transmit antennas transmitted at the tth OFDM symbol period is given as

$$\bar{\mathbf{C}}^t = \begin{pmatrix} c_1^t(0) & c_2^t(0) & \cdots & c_{M_t}^t(0) \\ c_1^t(1) & c_2^t(1) & \cdots & c_{M_t}^t(1) \\ \vdots & \vdots & \ddots & \vdots \\ c_1^t(N-1) & c_2^t(N-1) & \cdots & c_{M_t}^t(N-1) \end{pmatrix} \in \mathbb{C}^{N \times M_t}, \tag{43}$$

where $\mathbb{C}^{n \times m}$ represents the complex field of dimension $n \times m$. $\bar{\mathbf{C}}^t$ must satisfy the power constraint $E\|\bar{\mathbf{C}}^t\|_F^2 = N$, where $\|\bar{\mathbf{C}}^t\|_F$ is the Frobenius norm of matrix $\bar{\mathbf{C}}^t$.

A STF codeword has an additional time dimension added to the above space-frequency codeword, as it is formed by T consecutive OFDM symbols, and can be represented as

$$\bar{\bar{\mathbf{C}}} = \left[\bar{\mathbf{C}}^t \ \bar{\mathbf{C}}^{t+1} \ldots \ \bar{\mathbf{C}}^T\right] \in \mathbb{C}^{N \times TM_t}. \tag{44}$$

The transmitter applies an N-IFFT to each column of the matrix $\bar{\mathbf{C}}^t$.

The overall CFR over the nth subcarrier can be represented as an $M_t \times M_r$ matrix, $\mathbf{H}(n)$, given by

$$\mathbf{H}(n) = \sum_{l=0}^{L-1} \mathbf{h}(l) e^{-j2\pi \frac{n \cdot l}{N}}, \quad n = 0, 1, \ldots, N-1, \tag{45}$$

where $\mathbf{h}(l)$ is the CIR matrix of size $M_t \times M_r$, $l = 0, \ldots, L-1$. Denoting $\mathbf{C}(n) \in \mathbb{C}^{T \times M_t}$ as the codeword to be mapping over the nth tone (before the IFFT), and $\mathbf{r}(n) \in \mathbb{C}^{T \times M_r}$ as the received matrix, the MIMO-OFDM input-output relationship can be represented

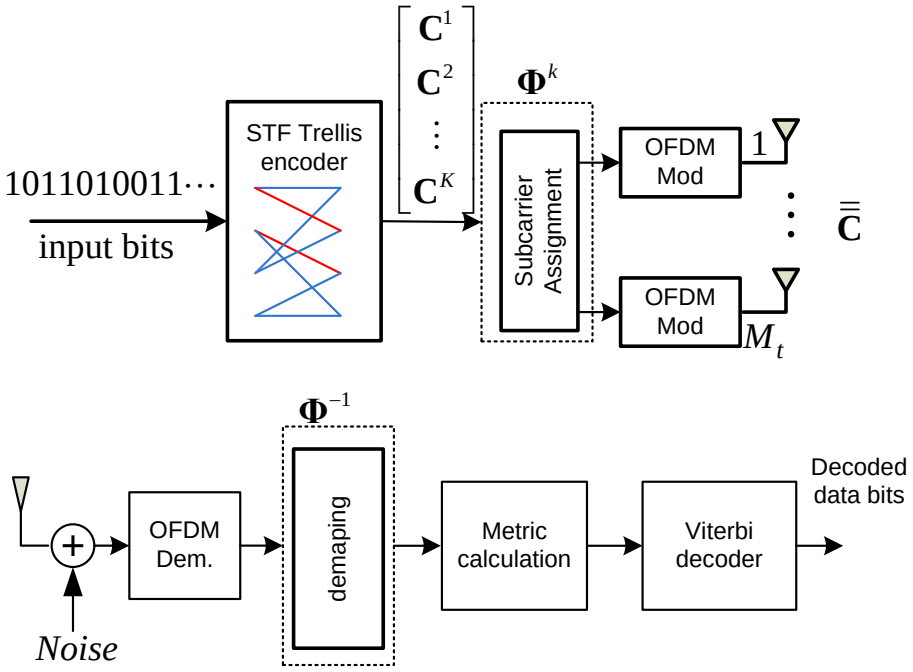

Figure 14. Transceiver model.

as follows:

$$\mathbf{r}(n) = \mathbf{C}(n)\,\mathbf{H}(n) + \mathcal{N}(n) \qquad n = 0, 1, \ldots, N-1 \tag{46}$$

where $\mathcal{N}(n) \in \mathbb{C}^{T \times M_r}$ is the noise matrix over the nth subcarrier (Liu *et al.*, 2002).

The transceiver system to be used is shown in Figure 14. The first stage of information processing in the transmitter is the trellis encoder. At the beginning of the transmission, the trellis encoding process starts in state zero. Similar to the method described by Jafarkhani and Seshadri (2003), at kth coding step, depending on the input information bits and the current state in the trellis encoder, a codeword $\mathbf{C}^k$ is selected from a constellation of possible codewords. Then, there is a transition towards the next state in the trellis, and the encoding process is performed again to obtain a frame with K codewords. The last codeword to be sent in the frame, at $k = K$, must be selected such that it merges to state zero in the trellis. After, the frame is mapped to the N subcarriers and transmitted by the M_t transmit antennas over the

frequency selective channel. As a result, a STF Trellis Code (STFTC) $\bar{\bar{\mathbf{C}}}$ is built. Next, OFDM demodulation process is performed at the receiver, and similar to the case of the SOSTTCs, a Maximum Likelihood (ML) Viterbi decoding finds the most likely valid path that starts from state zero and merges to state zero after K blocks. This process is described in more detail later in a subsequent section.

III.3 Design Criteria

Considering the channel model described in the previous section, Su *et al.* (2005) showed that the maximum achievable diversity gain by using a Space-Time-Frequency code, is equal to $LM_tM_r\mathcal{T}$, where $\mathcal{T}$ is the rank of the channel temporal correlation matrix. In order to derive the design criteria for SF trellis codes, according to the Pairwise Error Probability (PEP) and its upper bound analysis shown by Liu and Chong (2004), it is not necessary to know the multipath and delay effects of the channel. In this section, we discuss the design criteria for our proposed full diversity STFTC according to criteria derived in Liu and Chong (2004) with appropriate adjustments.

For simplicity, in the sequel, we consider a scenario with $M_t = 2$ transmit antennas. However, it is noteworthy that the method described here can be extended in a straightforward way to $M_t > 2$. We assume that the fading is quasi-static over two OFDM symbols, i.e. $\mathcal{T} = 1$. As a result of considering a quasi-static channel, the Space-Time-Frequency coding cannot provide additional temporal diversity advantage. Despite this, in such scenario we propose STFTC that provides reduced ML decoding.

Let K be the frame length and $\mathbf{C}^k$ be the branch output at the kth coding step of the trellis encoder. Let us consider that $\mathbf{C}^k$ is an Alamouti codeword (Alamouti, 1998) for two complex symbols c_1 and c_2.

Also, let $\bar{\bar{\mathbf{C}}} = [\mathbf{c}_1\ \mathbf{c}_2\ -\mathbf{c}_2^*\ \mathbf{c}_1^*] \in \mathbb{C}^{(K\times 2)\times 2}$ be the transmitted coded sequence such that, at a given symbol period, the OFDM symbol $\mathbf{c}_1 = (c_1^1 c_1^2 \ldots c_1^K)^T$ is transmitted from the first antenna, and the symbol sent from the second antenna is $\mathbf{c}_2 = (c_2^1 c_2^2 \ldots c_2^K)^T$; superscript $(\cdot)^T$ denotes the vector transpose. In the next symbol period, the OFDM symbol $-\mathbf{c}_2^*$ is transmitted from the first antenna, and the symbol transmitted from the second antenna is $\mathbf{c}_1^*$. At the receiver, a maximum likelihood decoder might decide erroneously in favor of the coded sequence $\bar{\bar{\mathbf{E}}} = [\mathbf{e}_1\ \mathbf{e}_2\ -\mathbf{e}_2^*\ \mathbf{e}_1^*]$.

As derived by Liu and Chong (2004), when the branch output is a symbol vector, the diversity order of SF trellis codes varies from rM_r to $\delta_H M_r$, where r and δ_H are the minimum rank and minimum symbol Hamming distance over all pairs of distinct coded sequences, respectively. Moreover, in order to achieve the maximum diversity $(M_t M_r L)$, it is a necessary condition that $\delta_H \geq M_t L$. Unlike Liu and Chong (2004), in our proposed STFTCs the branch output is an orthogonal matrix.

Let $\mathbf{D}^k = \mathbf{C}^k - \mathbf{E}^k$ be a branch difference matrix between $\mathbf{C}^k$ and $\mathbf{E}^k$, where $\mathbf{C}^k$ and $\mathbf{E}^k$ denote the kth codeword in coded sequence $\bar{\mathbf{C}}$ and $\bar{\mathbf{E}}$, respectively. A codeword distance matrix is defined as

$$\mathbf{A}^k = (\mathbf{D}^k)^H \mathbf{D}^k, \tag{47}$$

where $(\cdot)^H$ denotes the transpose conjugate.

Next, we define $\rho(\bar{\mathbf{C}}, \bar{\mathbf{E}})$ as the set of instances $1 \leq k \leq K$ at which $\mathbf{C}^k \neq \mathbf{E}^k$, and δ_H as the number of elements in $\rho(\bar{\mathbf{C}}, \bar{\mathbf{E}})$.

If $\mathbf{A}^k$ is a rank-two matrix for all $k \in \rho(\bar{\mathbf{C}}, \bar{\mathbf{E}})$, it can be shown that the diversity takes values from $2M_r$ to $2M_r\delta_H$, and the maximum achievable diversity order of the proposed STFTCs over any FSC with two transmit antennas and L independent taps

is

$$G_{d_{\max}} = 2M_r \cdot \min\{\delta_H, L\} \tag{48}$$

Furthermore, the distance criterion derived by Liu and Chong (2004) can be rewritten as the maximization of the minimum product of the coding gain distance CGD and the modified product distance MPD, which we denote as

$$\text{maximize}\left\{\min\left(CGD \cdot MPD\right)\right\}, \tag{49}$$

where

$$CGD = \det\left(\sum_k \mathbf{A}^k\right), \tag{50}$$

$$MPD = \prod_k \left(1 + \left\|\mathbf{D}^k\right\|_F^2\right), \tag{51}$$

and $k \in \rho(\bar{\mathbf{C}}, \bar{\mathbf{E}})$.

Note that the above design criteria do not need any knowledge of the channel delay profiles. Nevertheless, a small number of multipaths or a short root-mean square delay spread (τ_{rms}) produces a strong frequency domain correlation so both the diversity and coding gain can be degraded. Hence, in order to eliminate the dependence on the channel delay profiles, it is common to use an interleaver between a trellis encoder and an OFDM modulator to achieve reasonable robust code performance (Lu and Wang, 2003).

Consequently, the following design steps are proposed:

1. Perform set partitioning for the available codewords analogous to SOSTTC's set partitioning. The set partitioning metric is the product $CGD \cdot MPD$ over all possible pairs of distinct codewords.

2. Expand the available codewords constellation as necessary to design full-rate STFTCs.

3. Codewords that do not belong to the same codewords constellation are assigned to different states. Moreover, assign codewords diverging from (or merging into) a state such that $\mathbf{A}^k$ must have full rank, and all pairs of codewords diverging from or merging to a state must be separated by the largest product $CGD \cdot MPD$.

4. In order to achieve the multipath diversity provided by the channel, $\delta_H \geq L$ must be satisfied. It can be shown that the coding gain increases when δ_H is increased.

In the next sections, we present two STF trellis coding schemes, using the above design criteria, to achieve rate-one, high coding gain and multipath diversity.

III.4 Extended Space-Time-Frequency Trellis Codes

In this section we propose the Ex-SOSTFTCs such that, in order to increase the minimum δ_H and to achieve the channel multipath diversity, parallel transitions are avoided. Moreover, the distance matrix $\mathbf{A}^k$ is full-rank over all pairs of codewords.

III.4.1 Codeword structure

In order to exploit the rich diversity resources in a wideband channel, it has been shown that two critical design parameters (for a trellis code over a MIMO-OFDM system) are the effective length δ_H and the use of random interleaving. Furthermore, the code performance depends on both code structure and the channel profile. The code structure for our proposed codes is as follows.

Besides the rotation parameter θ, let ϕ be an extra-rotation parameter between zero and 2π in the original SOSTTCs as proposed in (Zhu and Jafarkhani, 2006). Let us set $\theta = 0$, assuming that space goes horizontally and different rows are transmitted at consecutive OFDM symbols, we define the kth codeword to be transmitted at subcarrier $k = 1, 2, \ldots, N$ as

$$\mathbf{C}^k(x_1, x_2, \phi) = \begin{pmatrix} x_1 e^{j\phi} & x_2 e^{j\phi} \\ -(x_2 e^{j\phi})^* & (x_1 e^{j\phi})^* \end{pmatrix} \tag{52}$$

where $x_i = e^{j\frac{2\pi}{M}m}$ represents an M-Phase Shift Keying (M-PSK) symbol, and $m = 0, 1, \ldots, M-1$ represents the index of the symbols for an M-PSK constellation with size $M = 2^b$. Note that $2b$ data bits go into the trellis encoder in each coding step, and an Ex-SOSTFTC consists of $K = N$ codewords $\mathbf{C}^k$.

III.4.2 Set partitioning

Let S be the set of all possible codewords $\mathbf{C}(x_1, x_2, \phi)$ to be transmitted with a cardinality of $|S| = M^2$. In order to design a trellis code, first we do the partition of the set S by following the general method derived by Jafarkhani and Seshadri (2003), such that the product $(CGD \cdot MPD)$ between codeword pairs at each level is maximum.

Figure 15 shows the set partitioning for a QPSK constellation, where $R = 2$ bit/s/Hz with $Mt = 2$. Note that the pairs of numbers at the leaves of the tree represent the indices of the symbols QPSK to be transmitted at kth coding step in the codeword $\mathbf{C}^k(x_1, x_2, \phi)$. Moreover, a codeword construction example is illustrated at the bottom of Figure 15. On the right side of the Figure 15, we can see both the maximum CGD and MPD between subsets at each nivel of the partitioning tree.

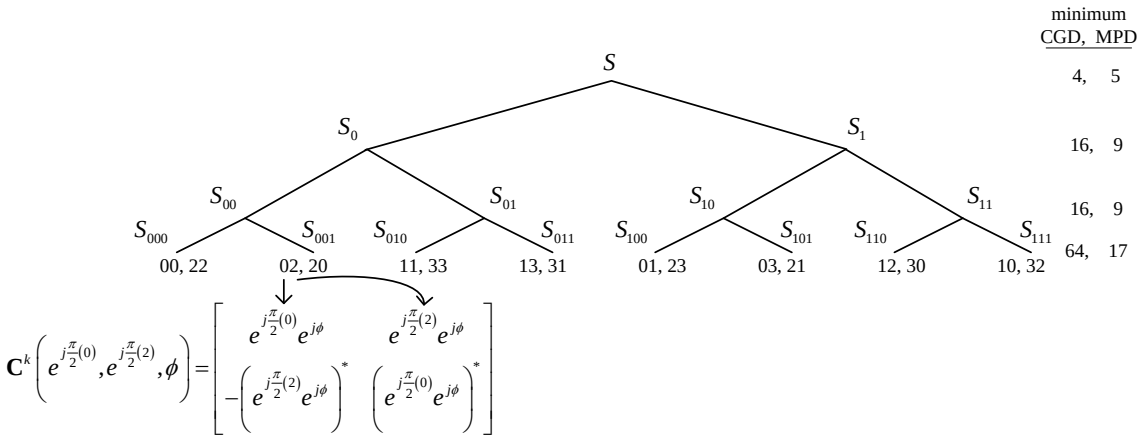

Figure 15. Set partition for QPSK using two transmit antennas.

III.4.3 Design of Ex-SOSTFTCs

In this subsection, we show how to use the set partitioning derived in previous section to design trellis codes. In order to increase the system performance in multipath channels, we avoid the parallel transitions constraint, such that for a rate of b bits/(s Hz), at least M^2 states are needed in the trellis structure for Ex-SOSTFTC.

An example for a 16-state Ex-SOSTFTC with QPSK is presented in Figure 16. For the sake of brevity, we denote $\tilde{S}_i = S_{\text{xxxx}}$, where $0 \leq i \leq 15$ and x can be 0 or 1, for the subsets given in the Figure 15. An optimal rotation parameter value that maximizes the minimum product ($CGD \cdot MPD$) for Ex-SOSTFTC with QPSK, shown in Figure 16 is $\phi = \frac{\pi}{4}$.

From Figure 16, any valid codeword starts from state one and ends at state one. Due to the structure of the trellis, two codewords may differ in 2 o more trellis transitions. Then, the smallest number of transitions (coding steps) is 2. Considering that the path of an Ex-SOSTFTC codeword called $\mathbf{C}$ stays in state one during both transitions, i.e. the path $1 \to 1 \to 1$, the corresponding codewords to be sending are

$$C^1(e^{j\frac{\pi}{2}(0)}, e^{j\frac{\pi}{2}(0)}, \phi = 0),\ C^2(e^{j\frac{\pi}{2}(0)}, e^{j\frac{\pi}{2}(0)}, \phi = 0) \tag{53}$$

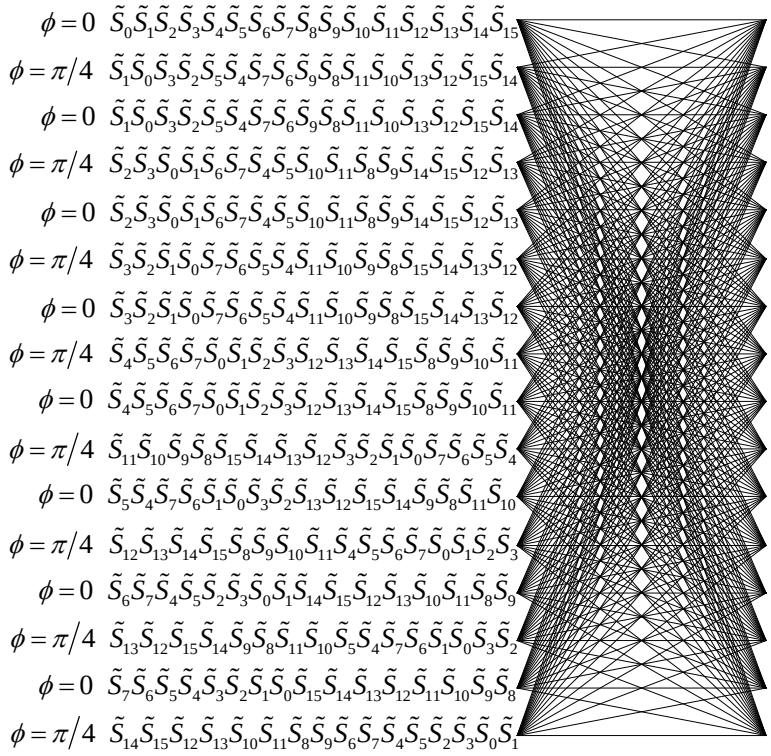

Figure 16. A 16-state Ex-SOSTFTC at rate of 2 bits/s/Hz using QPSK.

Then, by analyzing another posible codewords $\mathbf{E}$ to be transmitted in two transitions, we get that the minimum product $CGD \cdot MPD$ of the 16-state codeword in two transitions is 36×45, which is obtained if codeword $\mathbf{E}$ follows the paths $1 \rightarrow 9 \rightarrow 1$, $1 \rightarrow 11 \rightarrow 1$, or $1 \rightarrow 13 \rightarrow 1$.

Figure 17 illustrates the case when $\mathbf{E}$ goes through $1 \rightarrow 9 \rightarrow 1$. From Figure 16, we can see that the codewords to be transmitted in $\mathbf{E}$ are $\tilde{S}_8$ and $\tilde{S}_4$, and those are expressed as

$$E^1(e^{j\frac{\pi}{2}(0)}, e^{j\frac{\pi}{2}(1)}, \phi = 0),\ E^2(e^{j\frac{\pi}{2}(1)}, e^{j\frac{\pi}{2}(1)}, \phi = 0) \tag{54}$$

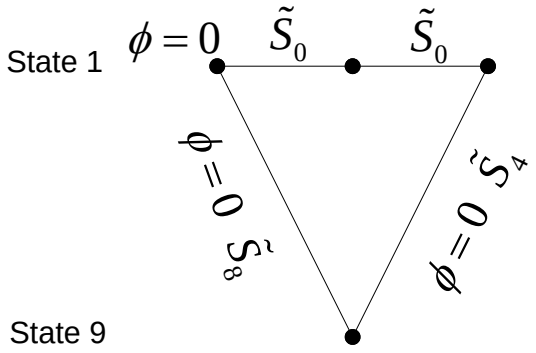

Figure 17. Two typical paths differing in 2 transitions.

The minimum product $CGD \cdot MPD$ for this case is calculated as follows:

$$\begin{aligned} D^1 &= C^1 - E^1 \\ D^2 &= C^2 - E^2 \\ A^1 &= (D^1)^H D^1 \\ A^2 &= (D^2)^H D^2 \end{aligned}$$

$$CGD = \det\left(A^1 + A^2\right) = 36 \tag{55}$$

$$MPD = \left(1 + \|D^1\|^2\right)\left(1 + \|D^2\|^2\right) = 45 \tag{56}$$

Moreover, considering that a codeword $\mathbf{C}$ stays in state one during three transitions, the minimum product $CGD \cdot MPD$ achieved by the proposed codeword is still 36×45. This is true for a codeword $\mathbf{E}$ going through the paths $1 \to 9 \to 5 \to 1$, $1 \to 11 \to 6 \to 1$, or $1 \to 13 \to 7 \to 1$. We can continue a similar analysis for more than 3 transitions, but it can be seen that the minimum product occurs in the case of 2 transitions.

In summary, the proposed 16-state code in Figure 16 has a minimum product $CGD \cdot MPD$ of 36×45 and a $\delta_H = 2$. Therefore, the maximum achievable diversity is $2M_r \cdot \min(2, L)$.

Full diversity Ex-SOSTFTCs with high coding gain can be systematically designed using both, the corresponding set partitioning and the design rules described above for different rates and different number of states.

III.4.4 Decoding of Extended-STF Trellis Codes

Next, let us describe the structure of the decoder. To find the most likely valid path in the trellis, we use a Viterbi algorithm for the Maximum Likelihood decoding of Ex-SOSTFTCs. Assuming that the channel is quasi-static over two OFDM symbols duration and perfect channel state information at the receiver. Let $\mathbf{H}(n)$ be the channel matrix during the transmission of codeword $\mathbf{C}^k$, and $\mathbf{y}(n)$ the received signal at two consecutive OFDM symbols over the nth subcarrier. The Maximum-Likelihood (ML) decoding rule is given by

$$\hat{\hat{\mathbf{C}}} = \arg \min_{(x_1,x_2)} \sum_{n=1}^{N} \|\mathbf{y}(n) - \mathbf{C}^n \mathbf{H}(n)\|_F^2 \tag{57}$$

Since the channel is quasi-static over two adjacent OFDM symbols, there are no temporal diversity gains offered by the channel, and there is a delay of two OFDM symbols associated with the decoding procedure. However, the decoding complexity of the Ex-SOSTFTCs is reduced.

III.5 Quasi-Orthogonal Space-Time-Frequency Trellis Codes

In what follows, we propose high-coding gain QOSTFTCs for two transmit antennas. Generally speaking, it is very difficult to prevent parallel trellis transitions from happening, specially for systems with a large number of transmit antennas and/or a high

order constellation modulation. However, the proposed QOSTFTCs have a reduced number of states in the trellis with parallel transitions, because it is possible to use an adequate full-rank codeword structure containing δ_H independent orthogonal matrices, such that the multipath diversity and coding gain can be increased despite the parallel transitions. First we define the codeword structure of a quasi-orthogonal STF code for two transmit antennas by assuming a 2-ray channel model. Afterwards we study the set partitioning using BPSK and QPSK constellations. Then we design full space and frequency diversity QOSTF trellis codes with high coding gain without sacrificing the rate of the code.

III.5.1 Codeword structure

Let us assume a 2-ray channel model. Then, we rearrange the general class of QOSTBCs given by the equation (19) in the codeword matrix

$$\mathbf{G}^k = \frac{1}{\sqrt{2}} \begin{pmatrix} x_1 + \widetilde{x}_3 & x_2 + \widetilde{x}_4 \\ -(x_2 + \widetilde{x}_4)^* & (x_1 + \widetilde{x}_3)^* \\ x_1 - \widetilde{x}_3 & x_2 - \widetilde{x}_4 \\ -(x_2 - \widetilde{x}_4)^* & (x_1 - \widetilde{x}_3)^* \end{pmatrix} \in \mathbb{C}^{4\times 2} \tag{58}$$

where space goes horizontally, (x_1, x_2) belong to a M-PSK constellation $\mathcal{A}$ and $(\tilde{x}_3, \tilde{x}_4)$ belong to the rotated constellation $\mathcal{A}e^{j\phi}$. From Table I, the optimal rotation parameter is $\phi = \pi/M$ since it provides the maximum coding gain for the code in (58) (Fazel and Jafarkhani, 2008). With QPSK, $2 \times 2b = 8$ data bits will be feed to the QOSTF trellis encoder in each coding step and these bits select a codeword from the 256 possible codewords. It is noteworthy that by rearranging the general class of QOSTBCs derived in equation (19), such that $\mathbf{G}^k \in \mathbb{C}^{2L\times 2}$ in (5), the method described here can be extended in a straightforward way to $L > 2$.

III.5.2 Set partitioning

Next, we provide a complete study of set partitioning for BPSK and QPSK constellations for two transmit antennas and $L = 2$.

Let $\mathbf{G}_1^k(x_1, x_2, \tilde{x}_3, \tilde{x}_4)$ and $\mathbf{G}_2^k(y_1, y_2, \tilde{y}_3, \tilde{y}_4)$ be two codewords as defined in (58), full diversity is achieved if the CGD given as

$$\begin{aligned} \mathrm{CGD}(\mathbf{G}_1^k, \mathbf{G}_2^k) = \frac{1}{4}\Bigg(\sum_{i=1}^{2} |(x_i - y_i) + (\widetilde{x}_{i+2} - \widetilde{y}_{i+2})|^2 + \\ |(x_i - y_i) - (\widetilde{x}_{i+2} - \widetilde{y}_{i+2})|^2\Bigg)^2 \end{aligned} \tag{59}$$

is not zero. If the CGD becomes zero, then both two terms in Eq. (59) must be zero; this happens when $x_i = y_i$. Note that by rotating (x_1, x_2) instead of (x_3, x_4) results in a code with similar properties and the full diversity is still valid.

For this case, the total number of different codewords $\mathbf{G}$ to be partitioned is M^{2L}, and the total pairwise combinations $(\mathbf{G}_1, \mathbf{G}_2)$ with $\det(A(\mathbf{G}_1, \mathbf{G}_2)) \neq 0$ is given by the binomial coefficient $\binom{M^{2L}}{2}$. By performing an exhaustive search, we can find the best set partitioning for a given set. The minimal product $CGD \cdot MPD$, between codewords at each level of an optimal set partitioning, must be maximum. Such an exhaustive search may be time consuming for large constellations. However, since it is done once and only to design the codes, the high complexity may be acceptable.

Figure 18 shows the set partitioning for BPSK, where the first two index correspond to the symbols x_1 and x_2, and the last two index represent the symbols x_3 and x_4. The rotation is $\phi = \frac{\pi}{2}$ and $0, 1$ represent $1, -1$, respectively. Also, $(\tilde{x}_3, \tilde{x}_4) \in e^{j\phi}\mathcal{A} = \{j, -j\}$, after applying the rotation ϕ.

Note that all possible combinations of input symbols using the indexes $0, 1$ are showed in the branches of the set partitioning for BPSK ($M = 2$) in Figure 18. We

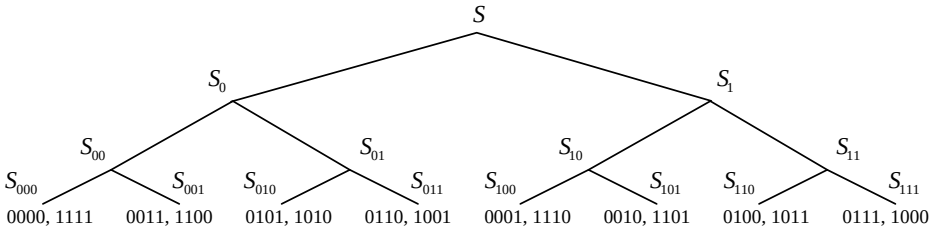

Figure 18. Set partitioning for BPSK.

can use this property to perform set partitioning when $M = 4$. Figure 19 shows the combination pattern that follows the BPSK set partitioning.

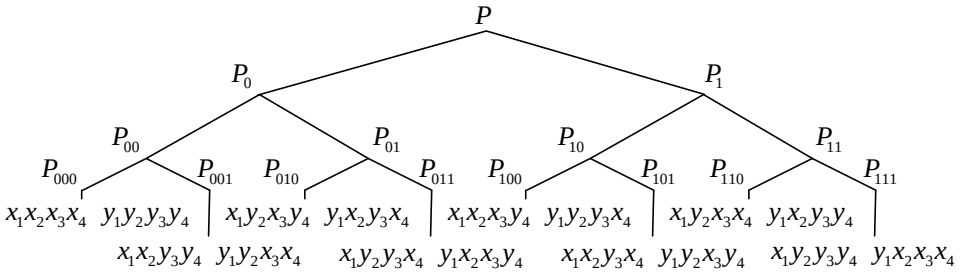

Figure 19. Set partitioning pattern follows with $M = 2$.

The procedure to extend this pattern to a QPSK constellation using two transmit antennas is as follows: First let us consider that the QPSK symbols $\{1, j, -1, -j\}$ in a codeword $\mathbf{G}$ are represented by the indices $m = 0, 1, 2$ and 3, respectively. Next, let us consider all posible codewords $\mathbf{G}$ containing only the indices $0, 1$, i.e. $2^4 = 16$ codewords. Then, we apply the partition pattern horizontally as described in Fig. 19. As an example, the pattern sequence $x_1x_2x_3x_4$ correspond to the indices 0000, the pattern $y_1y_2y_3y_4$ to the indices 1111, $x_1x_2y_3y_4$ to 0011, and so on. Afterward, for each one of these codewords, we calculate its corresponding codeword that maximizes the code gain distance between them. As an example, the CGD between codewords formed with the indices 0000 and 2222 is 256, and so on for all combination pairs. Then, we apply the pattern vertically by considering each quadruplet pair as a new $\{x_1x_2x_3x_4,\ y_1y_2y_3y_4\}$ pair, and thus increase the number of elements in a subset by a

Table II. Example of a vertical expansion to construct a new subset.

Pattern	Indices
$x_1x_2x_3x_4$	0000
$y_1y_2y_3y_4$	2222
$x_1x_2y_3y_4$	0022
$y_1y_2x_3x_4$	2200
$x_1y_2x_3y_4$	0202
$y_1x_2y_3x_4$	2020
$x_1y_2y_3x_4$	0220
$y_1x_2x_3y_4$	2002
$x_1x_2x_3y_4$	0002
$y_1y_2y_3x_4$	2220
$x_1x_2y_3x_4$	0020
$y_1y_2x_3y_4$	2202
$x_1y_2x_3x_4$	0200
$y_1x_2y_3y_4$	2022
$x_1y_2y_3y_4$	0222
$y_1x_2x_3x_4$	2000

factor of 16. Table II shows the subset formed by vertically apply the partition pattern by considering the codewords $x_1x_2x_3x_4 = 0000$ and $y_1y_2y_3y_4 = 2222$.

Therefore, we obtain 16 subsets with 16 codeword pairs each one. We show this partial set partitioning in Table III.

Finally, one must verify that the new subset contains the maximum code gain distance at each level of set partitioning by switching some subsets as needed. As an example, from Table III, the minimum CGD between the subsets P_{xxxx0} and P_{xxxx1} is 16, where x can be 0 or 1. It appears that it is necessary to exchange some subsets between these subsets to achieve a maximum CGD. In the set P_0 we need to switch subsets P_{00001} with P_{00011}, $P_{00101} \leftrightarrow P_{00111}$, $P_{01001} \leftrightarrow P_{01011}$ and $P_{01101} \leftrightarrow P_{01111}$. Similarly, in the set P_1 the subsets that must be switched are P_{10001} with P_{10011}, $P_{10101} \leftrightarrow P_{10111}$, $P_{11001} \leftrightarrow P_{11011}$ and $P_{11101} \leftrightarrow P_{11111}$. By doing so, the minimum code gain distance increases from 16 to 64 between the new subsets S_{xxxx0} and S_{xxxx1}.

Table III. Partial set partitioning for QOSTBCs with QPSK.

P																
P_0								P_1								
P_{00}				P_{01}				P_{10}				P_{11}				
P_{000}		P_{001}		P_{010}		P_{011}		P_{100}		P_{101}		P_{110}		P_{111}		
P_{0000}	P_{0001}	P_{0010}	P_{0011}	P_{0100}	P_{0101}	P_{0110}	P_{0111}	P_{1000}	P_{1001}	P_{1010}	P_{1011}	P_{1100}	P_{1101}	P_{1110}	P_{1111}	
0000	1111	0011	1100	0101	1010	0110	1001	0001	1110	0010	1101	0100	1011	0111	1000	
2222	3333	2233	3322	2323	3232	2332	3223	2223	3332	2232	3323	2322	3233	2333	3222	
0022	1133	0033	1122	0123	1032	0132	1023	0023	1132	0032	1123	0122	1033	0133	1022	
2200	3311	2211	3300	2301	3210	2310	3201	2201	3310	2210	3301	2300	3211	2311	3200	
0202	1313	0213	1302	0303	1212	0312	1203	0203	1312	0212	1303	0302	1213	0313	1202	
2020	3131	2031	3120	2121	3030	2130	3021	2021	3130	2030	3121	2120	3031	2131	3020	
0220	1331	0231	1320	0321	1230	0330	1221	0221	1330	0230	1321	0320	1231	0331	1220	
2002	3113	2013	3102	2103	3012	2112	3003	2003	3112	2012	3103	2102	3013	2113	3002	
0002	1113	0013	1102	0103	1012	0112	1003	0003	1112	0012	1103	0102	1013	0113	1002	
2220	3331	2231	3320	2321	3230	2330	3221	2221	3330	2230	3321	2320	3231	2331	3220	
0020	1131	0031	1120	0121	1030	0130	1021	0021	1130	0030	1121	0120	1031	0131	1020	
2202	3313	2213	3302	2303	3212	2312	3203	2203	3312	2212	3303	2302	3213	2313	3202	
0200	1311	0211	1300	0301	1210	0310	1201	0201	1310	0210	1301	0300	1211	0311	1200	
2022	3133	2033	3122	2123	3032	2132	3023	2023	3132	2032	3123	2122	3033	2133	3022	
0222	1333	0233	1322	0323	1232	0332	1223	0223	1332	0232	1323	0322	1233	0333	1222	
2000	3111	2011	3100	2101	3010	2110	3001	2001	3110	2010	3101	2100	3011	2111	3000	

Figure 20 shows the final set partitioning with QPSK when $\phi = \pi/4$, where the minimum CGD and the minimum MPD between subsets S_0 and S_1 is 4 and 9, respectively..

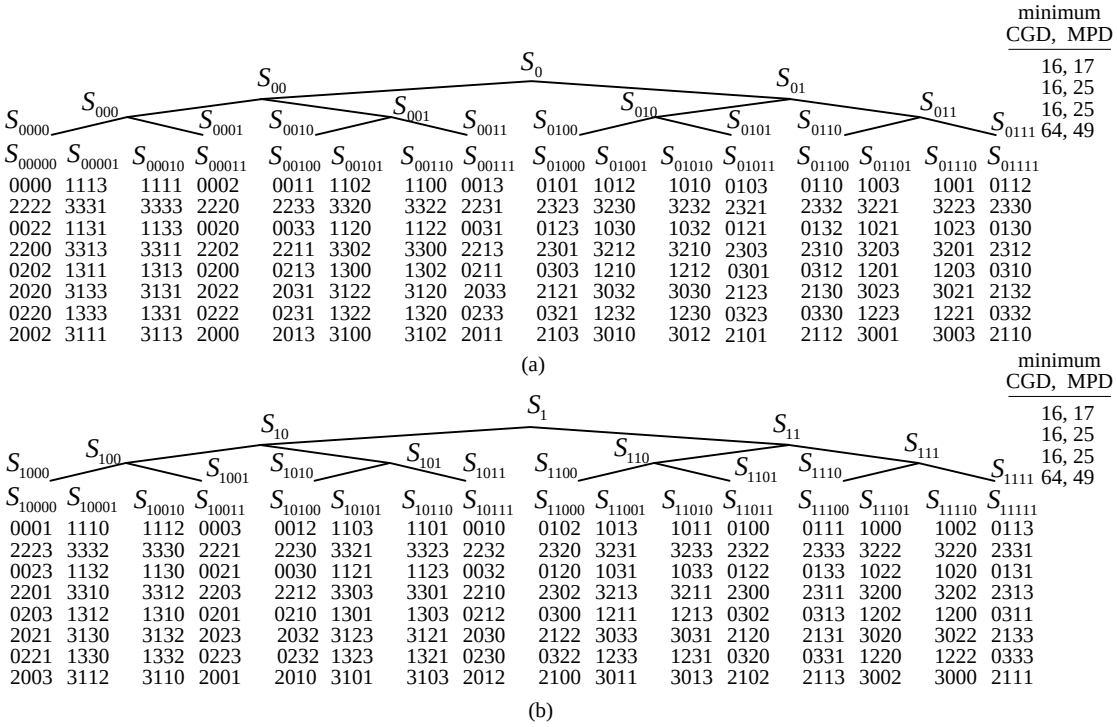

Figure 20. Final set partitioning using QOSTBCs with QPSK.

III.5.3 QOSTFTCs design

Due to the symmetry of the codeword defined by Equation (58), if we now rotate (x_1, x_2) instead of $(\tilde{x}_3, \tilde{x}_4)$, i.e. $(x_1, x_2) \in \mathcal{A}e^{j\phi}$ and $(\tilde{x}_3, \tilde{x}_4) \in \mathcal{A}$, it results in a code with similar properties and the full diversity is still achieved. This will give us a new degree of freedom and additional constellation matrices to pick from. In order to expand the constellation of matrices, let ϕ_1 and ϕ_2 be the rotation angles for the symbols (x_1, x_2) and $(\tilde{x}_3, \tilde{x}_4)$, respectively. Then, we set $(\phi_1 = 0, \phi_2 = \pi/4)$, or $(\phi_1 = \pi/4, \phi_2 = 0)$ with QPSK. For the sake of brevity, let $c_1^k = x_1 + \tilde{x}_3$, $c_2^k = x_2 + \tilde{x}_4$, $c_3^k = x_1 - \tilde{x}_3$ and

$c_4^k = x_2 - \tilde{x}_4$ be the transmitted symbols at the kth ($k = 1, \ldots, N/2$) codeword. The proposed QOSTFTC is defined as

$$\mathbf{C}_{STF} = \frac{1}{\sqrt{2}} \begin{bmatrix} c_1^1 & c_2^1 & -c_2^{1*} & c_1^{1*} \\ c_3^1 & c_4^1 & -c_4^{1*} & c_3^{1*} \\ c_1^2 & c_2^2 & -c_2^{2*} & c_1^{2*} \\ c_3^2 & c_4^2 & -c_4^{2*} & c_3^{2*} \\ \vdots & \vdots & \vdots & \vdots \end{bmatrix} \in \mathbb{C}^{N \times 2 \times 2}. \tag{60}$$

Following the design criteria and the set partition given in Figure 20, Figure 21 shows the proposed 2 and 4-state QOSTFTCs with QPSK.

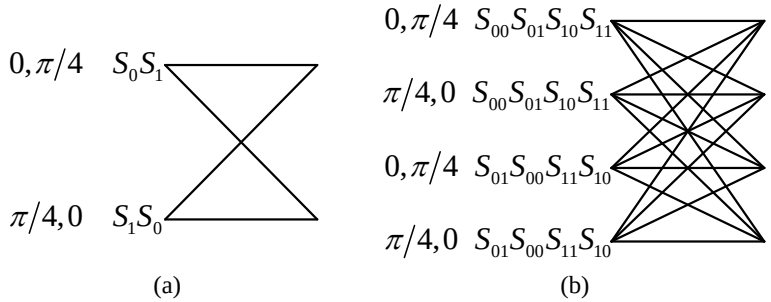

Figure 21. 2-state and 4-state QOSTFTCs at rate of 2 bits/s/Hz using QPSK.

Similar to 4-state QOSTFTC, we use a simple systematic design method to assign the subsets in the proposed 16-state QOSTFTC, which is illustrated in Figure 22. For the sake of brevity, we represent $\tilde{S}_{\text{decimal}} = S_{\text{xxxx}}$, where S_{xxxx} represents the subsets given in Fig. 20, and x can be 0 or 1. Note that in general, we use a simple systematic design method to assign the subsets in the trellis, and that $2 \times 2b = 8$ data bits are input to the QOSTF trellis encoder in each coding step and these bits pick a codeword up from 256 possible codewords.

Due to the independence of the Alamouti elements in the sub-blocks of (58), the proposed QOSTFTCs provide a minimum $\delta_H = 2$ and a diversity identical to that of

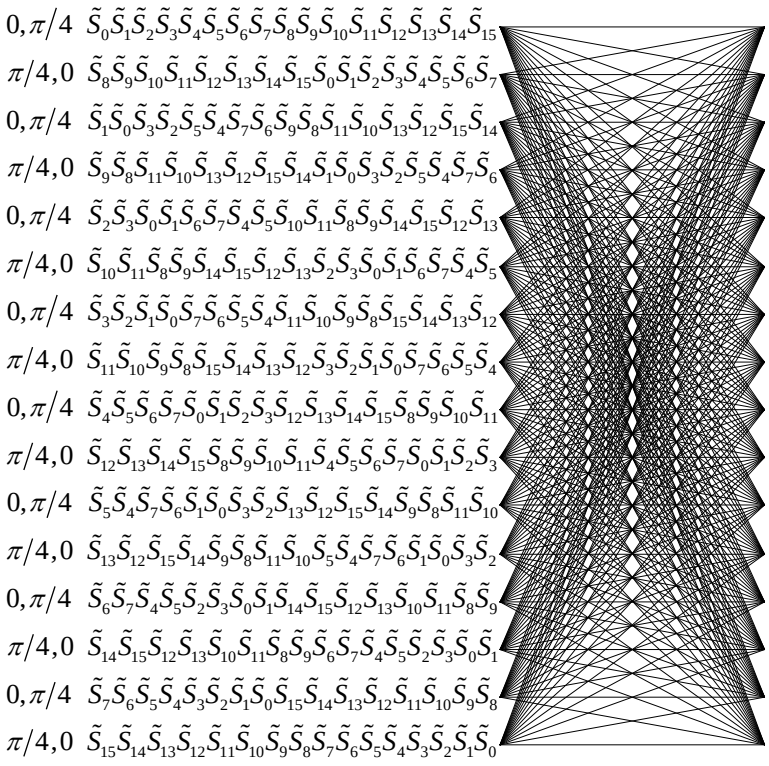

Figure 22. A 16-state QOSTFTC at rate of 2 bits/s/Hz using QPSK.

the proposed 16-state Ex-SOSTFTC. For the 2-state code in Fig. 21(a), the minimum product $CGD \cdot MPD$ for the paths with 2 or more transitions is more than the minimum product for parallel transitions. Therefore, the minimum $CGD \cdot MPD$ of the 2-state code is 16×17. For the 4-state code in Fig. 21(b), the minimum product is 16×25 which is also dominated by the parallel transitions. Similarly, for the 16-state QOSTFTC, the minimum product $CGD \cdot MPD$ is 64×49.

III.5.4 Decoding of QOSTF Trellis Codes

In what follows, we provide details of the decoding procedure for the code in (60). We assume perfect channel state information at the receiver. For simplicity, we assume

a single receive antenna. Let $\mathbf{h}[n] = [H_1(n)\ H_2(n)]^T$ be the channel gain vector between transmit antennas and the single-receive antenna at nth subcarrier. Also let $\mathbf{y}[n] = [r^1(n)\ r^2(n)]^T$ be the received signal at two consecutive OFDM symbols at nth subcarrier. The Viterbi algorithm is used for the ML decoding of QOSTFTC and solves the minimum from the accumulated branch metric along the survivor paths as:

$$\begin{aligned}\hat{\tilde{\mathbf{C}}} = \underset{\{c_1^n,\ldots,c_4^n\}}{\operatorname{argmin}} \sum_{n=1}^{N/2} \big\{ &\|\mathbf{y}[2n-1] - \boldsymbol{A}(c_1^n, c_2^n)\mathbf{h}[2n-1]\|_F^2 \\ + \quad &\|\mathbf{y}[2n] - \boldsymbol{A}(c_3^n, c_4^n)\mathbf{h}[2n]\|_F^2 \big\}.\end{aligned} \tag{61}$$

where $\boldsymbol{A}(c_i^k, c_j^k) = \begin{bmatrix} c_i^k & c_j^k \\ -c_j^{k*} & c_i^{k*} \end{bmatrix}$, $i \neq j$ is the Alamouti matrix.

The orthogonality of the inner building blocks makes it possible to simplify the complexity of the decoding process by combining the set partitioning and separate decoding of the inner QOSTFTCs; furthermore it allows a pairwise Maximum-Likelihood decoding using the Viterbi algorithm. It is important to note that the decoding process results in a delay of two OFDM symbols.

III.5.5 Diversity of QOSTFTCs

In this subsection, we discuss on the diversity of the STF code given by Equation (60). Let us consider the MIMO-OFDM system described in Section III.2, which is equipped with N subcarriers and two spatially uncorrelated transmit antennas, with L independent path gains $\alpha_{i,j}(l)$ between each pair of transmit and receive antennas. Moreover, the STF codeword is formed by T independent OFDM symbols. Assuming that the second order statistics of the time correlation is the same for all transmit and receive antenna pairs and all paths (the correlation values do not depend on i, j and l),

the diversity gain of a STF code is determined by the minimum rank of $\Lambda \circ \mathbf{R}$ over all pairs of distinct codewords $\mathbf{C}$ and $\mathbf{E}$ ($\circ$ denote the Hadamard product of two matrices), which was defined by Su *et al.* (2005) as

$$G_d = \min_{\mathbf{C},\mathbf{E}} \operatorname{rank}(\Lambda \circ \mathbf{R}) \tag{62}$$

where

$$\Lambda = \begin{pmatrix} \mathbf{D}_{STF}^1 \\ \mathbf{D}_{STF}^2 \\ \vdots \\ \mathbf{D}_{STF}^T \end{pmatrix} \begin{pmatrix} \mathbf{D}_{STF}^1 \\ \mathbf{D}_{STF}^2 \\ \vdots \\ \mathbf{D}_{STF}^T \end{pmatrix}^H, \tag{63}$$

$$\mathbf{D}_{STF}^t = \mathbf{C}_{STF}^t - \mathbf{E}_{STF}^t \quad \forall\, t \in \{1, \ldots, T\}, \tag{64}$$

$$\mathbf{R} = \mathbf{R}_t \otimes \mathbf{R}_f. \tag{65}$$

$\mathbf{R}_f \in \mathbb{C}^{N \times N}$ and $\mathbf{R}_t \in \mathbb{C}^{T \times T}$ represents the frequency correlation matrix of the channel and the temporal correlation matrix, respectively. If the minimum rank of $\Lambda \circ \mathbf{R}$ is ν for any pair of distinct codewords $\mathbf{C}$ and $\mathbf{E}$, the STF code achieves a diversity order of νM_r (Su *et al.*, 2005). Since the rank of Λ is at most M_t and the rank of $\mathbf{R}_f$ is at most L, and by denoting $\operatorname{rank}\{\mathbf{R}_t\}$ as $\mathcal{T}$, then

$$\operatorname{rank}(\Lambda \circ \mathbf{R}) \leq \min\{TN, M_t L \mathcal{T}\}. \tag{66}$$

Since $M_t = 2$ and $T = 2$, the maximum achievable diversity is $\min\{2M_r N,\ \ 2M_r L\mathcal{T}\}$. However, according to the codeword design criteria derived in Section III.3, we assume that the channel stays constant over $T = 2$ OFDM symbol duration, and the rank of

the temporal correlation matrix is $\mathcal{T} = 1$. As a result, STF coding cannot provide the temporal diversity advantage, and the maximum achievable diversity is

$$2M_r \cdot \min\{N, L\}. \tag{67}$$

One necessary condition to be considered in the definition of the matrix Λ is that the number of subcarriers should be at least equal to the number of paths of the impulse response of the channel, i.e. $N \geq L$. Then, the maximum achievable diversity is only $2M_rL$. In accordance with this, by combining trellis coding with orthogonal ST block codes, Section III.3 shows that the maximum achievable diversity of our proposed STF trellis codes is $2M_r \cdot \min\{L, \delta_H\}$.

III.6 Simulation Results and Discussions

In this section, we provide numerical results by Monte-Carlo simulations for the codes that we designed in Sections III.4 and III.5, over a MIMO-OFDM system equipped with two transmit antennas and a single receive antenna. In all simulations, the cyclic prefix length is long enough to combat ISI, and the multipath gains are assumed to be statistically independent, identically distributed and complex Gaussian random variables. All multipaths undergo independent Rayleigh fading and the average symbol power per transmit antenna is assumed to be $E_s = \frac{1}{M_t}$ and the noise variance is $\frac{1}{SNR}$. Also, we assume that the channel is quasi-static over two OFDM symbols duration (a frame) and changes independently for each frame, and the receiver has perfect channel state information. The quasi-static channel condition cannot provide additional temporal diversity advantage ($\mathcal{T} = 1$), however it provides a reduced and independent maximum likelihood decoding complexity. The performance curves are described by means of Frame Error Rate (FER) versus the receive SNR using a QPSK constellation.

The proposed schemes are compared with those of the existing 16-state super-orthogonal space-time-frequency trellis code (SOSTFTC) derived by Aksoy and Aygölü (2007). Furthermore, for the sake of comparison, we also evaluate the performance of the QOSTFBC with QPSK designed by Fazel and Jafarkhani (2008). All comparisons are performed under an identical scenario. In order to observe the robustness of the proposed STF trellis codes, a random interleaver is not applied. The decoding complexity of our Ex-SOSTFTC is similar to that of the SOSTFTC proposed by Aksoy and Aygölü (2007), while in the case of QOSTFTC over quasi-static channel, we benefit from a reduced decoding complexity.

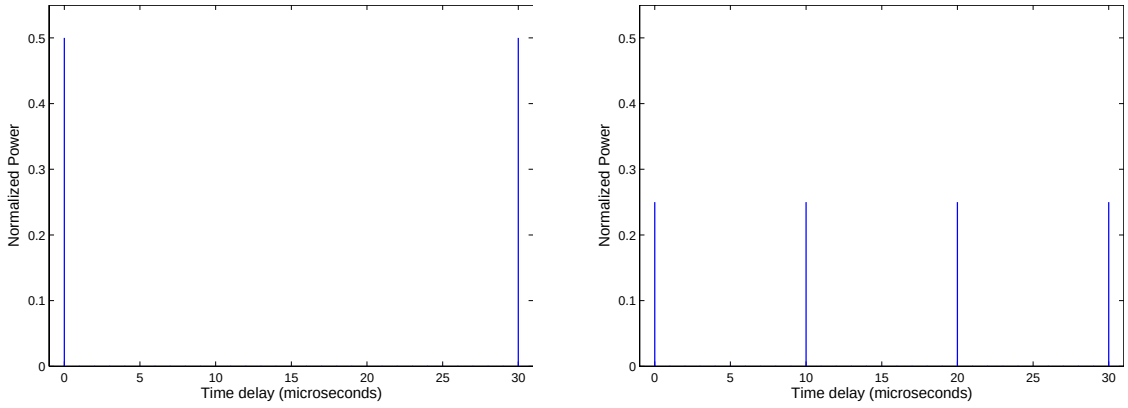

(a) (b)

Figure 23. Uniform power delay profile a) two-ray, b) four-ray channel model.

For the sake of a complete performance analysis, we simulated the system over the following channel scenarios:

1. Each transmit antenna is equipped with an OFDM modulator with $N = 128$ subcarriers over a total bandwidth of 1 MHz, and

   (a) The code performance is evaluated in a 2-ray equal power channel model with a maximum delay spread of $\tau_{\max} = 30$ μs (to represent underlying fading environment), where the paths are equally spaced, as shown in Figure 23(a).

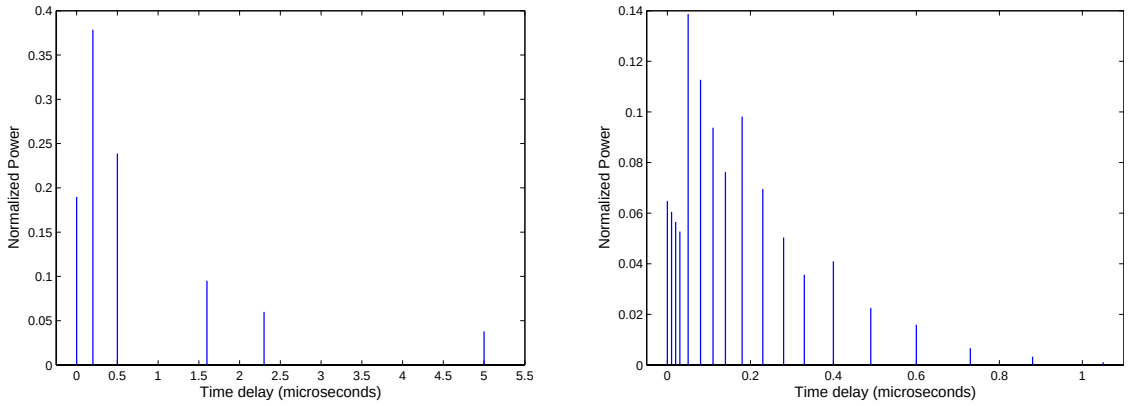

(a) (b)

Figure 24. Power delay profile of a) six-ray COST207-TU, b) HiperLAN/2 indoor channel model C.

(b) The channel is a 4-ray equal power channel model with delay spread between paths of $\tau_{\max} = 10$ μs, which is shown in Figure 23(b).

2. The OFDM modulation has $N = 128$ subcarriers, and the OFDM block duration is 128 μs over a total bandwidth of 1 MHz. In this scenario, we adopt a six-ray typical urban (TU) power delay profile (Stuber, 2001), which is shown in Figure 24(a).

3. We use a 64-tone OFDM system with a total bandwidth of 20 MHz. In order to model a more realistic frequency selective fading channel, we adopt the HiperLAN/2 indoor channel model from (Medbo and Schramm, 1998).

In figures 25 and 26 we study the performance of the Ex-SOSTFTC and QOSTFTCs designed in Section III.4 and III.5, over the channel scenario 1(a).

We can see from the FER curves in figures 25 and 26, that because of the trellis encoding, the 2-state, 4-state and 16-state QOSTFTCs achieve an additional coding gain of about 2 dB, 3 dB, and 4.5 dB, respectively, when compared with the existing QOSTFBC.

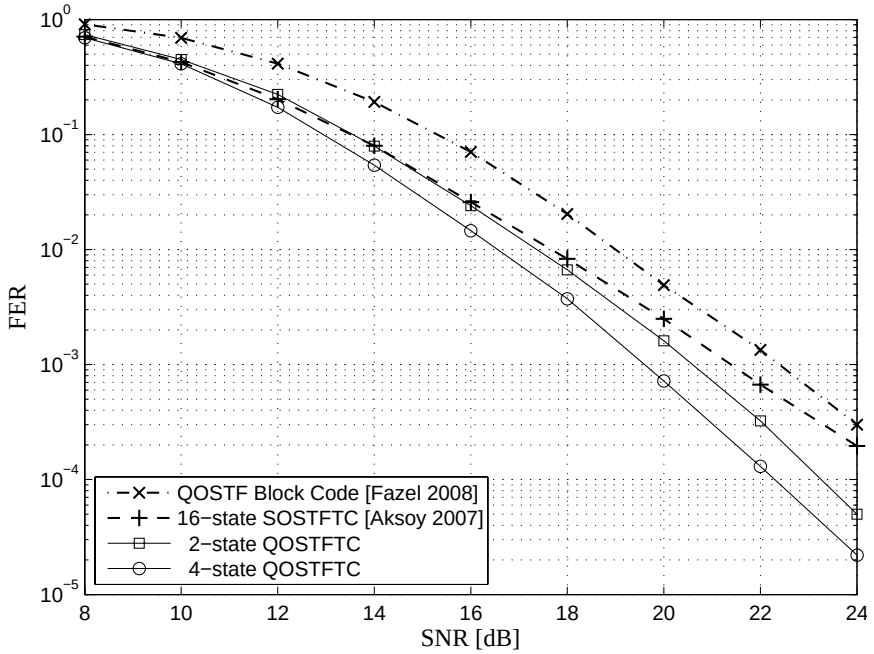

Figure 25. Performance of 2-state and 4-state Quasi-Orthogonal STF trellis codes, in a two-tap equal-power channel, where the delay spread between paths is 30 μs; at 2 bits/s/Hz with QPSK.

It can be seen from the slopes of the performance curves in figures 25 and 26, that both Ex-SOSTFTC and QOSTFTCs achieve the full-diversity order of 4. A practical calculus of the diversity, or diversity gain, is done by evaluating the slope of the FER curve as G_d = curve slope $m = \frac{10(\log(\mathrm{FER}_2) - \log(\mathrm{FER}_1))}{\mathrm{SNR}_2 - \mathrm{SNR}_1}$, where FER_i is the frame error probability at an SNR equal to SNR_i dB, $i = \{1, 2\}$. Note that the existing 16-state SOSTFTC (16-SO) designed by Aksoy and Aygölü (2007), which also uses orthogonal codewords as branch outputs in the trellis encoder, has a diversity order of 3.

By observing Figure 25 at FER of 10^{-3}, the proposed 4-state QOSTFTC (4-QO) and 2-state QOSTFTC (2-QO) have a superior performance over that of existing 16-SO by almost 2 dB and 1 dB, respectively. Similarly, we see from Figure 26 at FER of 10^{-3}, that the 16-state QOSTFTC (16-QO) and 16-state Ex-SOSTFTC (16-Ex) outperform that of existing 16-SO by almost 3 dB and 0.5 dB, respectively.

In figures 27 and 28, the performance of the Ex-SOSTFTC and QOSTFTCs are

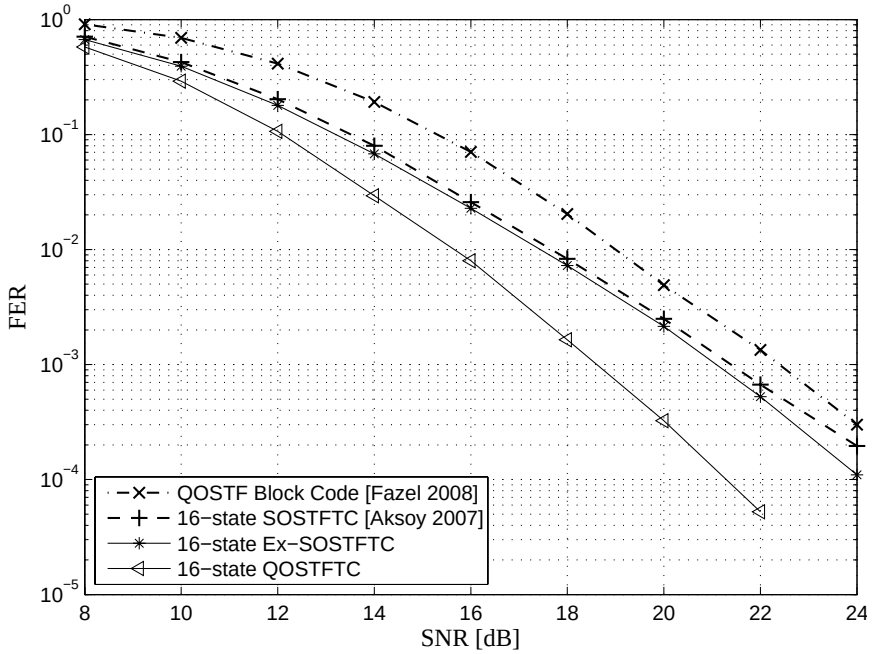

Figure 26. Performance of 16-state Extended Super-Orthogonal and 16-state Quasi-Orthogonal STF trellis codes, in a two-tap equal-power channel, where the delay spread between paths is 30 μs; at 2 bits/s/Hz with QPSK.

compared with codes of (Fazel and Jafarkhani, 2008) and (Aksoy and Aygölü, 2007), for the channel scenario 1(b), a four-tap equal-power fading channel. As seen from the FER curve in Fig. 28, at a FER of 10^{-3} our proposed 16-QO and 16-Ex outperform the 16-SO proposed by Aksoy and Aygölü (2007) by more than 2.2 dB and 0.6 dB, respectively. Besides, the FER curves in Figure 27 show that the 4-QO provides a performance similar to that of the 16-SO.

The effects of the number of paths in performance is not the same for all codes. While increasing the number of paths improves the performance of 16-QO and 16-Ex, it degrades the performance of 4-QO and 2-QO. Note that we have designed codes for a two-tap channel and therefore the maximum achievable diversity is four independent of the actual number of taps in the system. Of course, if the same approach is utilized to design codes for higher number of taps, a higher diversity will be achieved.

In what follows, we evaluate the performance of the proposed 16-state Ex-SOSTFTC

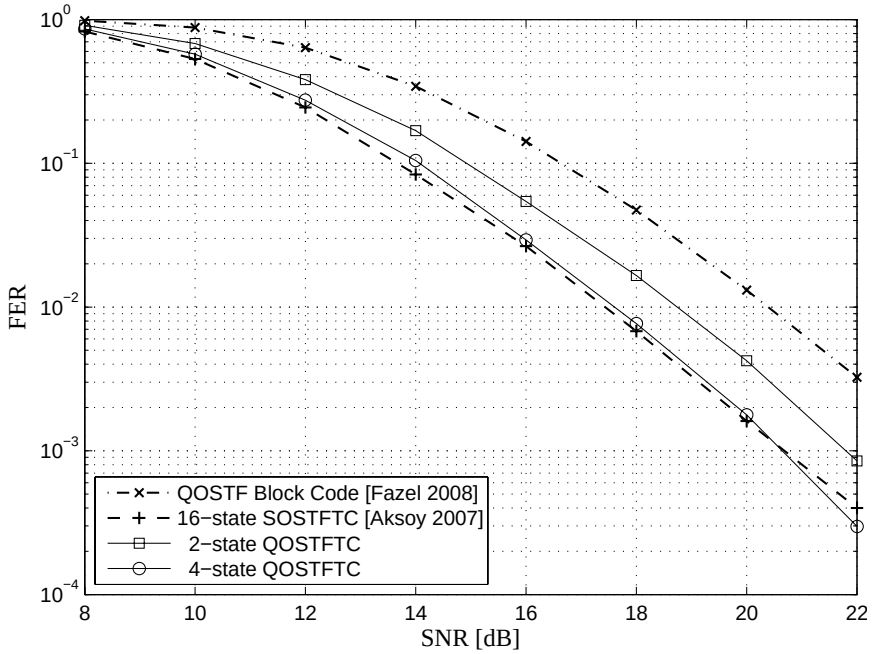

Figure 27. Performance of 2-state and 4-state Quasi-Orthogonal STF trellis codes, in a four-tap equal-power channel, where the delay spread between paths is 10 μs; at 2 bits/s/Hz with QPSK.

(16-EX) and 16-QOSTFTC (16-QO). These codes are compared with the 16-SO code of Aksoy and Aygölü (2007), for the channel scenario 2, the six-ray COST207 typical urban channel model. As can be seen from Figure 29, both proposed codes outperform the 16-SO by 0.8 dB and 0.4 dB, respectively.

It is worth mentioning that, we have significatively changed the frequency selectivity of the channel. For the scenarios 1(a) and 1(b), the root mean square (r.m.s.) delay spreads are higher than that r.m.s delay spread of channel scenario 1. As a result, the correlation between adjacent subcarriers increases in channel scenario 2. According to discussion in Section II.1.1, the coherence bandwidth B_c defined in Equation (6), is not large enough to produce a frequency selective channel.

In order to illustrate this phenomena, Figure 30 shows the FER performance under the HipeLAN/2 channel scenario. The slope curves in Figure 30 show that at a Frame Error Rate of 10^{-3} over the channel scenario 3, 16-QO outperforms the 16-SO code

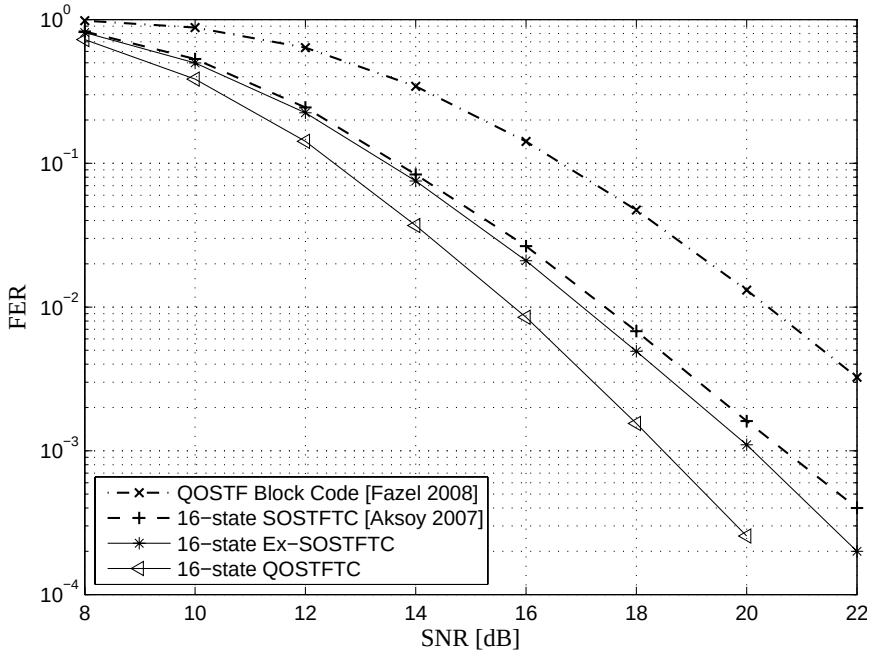

Figure 28. Performance of 16-state Extended Super-Orthogonal and 16-state Quasi-Orthogonal STF trellis codes, in a four-tap equal-power channel, where the delay spread between paths is $10\,\mu$s; at 2 bits/s/Hz with QPSK.

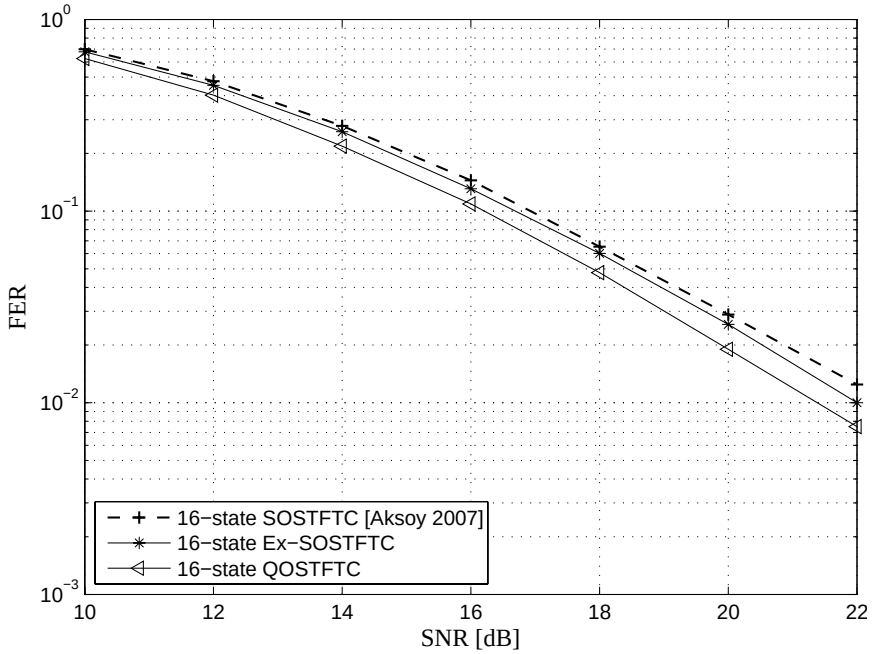

Figure 29. FER Performance for 6-ray COST207-TU channel model, where the rms delay spread is $1.1\,\mu$s; at 2 bits/s/Hz with QPSK.

by almost 1.5 dB. Note that the HiperLAN/2 channel model is more hostile than the six-ray COST207-TU. However, like the COST207-TU channel scenario, the correlation

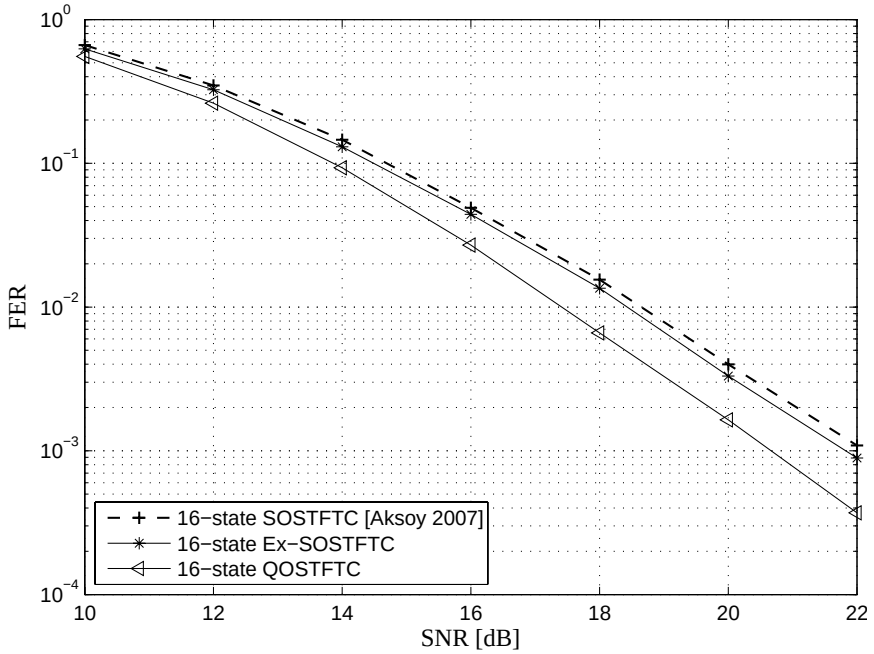

Figure 30. FER Performance for ETSI/BRAN channel model C, where the rms delay spread is 150 ns; at 2 bits/s/Hz with QPSK.

between adjacent subcarriers is high in this channel scenario, and the maximum order of diversity can not be achieved by any coding scheme. Random interleaver would break the correlation between subcarriers (Tan and Stuber, 2004; Akay and Ayanoglu, 2006), and apparently affect the parameters corresponding to the correlation i.e., the paremeters $\sigma(k)$ and $\eta(k)$ derived by Liu and Chong (2004). Then, these parameters significantly dominate the PEP given by Equation (20) of (Liu and Chong, 2004). Consequently this strongly affects the design of STF codes.

However, as we mentioned in the introduction of the Chapter, the interesting part of the design criteria for SF trellis codes proposed in Liu and Chong (2004) is that those codes do not need any knowledge of multipath and delay effects of the channel. Therefore, we propose to maximize both, the minimum product $CGD \cdot MPD$ and the δ_H for the optimization of the proposed STF trellis codes. Then, taking into account the subcarrier correlation for the design of the interleaver is beyond the scope of this

work.

The superiority of our proposed 16-QO scheme over that of Aksoy and Aygölü (2007) is evident from all channel scenario simulations. Moreover, as simulation results suggest, without applying a channel interleaving strategy, our proposed Ex-SOSTFTC and the QOSTFTCs outperform both the Quasi-Orthogonal Space-Time-Frequency Block Code (Fazel and Jafarkhani, 2008) and the super-orthogonal space-time-frequency trellis code of Aksoy and Aygölü (2007). All of these observations are consistent with the proprieties of our proposed codes discussed in this chapter.

III.7 Chapter Summary

We have carried out, a design of rate-one, high-coding gain Ex-SOSTFTC and QO-STFTCs for MIMO-OFDM systems under a frequency selective fading channel. The proposed codes provide multipath diversity in addition to space diversity.
Furthermore, as simulation results suggest, without applying a channel interleaving strategy, our proposed Ex-SOSTFTC and the QOSTFTCs outperform the best available space-time-frequency trellis code in the literature.

If the channel is quasi-static over two adjacent OFDM symbols, there are no temporal diversity gains offered by the channel, and there is a delay of two OFDM symbols associated with the decoding procedure in all cases. However, the decoding complexity of the proposed STFTCs is reduced.

In order to achieve the full diversity order offered by the channel, STFTCs with larger δ_H are required. Note that we only consider $L = 2$ for the proposed designs, but it is straightforward to design similar codes for more than two taps. There are few

examples of STF trellis codes in the literature, and those are usually designed manually or by computer search, while our proposed codes are designed systematically.

Chapter IV

Differential Quasi-Orthogonal Space-Frequency Trellis Codes

IV.1 Introduction

In the Chapter III, we have discussed on the practical case when the Channel State Information (CSI) exists only at the receiver. In such a scenario, called coherent detection, the receiver estimates the path gains by using pilot signals that the transmitter send (Tarokh *et al.*, 1999b). Then the decoding process of data symbols is performed coherently during the same frame (one o more OFDM symbols). Non-coherent modulation is useful when the knowledge of CSI is not available. The non-coherent modulation simplifies the receiver structure by omitting channel estimation and carrier or phase tracking. Some examples of the non-coherent modulation techniques for single-antenna systems, are non-coherent frequency shift keying (NFSK) and differential modulation (Proakis, 2000). It has been shown that the frequency offsets due to local oscillator mismatch at the transmitter and receiver, and the Doppler induced by relative mobility between the transmitter and receiver, are typically small compared with the bandwidth of the transmitted signal (Madhow, 2008). Non-coherent communication exploits this

observation to eliminate the necessity for carrier synchronization, modeling the phase over the duration of a demodulation interval as unknown, but constant. However, the non-coherent communication cannot encode information in the signal phase, since the channel produces an unknown phase shift that would destroy such information. Nevertheless, if this unknown phase can be modeled as approximately constant over more than one symbol, then we can get around this problem by encoding information in the phase differences between successive symbols. This enables recovery of the encoded information even if the absolute phase is unknown. This method is known as Differential Phase Shift Keying (DPSK), and is robust against unknown channel amplitude as well as phase. Differential modulation is useful for a wireless mobile channel, where the amplitude and phase vary over time.

In a linear modulation of a Phase-Shift Keying (PSK) symbol sequence c_t over a transmit and one receive antenna, the output of the receive filter at time t obey the model

$$r_t = \alpha c_t + \eta_t \tag{68}$$

where α is the channel gain, and η_t is the noise. If the phase of α can vary arbitrarily fast with t, then there is no hope of conveying any information in the carrier phase. However, if α varies slowly enough that we can approximate it as piecewise constant over at least two symbol intervals, then we can use phase transitions to convey information.

Let us consider a DPSK modulation using a MPSK constellation, where $M = 2^b$. At $t = 0$, the transmitter sends an arbitrary symbol c_0. After, for each b input bits at time t, the transmitter selects a symbol s_t from the MPSK constelation. Then, the transmitted symbol c_t is defined as

$$c_t = c_{t-1} s_t \quad \text{for } t = 1, 2, \ldots \tag{69}$$

If the MPSK constellation is an unitary-energy constellation, then $|c_t|$ is always equal to one. Moreover, because the initial transmitted symbol is an MPSK symbol, c_t is also an MPSK symbol. To decode the transmitted symbol at time t, the optimal estimate is shown in (Jafarkhani, 2005) as

$$\hat{s}_t = \arg\min_{s_t} \left| r_t r_{t-1}^* - |\alpha|^2 s_t \right|, \tag{70}$$

where

$$r_t r_{t-1}^* = |\alpha|^2 s_t + \mathcal{N}, \tag{71}$$

the path gain α is assumed constant during times $t-1$ and t, and $\mathcal{N}$ is a Gaussian noise. Since all constellation points in a MPSK constellation are on the same circle, the factor $|\alpha|^2$ will not change the detection regions, we can rewrite (70) as

$$\hat{s}_t = \arg\min_{s_t} \left| r_t r_{t-1}^* - s_t \right|, \tag{72}$$

As a result of ignoring $|\alpha|^2$, under the same transmission power, compared with the corresponding coherent detection, there is approximately a 3 dB loss in performance for this differential detection scheme (Jafarkhani, 2005).

Therefore, the existence of detection schemes that neither require the channel knowledge nor the pilot symbol transmission, motivated us to study differential detection for the case of Multiple-Input Multiple-Output (MIMO) systems.

In recent years, it has been shown that space-frequency coded Multiple-Input Multiple-Output-Orthogonal Frequency Division Multiplexing systems are capable of achieving maximum diversity over a frequency selective channel (FSC) (Su *et al.*, 2005). In most cases, space-frequency coding schemes assume that the receiver has an accurate estimate of the Channel State Information. This assumption is reasonable when the channel changes slowly compared with the symbol rate. However, acquiring knowledge of the

Channel State Information for an FSC with many taps is prohibitively complex. As a result, exploiting the available spatial, time and frequency diversities, if neither the transmitter nor the receiver knows the CSI, have been just recently addressed in the literature. To name a few, for example in the case of space-time coding schemes, in order to achieve the space-time diversity, unitary space-time codes were proposed by Hochwald and Marzetta (2000) and by Hochwald *et al.* (2000). Differential unitary space-time code and differential modulation were proposed in (Hochwald and Sweldens, 2000) and (Hughes, 2000), called Differential Unitary Space–Time Modulation (DUSTM). A first differential coding scheme based on OSTBCs for a slow Rayleigh fading channel was proposed in Tarokh and Jafarkhani (2000). The generalization of this differential scheme to more than two transmit antennas is derived in (Tarokh and Jafarkhani, 2001). A elegant differential modulation scheme based on quasi-orthogonal codes is derived by Zhu and Jafarkhani (2005).

In order to achieve space-frequency (SF) diversity, differential and non-coherent MIMO-OFDM systems were proposed in (Su and Liu, 2005; Borgmann and Bölcskei, 2005; Ma *et al.*, 2005; Tao, 2006; Himsoon *et al.*, 2006; Hong *et al.*, 2006; Zhu and Jafarkhani, 2006; Li *et al.*, 2008), among others. However, the existing differential techniques have several drawbacks. For example, they have a large code size, which exponentially increases the coding and decoding complexity. Moreover, by trying to increase the data rate, they have a low coding gain.

Liu and Giannakis (2003) proposed a block differentially encoded OFDM (BD-OFDM) system. There, the authors split the set of generally correlated subchannels into subsets of independent subchannels to which the DUSTM of (Hochwald and Sweldens, 2000) and (Hughes, 2000) is then applied by treating each subchannel as a transmit antenna. However, such a scheme cannot exploit the available maximum diversity of

a MIMO-OFDM system. A frequency-domain differential scheme was proposed by Ma *et al.* (2005), where maximum diversity and good performance can be achieved by dividing an OFDM symbol into several subcarriers groups, and perform differential encoding and decoding between adjacent groups. However, in the implementation of Ma *et al.* (2005), the subcarrier grouping is not selected according to channel delay profile, and require constant CFR from group to group, which lead to severe error floor in FSCs. Differential Space-Frequency Trellis Codes (DSFTCs) presented by Hong *et al.* (2006), can obtain rate-one (1 symbol per subcarrier), spatial diversity, and a simple decoding complexity. Even though the DSFTCs increase the coding gain, the error floor is still significant.

Motivated on solving the drawbacks of the previous schemes, in this chapter we propose differential encoding schemes. We called to this schemes Differential Quasi-Orthogonal Space-Frequency Trellis Codes (DQOSFTCs). The proposed DQOSFTCs achieve high coding gain, and are capable of exploiting both spatial and frequency diversity over a MIMO-OFDM system with lack of CSI at the transmitter and at the receiver. In order to guarantee both rate-one and full-diversity, we use the structure of the generalized Quasi-Orthogonal Space-Time Block Code (QOSTBC) derived by Fazel and Jafarkhani (2008). We stress, however, that the construction in (Fazel and Jafarkhani, 2008) does not take into account the coding gain, and it is not suitable for differential encoded process.

In summary, the contributions in this chapter of Thesis are the following: 1) In order to get rate-one and high-coding gain, we obtain a sufficient number of full-diversity unitary quasi-orthogonal codes, and following a similar procedure as in Section III.5.2, we perform set partitioning. Then, we systematically design the unitary quasi-orthogonal SF trellis codes (QOSFTCs). 2) We propose to perform the differential encoding in

2 ways: a) over the frequency domain, b) over the time domain. 3) According to the number of orthogonal matrices (subblocks) within a QOSFTC, we divide the OFDM subcarriers into equidistant groups. In addition, we take advantage of orthogonality of the inner subblocks of the QOSFTCs, by using a simple Maximum-Likelihood (ML) decoder without requiring CSI at the receiver, which is formed by a differential decoder and a Viterbi decoder. Therefore, we obtain a simple differential encoding process, and the assumption of a constant CFR from group to group can be relaxed. Besides being computationally efficient and easy to implement, we show through numerical simulations that in the presence of FSCs, our proposed codes significantly outperform the existing DSFTCs.

IV.2 System Description

For simplicity, let us consider the channel model described in Section III.2. The MIMO-OFDM system is implemented with M_t transmit and M_r receive antennas. We assume that no spatial fading correlation exists between antennas. Each transmit antenna employs an N-subcarrier OFDM modulator. The general representation of a space-frequency codeword for M_t transmit antennas transmitted at the tth OFDM symbol period is shown in Equation (43). We denote the transmitted space-frequency code at the tth OFDM symbol period by $\bar{\mathbf{C}}^t = \left[\mathbf{c}_1^t \dots \mathbf{c}_{M_t}^t\right] \in \mathbb{C}^{N \times M_t}$, where $\mathbf{c}_i^t = [c_i^t(1) c_i^t(2) \dots \ c_i^t(N)]^T$ is transmitted from the ith antenna ($i = 1 \dots M_t$), and $c_i^t(n)$ is the complex data transmitted at the nth subcarrier ($n = 1, \dots, N$).

Figure 31 shows the transmitter, which combines a QOSTBC with trellis encoding, differential modulation, and space-frequency coding. At instant t, according to current state and the information input bits, the trellis encoder builds the kth unitary-QOSTBC

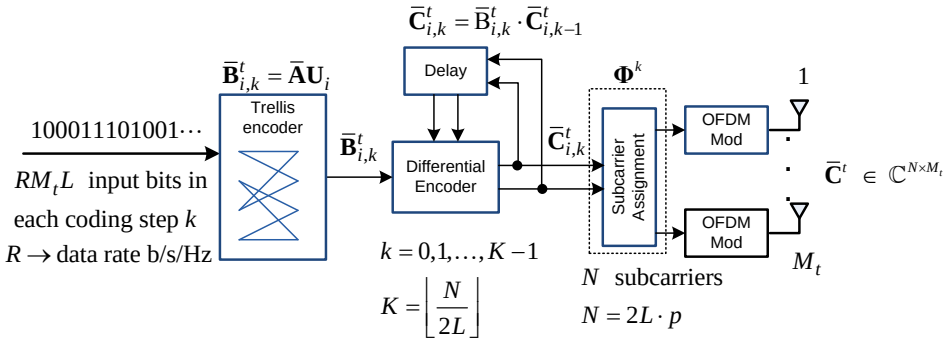

Figure 31. Differential Space-Frequency transmitter.

$\bar{\boldsymbol{B}}^t_{i,k}$. Then, $\bar{\boldsymbol{B}}^t_{i,k}$ is differentially encoded (as we will describe later) to obtain the data codeword, called $\bar{\boldsymbol{C}}^t_{i,k}$. Afterward, taking advantage of the inner construction of $\bar{\boldsymbol{B}}^t_{i,k}$, $\bar{\boldsymbol{C}}^t_{i,k}$ is mapped into OFDM tones, using subcarrier grouping. After K coding steps, we obtain the SF code matrix, $\bar{\mathbf{C}}^t$. Finally, the coded OFDM symbol $\bar{\mathbf{C}}^t$ is transmitted at instant t through the M_t transmit antennas. In order to recover the information data, the inverse process is performed at the receiver. The overall process is discussed in detail in subsequent sections.

IV.3 Differential encoding and subcarrier map

In this section, we derive the rate-one unitary QOSTBC construction, and describe two differential encoding designs. We also show the mapping of the differentially encoding codeword $\bar{\mathbf{C}}^t$ to the OFDM symbols.

IV.3.1 Unitary quasi-orthogonal block codes

The first stage of information processing in the transmitter is the trellis encoder. Similar to the coding process described in Section III.5, depending on the input information bits and the current state in the trellis encoder, a codeword is selected from a constellation

of possible unitary-QOSTBCs. Then, there is a transition towards the next state in the trellis, and the encoding process is performed again to obtain a frame with K codewords. Let us consider the general class of QOSTBC defined by Fazel and Jafarkhani (2008) as

$$\bar{\boldsymbol{A}} = \frac{1}{\sqrt{2L}} \begin{pmatrix} \mathbf{A}(S_1, S_2) & \dots & \mathbf{0} \\ \vdots & \ddots & \vdots \\ \mathbf{0} & \dots & \mathbf{A}(S_{2L-1}, S_{2L}) \end{pmatrix}, \tag{73}$$

where space goes horizontally, $\bar{\boldsymbol{A}} \in \mathbb{C}^{2L \times 2L}$. S_l $(l = 1, 2, \dots, 2L)$ are calculated as

$$[S_1 \ S_3 \dots S_{2L-1}]^T = \Phi[s_1 \ s_3 \dots s_{2L-1}]^T \tag{74}$$

$$[S_2 \ S_4 \dots S_{2L}]^T = \Phi[s_2 \ s_4 \dots s_{2L}]^T \tag{75}$$

where $\Phi = \mathbf{H}_d \times \text{diag}\{1, e^{j\phi_1}, \dots, e^{j\phi_{L-1}}\}$, $\mathbf{H}_d \in \mathbb{R}^{L \times L}$ is a Hadamard matrix, and $s_1, \dots, s_{2L}$ belong to a M-PSK constellation. $\mathbf{A}(S_x, S_y)$ denotes the Alamouti code (Alamouti, 1998) for any indeterminate symbols S_x, S_y, as defined in Equation (14).

In order to support a data rate of R, defined as the number of bits per subcarrier use (b/s/Hz), it is necessary for a sequence of RM_tL information bits to pick a codeword as (73) at each state transition of the trellis encoder. Then, we denote as $\mathcal{O}$ the set of all possible information codewords, which must have a cardinality of

$$|\mathcal{O}| = 2^{RM_tL}. \tag{76}$$

Furthermore, in the interest of performing differential encoding after trellis encoding, the information codewords to be transmitted must be unitary matrices, such that

$$\bar{\boldsymbol{A}}^H \bar{\boldsymbol{A}} = \mathbf{I}_{2L}, \tag{77}$$

where $\mathbf{I}_n$ is the $n \times n$ identity matrix.

Let us denote by O the set of all those codewords $\bar{\boldsymbol{A}}$ that satisfy the unitarity condition. For the sake of providing the required cardinality $|\mathcal{O}| = 2^{RM_tL}$, we introduce unitary rotation matrices

$$\mathbf{U}_i = \text{diag}(d_{i,1}, d_{i,2}, \ldots, d_{i,2L}), \tag{78}$$

where $i = 0, 1, \ldots, M$ denotes the ith rotation matrix and diag$(\cdot)$ denotes a diagonal matrix such that

$$\mathcal{O} = \{\text{O}\mathbf{U}_0, \ldots, \text{O}\mathbf{U}_M\}. \tag{79}$$

Thus, we express an information codeword from the trellis encoder output as

$$\begin{pmatrix} \mathbf{B}(S_1, S_2) & & & \\ & \mathbf{B}(S_3, S_4) & & \\ & & \ddots & \\ & & & \mathbf{B}(S_{2l-1}, S_{2l}) \end{pmatrix} =$$

$$\frac{1}{\sqrt{2L}} \begin{pmatrix} \mathbf{A}(S_1, S_2) & \mathbf{0} & \mathbf{0} & \mathbf{0} \\ \mathbf{0} & \mathbf{A}(S_3, S_4) & \mathbf{0} & \mathbf{0} \\ \mathbf{0} & \mathbf{0} & \ddots & \mathbf{0} \\ \mathbf{0} & \mathbf{0} & \mathbf{0} & \mathbf{A}(S_{2l-1}, S_{2l}) \end{pmatrix} \begin{pmatrix} d_1 & 0 & 0 & 0 & 0 \\ 0 & d_2 & 0 & 0 & 0 \\ 0 & 0 & \ddots & 0 & 0 \\ 0 & 0 & 0 & d_{2L-1} & 0 \\ 0 & 0 & 0 & 0 & d_{2L} \end{pmatrix}_i$$

$$\bar{\boldsymbol{B}}_i = \bar{\boldsymbol{A}}\mathbf{U}_i. \tag{80}$$

Since both $\bar{\boldsymbol{A}}$ and $\mathbf{U}_i$ are unitary matrices, then $\bar{\boldsymbol{B}}_i$ is also a unitary matrix. Due to the diagonal structure of (80), we can write the inner orthogonal matrices as

$$\mathbf{B}_i(S_{2l-1}, S_{2l}) = \frac{1}{\sqrt{2L}} \mathbf{A}(S_{2l-1}, S_{2l}) \text{ diag}(d_{i,2l-1}, d_{i,2l}), \tag{81}$$

where $l = 1, \ldots, L$. Then, we define the kth unitary codeword sent at period t from a trellis encoder as

$$\bar{\boldsymbol{B}}_{i,k}^{t} = \begin{pmatrix} \mathbf{B}_{i,k}^{t}(S_1, S_2) & \mathbf{0} & \ldots & \mathbf{0} \\ \mathbf{0} & \mathbf{B}_{i,k}^{t}(S_3, S_4) & \ldots & \mathbf{0} \\ \vdots & \ddots & \vdots & \vdots \\ \mathbf{0} & \mathbf{0} & \ldots & \mathbf{B}_{i,k}^{t}(S_{2L-1}, S_{2L}) \end{pmatrix}, \tag{82}$$

where $\bar{\boldsymbol{B}}_{i,k}^{t} \in \mathbb{C}^{2L \times 2L}$, $k = 0, 1, \ldots, K-1$, with

$$K = \left\lfloor \frac{N}{2L} \right\rfloor. \tag{83}$$

For convenience, we assume that $N = 2Lp$ for some integer p. Note that the essential structure of the QOSTBC derived by Fazel and Jafarkhani (2008) is preserved by the unitary matrix defined in (82), therefore the full-diversity of $M_t M_r L$ is still maintained.

IV.3.2 Subcarrier assignment

After picking the unitary codeword (82) from the trellis encoder output and the differential encoding process, we map the resultant codeword $\bar{\boldsymbol{C}}_{i,k}^{t}$ to the OFDM-subcarrier groups. Then, we express a SF construction for two transmit antennas and L subcarrier groups as

$$\bar{\mathbf{C}}^t = \begin{pmatrix} \mathbf{C}^t_{i,0}(S_1, S_2) \\ \vdots \\ \mathbf{C}^t_{i,K-1}(S_1, S_2) \\ \mathbf{C}^t_{i,0}(S_3, S_4) \\ \vdots \\ \mathbf{C}^t_{i,K-1}(S_3, S_4) \\ \vdots \\ \mathbf{C}^t_{i,0}(S_{2L-1}, S_{2L}) \\ \vdots \\ \mathbf{C}^t_{i,K-1}(S_{2L-1}, S_{2L}) \end{pmatrix} \tag{84}$$

where $\bar{\mathbf{C}}^t \in \mathbb{C}^{N \times 2}$.

IV.3.3 Differential encoding

For simplicity, in the sequel, we consider a scenario with $M_t = 2$ transmit antennas. The extension to more antennas is straightforward. In order to perform differential encoding keeping multipath diversity, we exploit the independence of the orthogonal matrices in (82) by partitioning the N subcarriers into L groups of subcarriers, with L representing the channel order. Then, we propose encoding differentially over the frequency domain (DF), and over the time domain (DT) as follows.

Differential encoding over the frequency domain (DF)

We consider that the channel remains constant during one OFDM symbol period and changes independently from symbol to symbol. We also consider that the correlation between adjacent subcarriers is high, which is a reasonable assumption if N is large

enough. Let $\bar{\boldsymbol{B}}_{i,k}^{t}$ be the kth information codeword generated in the trellis encoder at the tth OFDM symbol period for $k = 1, 2 \ldots, K-1$. In the differential encoder, the recursive construction of the unitary codeword $\bar{\boldsymbol{C}}_{i,k}^{t} \in \mathbb{C}^{2L \times 2}$ is given by

$$\mathbf{C}_{i,k}^{t}(S_{2l-1}, S_{2l}) = \begin{cases} \mathbf{I}_2, & k = 0 \\ \mathbf{B}_{i,k}^{t}(S_{2l-1}, S_{2l})\mathbf{C}_{i,k-1}^{t}(S_{2l-1}, S_{2l}), & k \geq 1. \end{cases} \tag{85}$$

The orthogonal property of the inner matrix $\mathbf{B}_{i,k}^{t}(S_{2l-1}, S_{2l})$ guarantees that $\bar{\boldsymbol{C}}_{i,k}^{t}$ $\in \mathcal{O}$ whenever $\bar{\boldsymbol{C}}_{i,k-1}^{t} \in \mathcal{O}$.

As an example, let us consider that $M_t = 2$ and $L = 2$, then the generation of the transmitted codeword $\bar{\mathbf{C}}_{i,k}^{t}$ for the Differential Encoding over the Frequency Domain (DF) at time t, follows the recursion

$$\bar{\mathbf{C}}_{i,0}^{t} = \begin{pmatrix} 1 & 0 \\ 0 & 1 \\ 1 & 0 \\ 0 & 1 \end{pmatrix} \qquad k = 0,$$

$$\bar{\mathbf{C}}_{i,1}^{t} = \begin{pmatrix} \mathbf{B}_{i,1}^{t}(S_1, S_2) \cdot \mathbf{C}_{i,0}^{t}(S_1, S_2) \\ \mathbf{B}_{i,1}^{t}(S_3, S_4) \cdot \mathbf{C}_{i,0}^{t}(S_3, S_4) \end{pmatrix} \qquad k = 1,$$

and so on until $k = K - 1$. At this step, a frame has been built.

Differential encoding over the time domain (DT)

In Differential Encoding over the Frequency Domain, the differential encoding process is performed at time t over each codeword $\bar{\boldsymbol{B}}_{i,k}^{t}$ from the trellis encoder output, with $k = 0, \ldots, K-1$. Now, we describe the Differential Encoding over the Time Domain

(DT), where differential encoding process is performed by mapping the codewords on adjacent OFDM symbols.

In this case we assume that the channel is quasi-static over one OFDM symbol period and slowly varies between adjacent OFDM symbols. Let $\bar{\boldsymbol{C}}_{i,k}^{t} \in \mathbb{C}^{2L\times 2}$ be the differential encoded matrix to be transmitted at the tth OFDM symbol period. At the beginning of the transmission ($t = 0$), the differential encoder sends $\mathbf{C}_{i,k}^{0}(S_{2l-1}, S_{2l}) = \mathbf{I}_2$ for all $k = 0, 1 \ldots, K-1$, where $l = 1, 2, \ldots, L$. Let $\bar{\boldsymbol{B}}_{i,k}^{t}$ be the kth information codeword generated in the trellis encoder at the tth OFDM symbol period, $t \geq 1$. The kth transmit codeword is generated as

$$\mathbf{C}_{i,k}^{t}(S_{2l-1}, S_{2l}) = \begin{cases} \mathbf{I}_2, & t = 0 \\ \mathbf{B}_{i,k}^{t}(S_{2l-1}, S_{2l})\mathbf{C}_{i,k}^{t-1}(S_{2l-1}, S_{2l}), & t \geq 1. \end{cases} \tag{86}$$

After of DT, the encoded matrices $\mathbf{C}_{i,k}^{t}(S_{2l-1}, S_{2l})$ will be mapped to the same sub-block (which contains similar subcarriers) of two adjacent time domain OFDM symbols.

To the sake of exposition, we explain this process as follows: First, at time $t = 0$, the encoder constructs a frame with K identity matrices $\mathbf{I}_2$. This frame is then transmitted as an OFDM symbol through the transmit antennas. Then, at the tth OFDM symbol period, $t > 0$, on each coding step k, the encoder picks the codeword $\bar{\boldsymbol{B}}_{i,k}^{t}$ from the trellis encoder output. Following the rule of subcarriers mapping, which is described in Subsection IV.3.2, submatrices $\mathbf{B}_{i,k}^{t}(S_{2l-1}, S_{2l})$ are mapped to their corresponding subcarriers group. Afterwards, the differential encoding is performed between adjacent codewords from the $(t-1)$ and tth frames. Consequently, codewords $\mathbf{C}_{i,k}^{t}(S_{2l-1}, S_{2l})$ have been obtained. Finally, the tth OFDM symbol containing the K differentially encoding codewords $\mathbf{C}_{i,k}^{t}(S_{2l-1}, S_{2l})$ is transmitted. This encoding process continues following the recursion procedure defined in Equation (86). Equation (87) illustrates

an example for the first frame to be transmitted in a Differential Encoding over the Time Domain.

$$\begin{pmatrix} \mathbf{C}_{i,0}^{t}(S_1,S_2) \\ \mathbf{C}_{i,1}^{t}(S_1,S_2) \\ \vdots \\ \mathbf{C}_{i,0}^{t}(S_3,S_4) \\ \mathbf{C}_{i,1}^{t}(S_3,S_4) \\ \vdots \\ \mathbf{C}_{i,0}^{t}(S_{2l-1},S_{2l}) \\ \vdots \end{pmatrix}^{t=1} = \begin{pmatrix} \mathbf{B}_{i,0}^{1}(S_1,S_2)\ \mathbf{I}_2 \\ \mathbf{B}_{i,1}^{1}(S_1,S_2)\ \mathbf{I}_2 \\ \vdots \\ \mathbf{B}_{i,0}^{1}(S_3,S_4)\ \mathbf{I}_2 \\ \mathbf{B}_{i,1}^{1}(S_3,S_4)\ \mathbf{I}_2 \\ \vdots \\ \mathbf{B}_{i,0}^{1}(S_{2l-1},S_{2l})\ \mathbf{I}_2 \\ \vdots \end{pmatrix} \tag{87}$$

Note that the transmission efficiency for Differential Encoding over the Time Domain is greater than its Differential Encoding over the Frequency Domain counterpart, since in every frame of the Differential Encoding over the Frequency Domain, the first codeword $\bar{\mathbf{C}}_{i,0}^{t}$ will not transmit information. Unlike Differential Encoding over the Frequency Domain, in the Differential Encoding over the Time Domain only the first frame will not transmit information. Moreover, we will show in Section IV.5 that the DF and DT schemes suffer from frequency selectivity and time variance, respectively.

IV.4 Differential QOSFTCs

In what follows, we propose rate-one differential QOSFTC designs for two transmit antennas, assuming a two-path fading channel model, i.e. $L = 2$. However, it is noteworthy that the method described here can be extended in a straightforward way to $L > 2$.

IV.4.1 Codeword sets

Let $S_1 = (s_1 + \tilde{s}_3)$, $S_3 = (s_1 - \tilde{s}_3)$, $S_2 = (s_2 + \tilde{s}_4)$ and $S_4 = (s_2 - \tilde{s}_4)$ be the symbols transmitted in (82) by setting $L = 2$, where the symbols s_1 and s_2 belong to a M-PSK constellation $\mathcal{A}$, and the symbols $\tilde{s}_3$ and $\tilde{s}_4$ belong to the rotated constellation $\mathcal{A}e^{j\phi}$. Also, let $\phi = \pi/M$ be the optimal rotation that provides the maximum coding gain for the code in (82), see Table I in Section II.2.2. In the sequel, for simplicity, we asume that the system employs a QPSK constellation. Therefore, a QPSK symbol is denoted as $s_i = e^{j\frac{\pi}{2}m}$, where $m = \{0, 1, 2, 3\}$ represents the index of the corresponding QPSK symbol.

Considering the unitary codewords $\bar{\boldsymbol{B}}_{i,k}^{t}$ defined in Equation 82, we obtain only 128 unitary codewords. Then, we use O to represent the subset of these unitary QOSTBCs. Therefore, in order to get a data rate of $R = 2$ b/s/Hz, we need two unitary matrices, $\mathbf{U}_0$ and $\mathbf{U}_1$, such that the overall set $\mathcal{O}$ of unitary QOSTBCs is

$$\mathcal{O} = \{\mathrm{O}\mathbf{U}_0, \mathrm{O}\mathbf{U}_1\}, \tag{88}$$

whose cardinality must be $|\mathcal{O}| = 256$.

Due to the symmetry in (82), if symbols $(s_1, s_2) \in \mathcal{A}e^{j\phi}$ and the symbols $(\tilde{s}_3, \tilde{s}_4) \in \mathcal{A}$, we get another subset of 128 different unitary codewords. We use P to represent them.

Let ϕ_1 and ϕ_2 be the rotation angles for the symbols (s_1, s_2) and $(\tilde{s}_3, \tilde{s}_4)$, respectively. Then, we assign $\Phi_0 = \{\phi_1 = 0, \phi_2 = \pi/4\}$ for the 128 unitary codewords belonging to set O, and $\Phi_1 = \{\phi_1 = \pi/4, \phi_2 = 0\}$ for the 128 unitary codewords that belong to set P. Thus, we obtain a new set as

$$\mathcal{P} = \{\mathrm{P}\mathbf{U}_0, \mathrm{P}\mathbf{U}_1\}, \tag{89}$$

such that $|\mathcal{P}| = 256$.

IV.4.2 Design criteria

Here we borrow the design criteria for differential space-time-frequency codes of Ma *et al.* (2005), which are identical to those proposed for differential super-orthogonal space-time trellis codes over flat channels in (Zhu and Jafarkhani, 2006). Let C_1 and C_2 be two codewords as defined in Equation (82) so that

i) Full diversity is achieved if the difference matrix given by

$$\mathbf{D} = C_1 - C_2, \tag{90}$$

has full rank over all possible pairs of distinct codewords C_1 and C_2.

ii) The minimum of the determinant defined as

$$CGD = \det\left(\mathbf{D}^H\mathbf{D}\right), \tag{91}$$

for all $C_1 \neq C_2$ corresponds to the Coding Gain Distance (CGD) and must be maximized.

IV.4.3 Set partitioning

Whereas in this thesis the differential modulation will be combined with space-frequency trellis codes over a MIMO-OFDM system, in order to achieve a better coding gain by using a trellis code structure, we need to do set partitioning.

Note that the codeword structure in Equation (82) guarantees the full diversity criterion. Moreover, the minimum CGD between codewords at each level of an optimal set partitioning must be maximized. First, in order to avoid expanding the original QPSK constellation, we need to search for the optimal values of the unitary rotation

matrices $\mathbf{U}_i$ $(i = 0, 1)$. In addition, the design criteria for the codewords in set $\mathcal{O}$ or $\mathcal{P}$ must be satisfied.

With numerical search, we obtain the optimal matrices

$$\mathbf{U}_0 = \begin{pmatrix} -1 & 0 & 0 & 0 \\ 0 & -j & 0 & 0 \\ 0 & 0 & 1 & 0 \\ 0 & 0 & 0 & -1 \end{pmatrix}, \tag{92}$$

and

$$\mathbf{U}_1 = \begin{pmatrix} 1 & 0 & 0 & 0 \\ 0 & -j & 0 & 0 \\ 0 & 0 & 1 & 0 \\ 0 & 0 & 0 & 1 \end{pmatrix}, \tag{93}$$

where $j = \sqrt{-1}$.

Applying $\mathbf{U}_0$ and $\mathbf{U}_1$ to the subsets of unitary QOSTBCs O and P respectively, we obtain $\mathcal{O}$ and $\mathcal{P}$, which are two sets of expanded unitary QOSTBCs. The resulting sets $\mathcal{O}$ and $\mathcal{P}$ contains 256 rate-one full-diversity unitary quasi-orthogonal codes using QPSK.

In order to perform the set partitioning procedure, in a first step, we partition the sets O and P following a procedure similar to the procedure in Section III.5.2. Here, at each level of an optimal set partitioning, we maximize the minimum CGD between codewords given in Equation (91). Then, after expanding the constellation matrices by using the unitary rotation matrices defined in Equations (92) and (93), we perform set partitioning to sets $\mathcal{O}$ and $\mathcal{P}$, following similar partition rules described above.

Fig. 32 shows the final set partition for $\mathcal{O}$ and $\mathcal{P}$ with QPSK and $L = 2$. The case when $\Phi_0 = \{\phi_1 = 0, \phi_2 = \pi/4\}$ is shown in Figure 32(a).

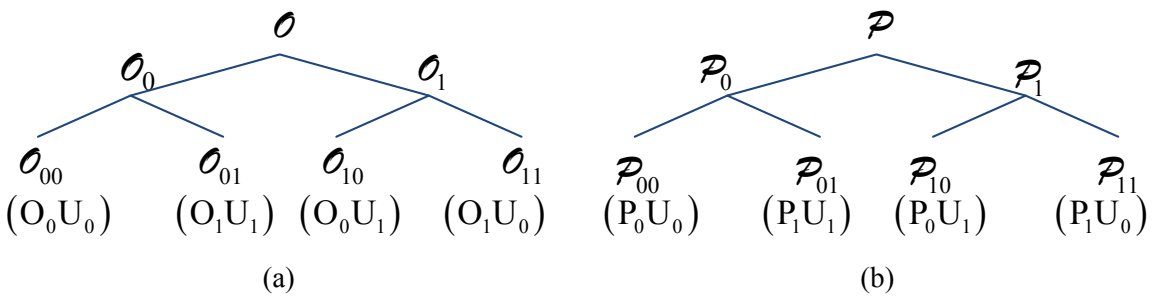

Figure 32. Final partitioning of sets (a) $\boldsymbol{\mathcal{O}}$ with Φ_0, and (b) $\boldsymbol{\mathcal{P}}$ with Φ_1.

In order to obtain the codewords $\bar{\boldsymbol{B}}_{i,k}$ in subset $\mathcal{O}_0$, we multiply the elements in the subset O_i $(i = 0, 1)$ by $\mathbf{U}_i$, i.e. $(\mathrm{O}_i\mathbf{U}_i)$. Figure 33(a) shows a partial set partition for unitary codewords $\bar{\boldsymbol{A}}$ (see Equation (73)) in subset O. We can obtain the codewords in subset $\mathcal{O}_1$ by multiplying the elements in subset O_i by $\mathbf{U}_j$ $(j = 1, 0)$, i.e. $(\mathrm{O}_i\mathbf{U}_j)$, $i \neq j$. Similarly, the set partition for $\mathcal{P}$ when $\Phi_1 = \{\phi_1 = \pi/4, \phi_2 = 0\}$ is shown in Figure 32(b). The partitioning steps are similar to those followed to obtain the set $\mathcal{O}$. Figure 33(b) shows the partitioning tree to subset P.

IV.4.4 Unitary Quasi-Orthogonal SF Trellis Codes

Now we explain how to use the proposed set partition schemes to systematically design rate-one full-diversity unitary Quasi-Orthogonal Space-Frequency Trellis Codes (QOSFTCs). A key concept is that those codewords that do not belong to the same set are assigned to different states. Moreover, we must assign codewords diverging (or merging) into a state such that both difference matrices have full rank, and the CGD between all pairs of codewords must be the largest CGD.

In Figure 34 we show the proposed 4-state and 8-state trellises containing branches with 64 and 32 parallel transitions, respectively. Similarly, Figure 35 shows a 16-state trellis structure with 16 parallel transitions on each one of the branches. Note that the

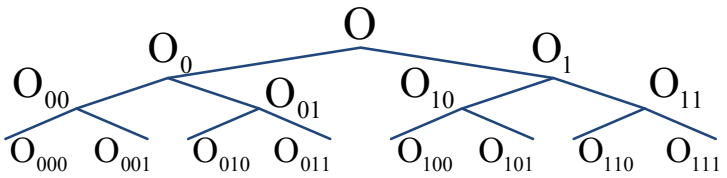

O_{000}	O_{001}	O_{010}	O_{011}	O_{100}	O_{101}	O_{110}	O_{111}
1113	1102	1012	0110	0001	1103	0102	0111
3331	3320	3230	2332	2223	3321	2320	2333
1131	1120	1030	0132	0023	1121	0120	0133
3313	3302	3212	2310	2201	3303	2302	2311
0002	0013	0301	1203	1310	0212	1011	1002
2220	2231	2123	3021	3132	2030	3233	3220
0020	0031	0323	1221	1332	0230	1033	1020
2202	2213	2101	3003	3110	2012	3211	3202
1311	1300	0103	1001	1112	0010	0300	0313
3133	3122	2321	3223	3330	2232	2122	2131
1333	1322	0121	1023	1130	0032	0322	0331
3111	3100	2303	3201	3312	2210	2100	2113
0200	0211	1210	0312	0203	1301	1213	1200
2022	2033	3032	2130	2021	3123	3031	3022
0222	0233	1232	0330	0221	1323	1231	1222
2000	2011	3010	2112	2003	3101	3013	3000

(a)

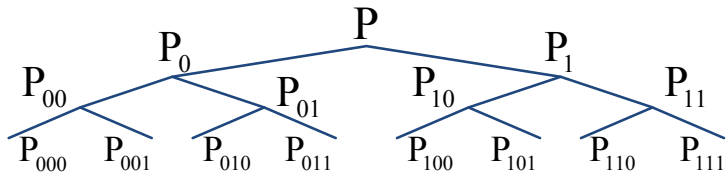

P_{000}	P_{001}	P_{010}	P_{011}	P_{100}	P_{101}	P_{110}	P_{111}
1113	1102	1012	0110	1110	0012	1013	1000
3331	3320	3230	2332	3332	2230	3231	3222
1131	1120	1030	0132	1132	0030	1031	1022
3313	3302	3212	2310	3310	2212	3213	3200
0002	0013	0301	1203	0201	1303	0100	0113
2220	2231	2123	3021	2023	3121	2322	2331
0020	0031	0323	1221	0223	1321	0122	0131
2202	2213	2101	3003	2001	3103	2300	2313
1311	1300	0103	1001	0003	1101	1211	1202
3133	3122	2321	3223	2221	3323	3033	3020
1333	1322	0121	1023	0021	1123	1233	1220
3111	3100	2303	3201	2203	3301	3011	3002
0200	0211	1210	0312	1312	0210	0302	0311
2022	2033	3032	2130	3130	2032	2120	2133
0222	0233	1232	0330	1330	0232	0320	0333
2000	2011	3010	2112	3112	2010	2102	2111

(b)

Figure 33. Partitioning for sets (a) O and (b) P, using QPSK.

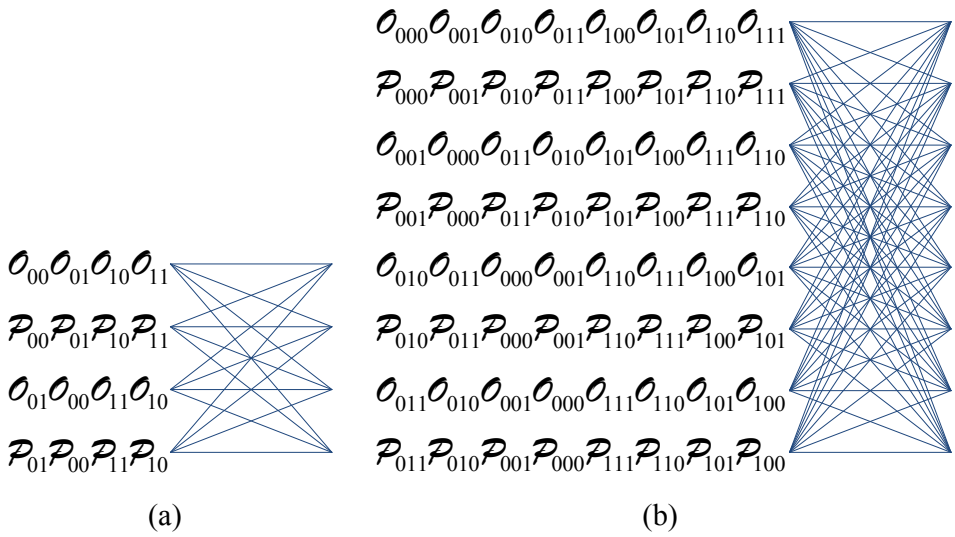

Figure 34. QOSTFTCs using QPSK (a) 4-state, (b) 8-state.

trellis design follows a systematic method. For brevity, in Figure 35 we denote a subset $\mathcal{O}_{xxxx}$ as $\mathcal{O}'_y$, where subscript y is the decimal representation of binary subscript $xxxx$. The same notation applies to the subsets $\mathcal{P}_{xxxx}$.

According to the current state and the 8 input bits, the trellis encoder builds the kth codeword $\bar{\boldsymbol{B}}^t_{i,k} \in \{\mathcal{O}, \mathcal{P}\}$ based on (82).

So far, we have considered the design of unitary QOSFTCs with two transmit antennas, a QPSK constellation and $L = 2$ independent delay paths on each pair of transmit-receive links. However, the proposed unitary QOSFTCs are general enough such that one can systematically design codes for $L > 2$ and more than two transmit antennas following similar procedures. In addition, we can design the unitary QOSFTCs for a 2^bPSK constellation, $b > 2$. In general, for any L and M_t using a 2^bPSK constellation, the total number of different codewords to be partitioned is $(2^b)^{M_t L}$. Therefore, the system complexity will be increased.

Note the inner codewords of resulting QOSFTCs are also unitary matrices. Also, full-diversity and high-coding gain unitary QOSFTCs with different number of states

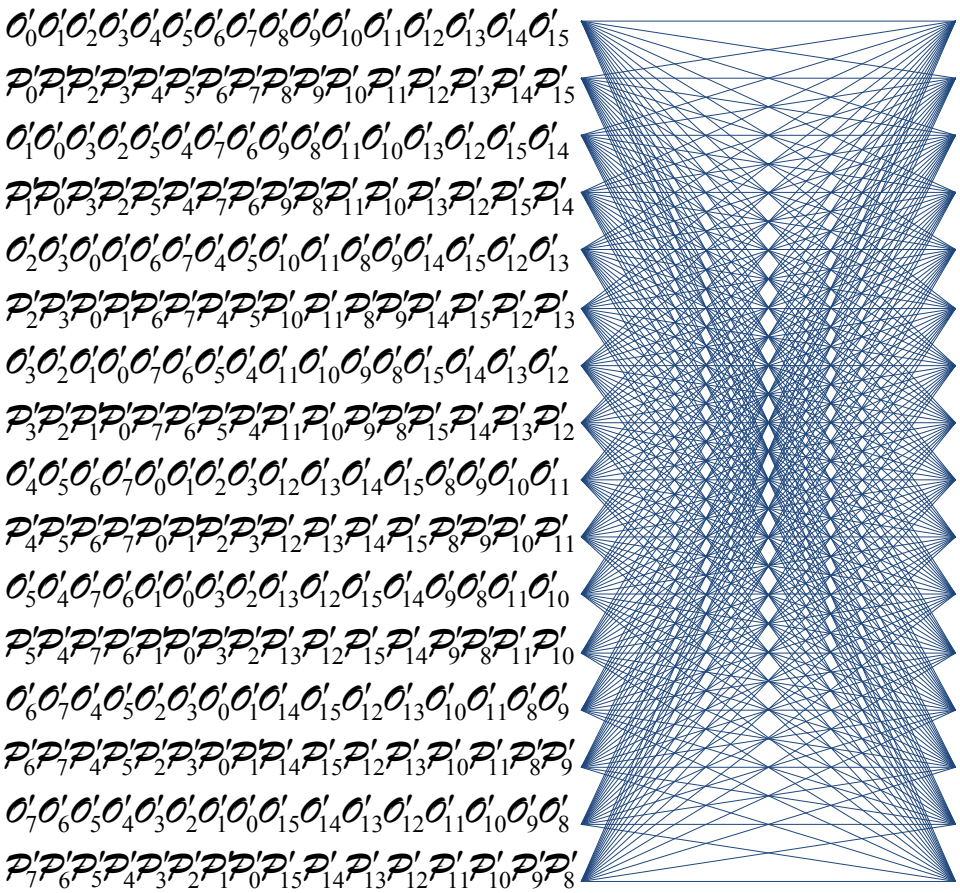

Figure 35. 16-state QOSTFTC using QPSK.

can be systematically designed using both the corresponding set partitioning and the design rules described above.

IV.4.5 Differential encoding of the QOSFTCs

In this section, we follow the differential encoding method presented in Section IV.3.3. After constructing the codeword $\bar{\boldsymbol{B}}_{i,k}^{t}$, in order to build a DF-QOSFTC or a DT-QOSFTC, we perform the Differential Encoding over the Frequency Domain, using Equation (85), or Differential Encoding over the Time Domain with (86), respectively. Then, at the tth OFDM symbol period we form a SF code as in (84) for $L = 2$, such

that

$$\bar{\mathbf{C}}^t = \begin{pmatrix} \mathbf{C}^t_{i,0}(S_1, S_2) \\ \vdots \\ \mathbf{C}^t_{i,K-1}(S_1, S_2) \\ \mathbf{C}^t_{i,0}(S_3, S_4) \\ \vdots \\ \mathbf{C}^t_{i,K-1}(S_3, S_4) \end{pmatrix} \tag{94}$$

IV.4.6 Decoding of DQOSFTCs

The successful differential decoding of the proposed DF-QOSFTCs and DT-QOSFTCs depends on the assumption that the fading channel remains constant over at least four adjacent subcarriers or two successive OFDM symbols, respectively. It is worth mentioning that both, orthogonality and independence of the inner building matrices in the proposed codes, make it possible to simplify the complexity of the decoding process by separating the decoding of these subblocks. In order to estimate the information submatrix $\mathbf{B}^t_{i,k}(S_{2l-1}, S_{2l})$, no CSI is required at the receiver. The proposed differential codes are decoded using Maximum-Likelihood (ML) decoding, comprised by the differential decoder derived by Hochwald and Sweldens (2000); Hughes (2000), and a Viterbi decoder.

Now, we consider the decoding for the Differential Encoding over the Frequency Domain. For the sake of brevity, and by taking advantage of the independence of inner submatrices of transmitted codewords, we first show the analysis by considering only the submatrix codeword $\mathbf{B}^t_{i,k}(S_1, S_2)$. Then, we will extend to the general case. For simplicity, in order to represent the receive equation for the kth submatrix $\mathbf{C}^t_{i,k}(S_1, S_2)$

to be transmitted over subcarriers n and $n+1$ at tth OFDM symbol, we denote

$$\mathbf{C}_k^t = \begin{bmatrix} \begin{bmatrix} S_1^k(2k-1) & S_2^k(2k-1) \end{bmatrix} & \mathbf{0} \\ \mathbf{0} & \begin{bmatrix} -S_2^{*k}(2k) & S_1^{*k}(2k) \end{bmatrix} \end{bmatrix} \in \mathbb{C}^{2\times 4}, \tag{95}$$

where $S_i^k(n)$ $(i=1,2)$ is the resulting symbol in accordance with the Equation (85) to be transmitted on subcarrier n. The matrix of channel coefficients in frequency domain during the transmission of kth codeword $\mathbf{C}_{i,k}^t(S_1,S_2)$ and corresponding subcarriers, can be represented as (see Equation (45))

$$\mathbf{H}_k^t = \begin{bmatrix} \mathbf{H}(2k-1) \\ \mathbf{H}(2k) \end{bmatrix} \in \mathbb{C}^{4\times M_r}. \tag{96}$$

Also let $\mathbf{y}_k^t = [y^1(n)\ y^2(n+1)]^T$ be the received signal in two adjacent subcarriers at nth OFDM symbol duration. Therefore, the receiver equation can be represented by

$$\mathbf{y}_k^t = \mathbf{C}_k^t \mathbf{H}_k^t + \mathcal{N}_k^t \tag{97}$$

where $\mathcal{N}_k^t \in \mathbb{C}^{2\times M_r}$ is the noise matrix over the subcarriers n and $n+1$. Since

$$\mathbf{y}_{k-1}^t = \mathbf{C}_{k-1}^t \mathbf{H}_{k-1}^t + \mathcal{N}_{k-1}^t, \tag{98}$$

and by observing Equation (85), we have

$$\begin{aligned} \mathbf{y}_k^t &= \mathbf{B}_{i,k}^t(S_1,S_2)\mathbf{C}_{k-1}^t\mathbf{H}_k^t + \mathcal{N}_k^t \\ &= \mathbf{B}_{i,k}^t(S_1,S_2)\,\mathbf{y}_{k-1}^t + \mathbf{C}_k^t\left(\mathbf{H}_k^t - \mathbf{H}_{k-1}^t\right) + \mathcal{N}_k^{\prime t}, \end{aligned} \tag{99}$$

where $\mathcal{N}_k^{\prime t} = \mathcal{N}_k^t - \mathbf{B}_{i,k}^t(S_1,S_2)\mathcal{N}_{k-1}^t$ is a noise matrix. By assuming $\mathbf{H}_k^t \approx \mathbf{H}_{k-1}^t$, simple receivers for Equation (99) were derived in (Hochwald and Sweldens, 2000; Hughes, 2000). Using this representation, we obtain the suboptimal Maximum Likelihood receiver (branch metric in the trellis decoder) of the kth block as follows

$$\begin{aligned}\mathbf{B}_{i,k}^{t}(S_1,S_2) &= \underset{\{s_1,s_2\}_k^t}{\operatorname{argmin}}\, p\left(\mathbf{y}_k^t|\mathbf{C}_k^t\right)\\ &= \underset{\{s_1,s_2\}_k^t}{\operatorname{argmin}} \left\|\mathbf{y}_k^t - \mathbf{B}_{i,k}^{t}(S_1,S_2)\mathbf{y}_{k-1}^t\right\|_F^2 .\end{aligned} \tag{100}$$

In order to decode the Differential QOSFTCs, we need to solve the minimum from the accumulated branch metric along the survivor paths on the trellis structure. Therefore, we combine the Viterbi algorithm with the receiver in Equation (100). For simplicity, let us assume a single receive antenna. Linking the number of transmitted codewords with the corresponding subcarriers, the general ML decoder for the DF-QOSFTCs is denoted as

$$\begin{aligned}\widehat{\widetilde{\mathbf{C}}} = \underset{\{s_1,s_2,s_3,s_4\}_k^t}{\operatorname{argmin}} \sum_{k=2}^{N/4} \Bigg\{ &\left\| \mathbf{y}^t \begin{bmatrix} 2k-1 \\ 2k \end{bmatrix} - \mathbf{B}_{i,k}^{t}(S_1,S_2)\ \mathbf{y}^t \begin{bmatrix} 2k-3 \\ 2k-2 \end{bmatrix} \right\|_F^2 \\ + &\left\| \mathbf{y}^t \begin{bmatrix} 2k-1+\frac{N}{2} \\ 2k+\frac{N}{2} \end{bmatrix} - \mathbf{B}_{i,k}^{t}(S_3,S_4)\ \mathbf{y}^t \begin{bmatrix} 2k-3+\frac{N}{2} \\ 2k-2+\frac{N}{2} \end{bmatrix} \right\|_F^2 \Bigg\}.\end{aligned} \tag{101}$$

Following a similar method, we can derive the expression for Maximum Likelihood decoder for the Differential Encoding over the Time Domain. However, in order to perform differential decoding for the DT-QOSFTCs, two consecutive received OFDM symbols are required. So, the ML decoder is given by

$$\begin{aligned}\widehat{\widetilde{\mathbf{C}}} = \underset{\{s_1,s_2,s_3,s_4\}_k^t}{\operatorname{argmin}} \sum_{k=1}^{N/4} \Bigg\{ &\left\| \mathbf{y}^t \begin{bmatrix} 2k-1 \\ 2k \end{bmatrix} - \mathbf{B}_{i,k}^{t}(S_1,S_2)\ \mathbf{y}^{t-1} \begin{bmatrix} 2k-1 \\ 2k \end{bmatrix} \right\|_F^2 \\ + &\left\| \mathbf{y}^t \begin{bmatrix} 2k-1+\frac{N}{2} \\ 2k+\frac{N}{2} \end{bmatrix} - \mathbf{B}_{i,k}^{t}(S_3,S_4)\ \mathbf{y}^{t-1} \begin{bmatrix} 2k-1+\frac{N}{2} \\ 2k+\frac{N}{2} \end{bmatrix} \right\|_F^2 \Bigg\},\end{aligned} \tag{102}$$

where $\mathbf{H}_k^t \approx \mathbf{H}_k^{t-1}$ is assumed.

IV.5 Simulation results

In this section, we provide simulation results to illustrate performances of our proposed differential QOSFTCs in comparison with some previously existing schemes. First, we describe the simulation parameters for the MIMO-OFDM system. Then, we discuss performance results over different channel scenarios.

We assume a 128-tone OFDM system with two transmit antennas, a single receive antenna, and a total bandwidth of 1 MHz. We add a cyclic prefix of 20 μs to avoid the ISI. The performance curves are described by means of OFDM Symbol Error Rate (SER) versus the received Signal-to-Noise Ratio (SNR). We simulate the system over the following channel scenarios:

1. A quasi-static channel with 2-path uniform power delay profile, which changes independently for each OFDM symbol. The delay between these 2 paths is one OFDM sample duration.

2. The channel is quasi-static over one OFDM symbol period and slowly changes between adjacent OFDM symbols by varying the normalized Doppler frequencies f_{Dn}, with

   (a) $f_{Dn} = 0.0025$ and

   (b) $f_{Dn} = 0.0125$,

   which correspond to mobile speeds of 6 and 30 m/s, respectively. To properly model a frequency selective channel, we adopt a typical urban (TU) six-ray power delay profile (Stuber, 2001), which is shown in Figure 24(a).

In order to validate the work we have carried out, we then compare the performance of our proposed DF-QOSFTCs and DT-QOSFTCs, to that of the 8-state Differential

Space-Frequency Trellis Code (DSFTC) derived by Hong *et al.* (2006), which is based on group codes with the same rate R =2 b/s/Hz. As can be seen from Figure 36 to Figure 39, our proposed codes all considerably outperform the existing DSFTC. Also, we have added a comparison with coherent QOSFTCs, and the result is a 3 dB difference, as happens with most well-designed differential schemes.

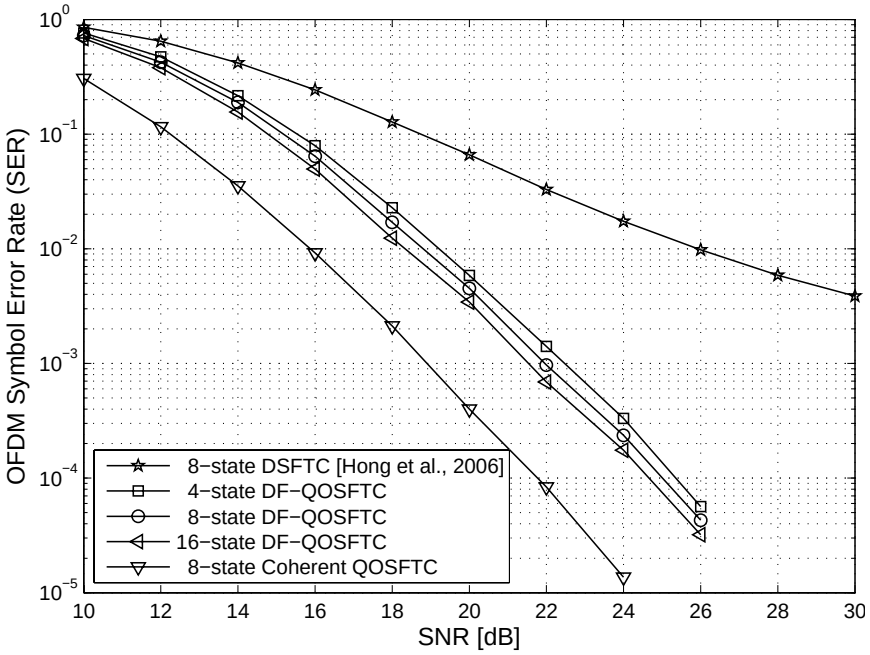

Figure 36. SER performance for the two-ray power delay profile, and R =2 b/s/Hz.

Figure 36 provides SER performance for the proposed DF-QOSFTCs, on a channel scenario with a two-ray power delay profile. For the sake of brevity, we call 4-DF, 8-DF and 16-DF to the 4-state, 8-state and 16-state DF-QOSFTCs, respectively. Similar notation is applying to the DT-QOSFTCs, i.e. 4-DT, 8-DT and 16-DT. We can see from the slopes of the SER curves in Figure 36, that all our proposed DF-QOSFTC achieve the full-diversity order of 4. Note that we have designed codes for $L = 2$ and therefore the maximum achievable diversity is four, independent of the actual number of taps in the system. Despite of the high correlation between adjacent subcarriers on

this channel scenario, we can observe that, the existing 8-state DSFTC design by Hong *et al.* (2006), suffers of a severe error floor. Also, we can see from the performance curves in Figure 36, that there is a coding gain difference of about 0.4 dB between codewords 16-DF, 8-DF and 4-DF. Therefore, we can conclude that, under a channel scenario highly correlated in frequency domain, the 8-DF codeword (which provides an excellent performance and a low decoding complexity) is a good choice for a simple MIMO-OFDM system.

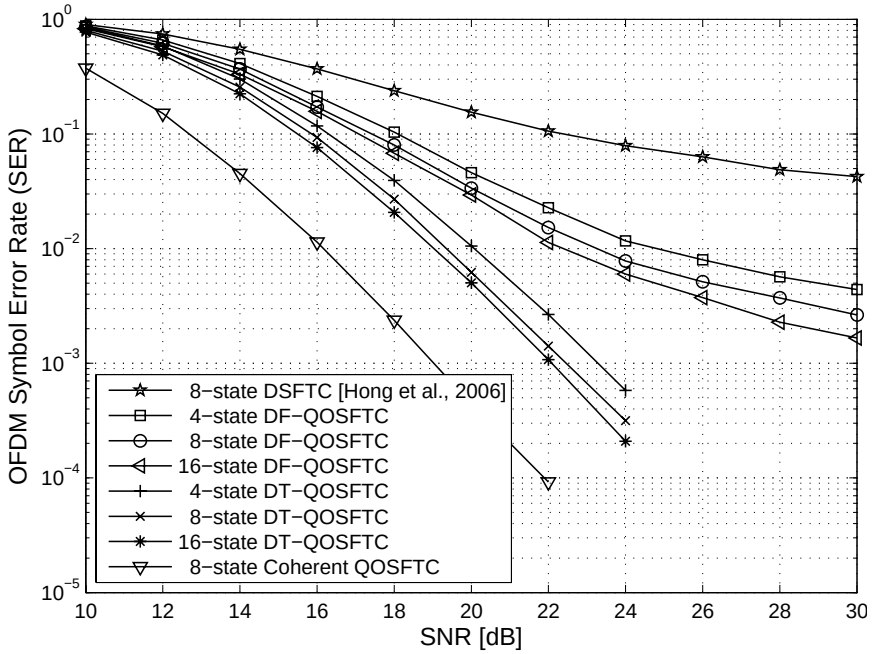

Figure 37. SER performance for the TU six-ray power delay profile, with a normalized Doppler frequency $f_{Dn} = 0.0025$, and R =2 b/s/Hz.

Figure 37 shows that DT-QOSFTCs over channel scenario 2(a), achieve the full-diversity order of 4. By observing Figure 37 at SER of 10^{-2}, the proposed 16-DT, 8-DT and 4-DT outperform the proposed 8-DF by 4.4 dB, 4.1 dB and 3.6 dB, respectively. Note that, similar to DF-QOSFTCs codes, the coding gain difference between the 16-DT and 8-DT is about 0.3 dB, while the difference between 8-DT and 4-DT is 0.4 dB. Moreover, although DF-QOSFTCs also reach coding gain under the channel scenario

2(a), at high SNRs, they suffer a diversity loss. This is because the success of the DF-QOSFTCs depends on a high correlation between adjacent subcarriers, which is not preserved in hostile Frequency Selective Channels. This effect can be mitigated either by increasing the number of subcarriers in the MIMO-OFDM system, or implementing codes for largest multipaths, $L > 2$. Thus, the number of subcarrier groups is increased leading to a better multipath-diversity gain. Also, we can see that for this six-ray typical urban channel scenario, the existent 8-state DSFTC does not work.

Next, for the sake of fairness, we compare the performance of the 8-state proposed codes versus existing 8-state DSFTC by varying f_{Dn}.

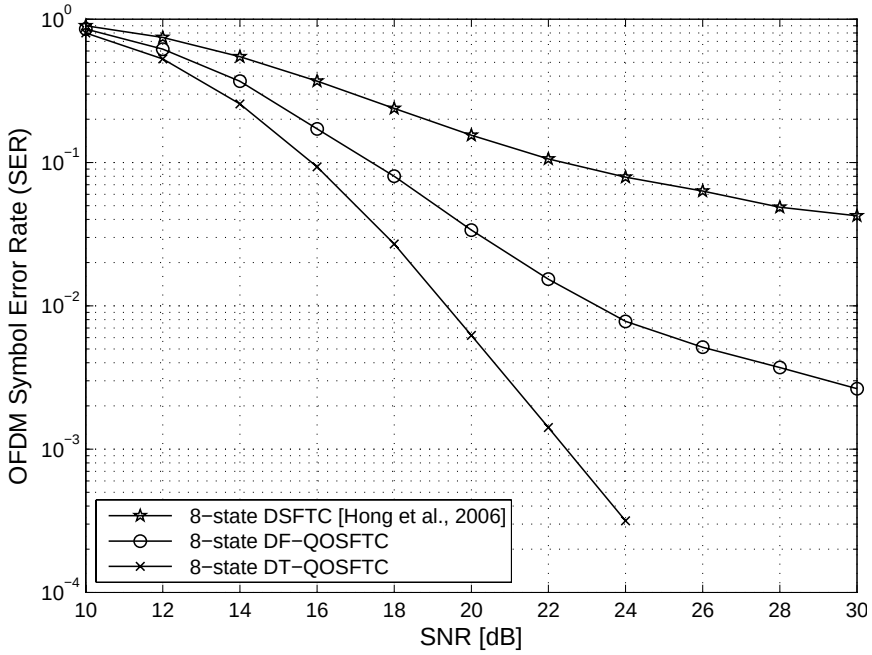

Figure 38. SER performance for all 8-states trellis codes, under a TU six-ray power delay profile, with a normalized Doppler frequency of $f_{Dn} = 0.0025$, and R =2 b/s/Hz.

We can see in figures 38 and 39, that both DF-QOSFTC and DSFTC have a robust performance in the case of time-varying channels. The SER performance does not depend on correlation between adjacent OFDM symbols for these schemes.

However, time variations of the channel affect the diversity of the DT-QOSFTC,

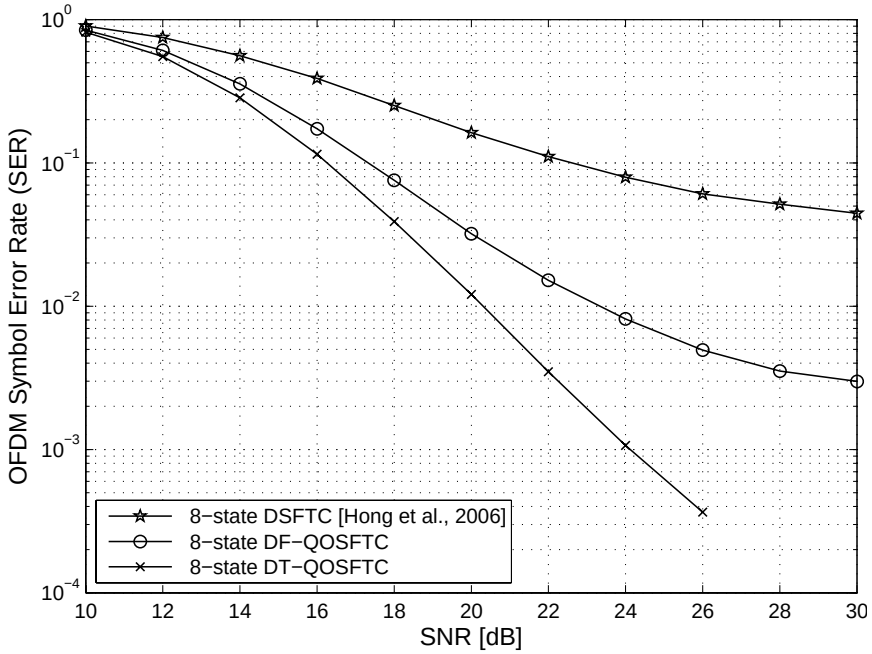

Figure 39. SER performance for all 8-states trellis codes, under a TU six-ray power delay profile, with a normalized Doppler frequency of $f_{Dn} = 0.0125$, and R =2 b/s/Hz.

because of the differences between the channel gain of subcarrier groups for adjacent OFDM symbols. Such effect is illustrated in figures 38 and 39. In channel scenarios 2(a) and 2(b), besides being highly selective in frequency, we have significatively changed the time selectivity. In the channel scenario 2(a), the coherent time is longer than coherence time of channel scenario 2(b). Therefore, the channel scenario 2(a) undergoes a slower variation over time domain than that experienced by the channel scenario 2(b). Then, the adjacent OFDM symbols in scenario 2(a) are more correlated in the time domain than those of channel scenario 2(b). This is consistent with the discussion in Section II.1.1.

Nevertheless, the DT-QOSFTC notably outperforms all other codes. As seen from the performance curves shown in Figure 38, for a TU six-ray power fading channel with a normalized Doppler frequency of $f_{Dn} = 0.0025$, at a SER of 10^{-2} the 8-DT have a superior performance over that of 8-DF by almost 3.8 dB. Besides, as illustrated in

Figure 39, for the same scenario but with a normalized Doppler frequency of $f_{Dn} = 0.0125$, at a SER of 10^{-2} the 8-DT outperform the 8-DF by almost 3 dB. Moreover, the transmission efficiency for the DT-QOSFTCs is greater than that achieved in the frequency domain by for example DF-QOSFTCs and that of the existing DSFTC. This improved performance is due to that, in the differential encoding over the time domain, only the first OFDM symbol will not transmit information. However, in the differential encoding over the frequency domain, on each OFDM symbol to be transmitted, the first codeword will not transmit information. In addition, under practical fading channels, significant gains can be achieved by increasing the number of states in a DT-QOSFTC and the simple decoding complexity is hold.

Clearly, as shown in all performance curves in this section, DSFTC derived by Hong *et al.* (2006) is not suitable to be implemented in most practical fading channels. On the other hand, the differential codes proposed here can be adjusted in both scenarios: frequency selective and time selective fading channels. Additionally, our codes achieve good performance, without requiring channel state information on both sides of the communication link. Also, our proposed codes are designed systematically and have a simple decoding complexity.

IV.6 Chapter Summary

In this chapter we have proposed rate-one differential space-frequency trellis codes for MIMO-OFDM systems, where CSI is not available at the transmitter and at the receiver. The proposed differential codes have been designed based on a generalized class of unitary quasi-orthogonal space-time block codes. Also by trellis encoding and grouping of OFDM-subcarriers, our proposed codes achieve full-diversity and high-coding gain

over practical FSCs. Of course, this performance is achieved at the expense of that the fading channel remains constant over at least four adjacent subcarriers or two successive OFDM symbols, for the proposed DF-QOSFTCs and DT-QOSFTCs, respectively.

Simulation results show that, compared to the existing DSFTC, the proposed codes provide better performance in all channel fading scenarios. Moreover, the independence of inner orthogonal matrices in the proposed codes, allows a reduced encoding and decoding complexity. Furthermore, because the differentially encoded codewords are transmitted within one OFDM symbol period, we obtain a reduced decoding delay.

The provided examples have only been able to achieve a maximum diversity order of four with two transmit antennas, but it is straightforward to design similar codes for more than two taps, and two transmit antennas. This, of course, is at the expense of increased decoding complexity.

In addition, unlike differential and noncoherent SF schemes in the literature, our proposed codes achieve rate one and can be designed in a simple systematic way.

Chapter V

Conclusions and Future Works

Reaching the end of this thesis, a brief summary of the main contributions and findings of this thesis are given in this chapter. Some suggestions on future research directions are discussed with a brief summary of the possible extensions to this work.

V.1 Conclusions

In this thesis, design and performance of space-time-frequency trellis codes and differential space-frequency trellis codes in MIMO-OFDM communication systems have been studied. The main objective has been to improve the performance of these coding schemes operating over frequency-selective channels.

In the first part, we focused on space-time-frequency trellis codes from orthogonal and quasi-orthogonal designs. Assuming perfectly known channel state information at the receiver, our proposed rate-one STF trellis codes are capable to achieve high coding gain and multipath diversity. To the sake of simplicity in our designs, we have assumed that the channel is quasi-static over two OFDM symbols duration (a frame) and changes independently from frame to frame. Such assumption provides a reduced maximum likelihood decoding complexity, at the expense of not achieving the additional

temporal diversity advantage available in the wireless channel.

In order to design Space-Time-Frequency trellis codes, we modify the design criteria for Space-Frequency trellis codes derived by Liu and Chong (2004). The advantage of such criteria is that it is not necessary any knowledge of multipath and delay effects of the channel. Moreover, considering that the trellis encoder output is an orthogonal matrix, we redefine the distance criterion between any possible pair of distinct STF codewords, as the maximization of the minimum product of the coding gain distance and the modified product distance. We have shown that by satisfying $\delta_H \geq L$, multipath diversity provided by the channel can be achieved. Also, the maximum achievable diversity in our designs has been denoted as the product of twice the number of receive antennas, the minimum value of δ_H and the number of multipaths L in the channel model.

Despite the fact that by increasing the effective length δ_H in a trellis code, the coding gain will increase; a random interleaving is also necessary. It has been shown that the random interleaving is a critical design principle, which helps to exploit the rich diversity resources in presence of frequency-selective channels. The random interleaver goal is to break the correlation between subcarriers into an OFDM symbol. Then, correlation parameters significantly dominate the Pairwise Error Probability of STF trellis codes, as observed from (Liu and Chong, 2004). Consequently, such parameters will affect the design of STF codes. However, taking into account the subcarrier correlation for the design of the interleaver is beyond the scope of this work. Thus, to observe the robustness of the proposed STF trellis codes, we did not apply an interleaver strategy in our designs.

In Chapter 3 we proposed two new STF trellis coding schemes considering two antennas at the transmitter. In the first design of this chapter, we have concentrated

on increasing the performance of the Space-Time-Frequency (STF) trellis codes using the rotated constellation concept from Zhu and Jafarkhani (2006), and we have avoided implementing parallel transitions in the trellis design, which restrict the performance in multipath channels. Therefore, we have extended the design of the Super-Orthogonal Space-Time Trellis Codes derived by Jafarkhani and Seshadri (2003) from a flat-fading channel case to a frequency-selective channel case, maintaining a low decoding complexity. In such first design, called Ex-SOSTFTC, the minimum effective length is set as $\delta_H = 2$. This value of δ_H avoids parallel transitions and allows to design the 16-state Ex-SOSTFTC, assuring that this scheme will work perfectly on a channel with at least two distinguishable paths ($L = 2$).

On the other hand, in systems using a higher order modulation and/or a larger number of transmit antennas, it is difficult to avoid parallel transitions in a trellis code design. Then, in order to enhance the achievable diversity and coding gain, we have systematically combined the full-rank quasi-orthogonal space-time block code from Fazel and Jafarkhani (2008) with a trellis code. We have designed the rate-one quasi-orthogonal space-time-frequency codes for two transmit antennas and an arbitrary number of receive antennas, operating over frequency-selective channels. It is noteworthy that following similar procedures as those described in Chapter 3, all the STF codes designs can be extended in a straightforward way to more than two transmit antennas.

The advantage of considering the full-rank QOSTBC as an inner block code in our trellis code, lies in the fact that its internal structure is based on orthogonal designs. In particular, such a QOSTBC containing δ_H independent orthogonal Alamouti matrices (Alamouti, 1998). Consequently, the multipath diversity and coding gain can be increased despite the parallel transitions. The maximum possible achievable diversity in this design is bounded by the number of such inner orthogonal matrices, i.e. by

δ_H. Therefore, for simplicity in the exposition and design of the QOSTFTCs, we have also assumed a frequency-selective channel model with two taps $L = 2$. By observing Equation (19), which define the general class of QOSTBCs, it is possible to extend the method described to design the QOSTFTCs, by making $L > 2$ in (58), i.e. considering more than two inner orthogonal matrices in our codes. At this point in the discussion, we emphasize that the maximum diversity achieved by our codes is four, independent of the actual number of taps in the frequency-selective channel. However, it is possible to use a similar approach to design STF codes for higher number of taps. Hence, linked to the number of tranmit/receive antennas in the system, a higher diversity can be achieved. In general, a major performance will be obtained at a cost of a more complex system. The choice of a particular approach depends on the tradeoff between complexity and performance.

To obtain good designs of QOSTFTCs, we have described a simplified set partitioning method for a QPSK constellation, applying a set pattern in both vertical and horizontal direction. We show examples of 4-states, 8-states and 16-states QOSTFTCs, with 64, 32 and 16 parallel transitions in the trellis encoder, respectively. In each one of these designs, due to the fact that 8 bits are feed to the encoder input, and the trellis codeword output is a matrix containing four QPSK symbols, the rate of transmission is one symbol for subcarrier use (rate-one codeword).

Due to the orthogonality presented by our designs, a simple pairwise Maximum-Likelihood decoding using the Viterbi algorithm was applied in the decoding process. However, the decoding process introduce a delay of two OFDM symbols for the proposed STF trellis codes.

We showed that our Ex-SOSTFTC and QOSTFTCs schemes outperform both existing quasi-orthogonal STF block coding and super-orthogonal STF trellis coding schemes

for MIMO-OFDM in the literature, in terms of performance.

Chapter 4 deals with Differential Quasi-Orthogonal Space-Frequency Trellis Code with lack of channel state information at the transmitter and at the receiver. In this chapter, the idea of Differential encoding was applied over frequency-domain and over time-domain for MIMO-OFDM systems. Both proposals are based on unitary rate-one quasi-orthogonal block codes, which we have been derived by first only considering those quasi-orthogonal block codes from (73) complying with the unitarity property. Then, we have introduced rotated unitary matrices to extend the set of unitary code-words. We have followed a similar set partitioning procedure as that for STF trellis codes. Therefore, our differential SF trellis codes can be systematically designed, and we showed that the codes can achieve rate-one, multipath diversity and good coding gain. Because current design criteria for this class of schemes has been widely studied, we have focused only on the design of SF trellis codes using such criteria. However, these design criteria could be studied in more detail, which is beyond the scope of this work.

In a first proposal, we have focused on differential Space-Frequency (SF) coding scheme within a single OFDM tone. We have named this coding scheme as Differential encoding of QOSFTC over frequency domain (DF-QOSFTC). In this proposal, we concluded that there is a little loss of transmission efficiency, because in every OFDM symbol in the Differential Encoding over the Frequency Domain (DF), the first codeword that will be send does not transmit information. In a second code design, we have proposed the Differential Encoding over the Time Domain (DT). We showed that the Differential Encoding over the Time Domain has better transmission efficiency that the DF, because only the first frame (two adjacent OFDM symbols) does not transmit information. A delay of two consecutive OFDM symbols is required in this scheme. In addition,

we have grouping the independent inner codes of the unitary quasi-orthogonal designs into adjacent subcarriers groups. By making this grouping technique, the assumption of constant channel frequency response from group to group has been alleviated, and performance was improved.

On the other hand, as the numerical results have shown that, both DF and DT schemes suffer from frequency selectivity and time variance when operating over highly frequency-selective and time-selective channels, respectively. This limitation of the DF is due to a big number of multipaths in the channel profile, or small number of tones within an OFDM symbol. As a result, correlation between adjacent carriers was low. Similarly, the performance of the differential QOSFTC Differential Encoding over the Time Domain scheme was studied, and it was shown that it fails to exploit full space-frequency diversity. This poor performance of the DT is due to higher Doppler frequency in the system, i.e. the coherence time is decreased. Therefore, we can assert that the success of our DF and DT schemes is dependent on having a system with good adjacent subcarriers and adjacent OFDM symbols correlations, respectively. Despite of this, compared to existing rate-one differential space-frequency trellis codes, under the same time-frequency-selective channel scenarios, our differential codes have a significantly higher performance. We have used a simple Maximum-Likelihood (ML) decoder without requiring CSI at the receiver, which is formed by a differential decoder and a Viterbi decoder. This decoding process is somewhat different between the two designs. In modern 4G systems, where the computing capacity is limited and battery life is vital, our differential schemes are interesting because we do not need an additional algorithm to determine the state of the channel, which consumes too many resources in a wireless system operating over frequency-selective channels.

V.2 Future works

We would like to finish this chapter with some recommendations for future possible works that extend the proposals presented here. In particular, future work could be oriented towards the following directions:

One of the direct extension of this work can be the design of space-time-frequency trellis codes by considering the existing correlation between subcarriers. From the analytical equations, we see that the performance depends on the rank of channel correlation matrix. Then, an extended coding scheme can be derived based on interleaving methods and by re-defining the Pairwise Error Probability, which must be associated with subcarrier correlation parameters.

In the analysis done for the design of STF trellis codes, we assume perfect channel estimation at receiver. In practice, channel estimation is imperfect. In broadband wireless systems transmission, the estimation error cannot be ignored because the number of training pilot symbols is limited by the fact of not decreasing the spectral efficiency. It would be interesting to analyze STF coding for imperfect channel estimation.

We also assume that there is not spatial correlation between antennas. If there is spatial correlation, one can analyze what happens with the error probability in order to derive the boundaries and design criteria for STF trellis coding schemes with spatial correlation.

We have concentrated on STF codes design for single user systems only. For multiple access channels, the single-user STF codes are commonly applied to each user independently. To the best of our knowledge, there is a few research on multiuser STF code design for the frequency-selective fading multiple access channels. In this way, designing full-diversity multiuser STF codes for modern broadband wireless systems is

a very interesting research area that involves a great challenge.

Throughout this thesis, we have exploited the spatial and frequency diversities available over frequency-selective fading channels. However, in some situations, the use of multiple antennas may not be practical due to the size and cost of the broadband mobile station. To overcome this issue, it has been recently proposed a new form of spatial diversity, called cooperative diversity, whereby diversity gains are achieved via the cooperation of nodes. Cooperative diversity allows a virtual antenna array to achieve spatial diversity gain in a distributed fashion. As we can see, there is a new and vast area, where the design of coding schemes able to exploit the spatial, time and frequency diversities is imminently necessary.

In the second part of this thesis, we have incorporated two differential detection schemes which do not require the knowledge of channel information at the receiver neither at the transmitter. By incorporating subcarrier grouping and using the unitary quasi-orthogonal block codes we have achieved maximum diversity gain with low complexity, but only in certain channel scenarios. One natural extension is to consider the generalization of Differential-QOSFTCs for diversity maximization over any fading channel scenario. Then, it is necessary to rethink the design criteria and redesign the subcarrier group technique, which should incorporate correlation parameters while maintaining the mathematical formulation tractable.

A novel coding scheme which takes ideas from conventional space-frequency coding and multi-hop networks is called Distributed space-frequency coding. Such a scheme allows to design a wireless relay network capable of significatively improving the performance. Most existing cooperative diversity schemes focus on the coherent detection. However, estimating the channel coefficients is more complicated than those encountered in MIMO-OFDM channel scenarios because the cooperative diversity schemes

involve both the broadcast phase and the relay phase. Motivated by the above, it is interesting to investigate the possibility of deploying differential space-frequency codes for cooperative networks operating over frequency selective channels.

Another interesting area of application for differential space-frequency codes is in emerging technologies, namely multi-band OFDM ultra-wideband MIMO and space-time-frequency codes (STFC MB-OFDM UWB systems). In the literature on this technology, channel state information is assumed to be known exactly at the receiver, thus allowing the receiver to perform coherent detection. However, the differential transmission in MB-MIMO-OFDM systems has not been fully examined.

References

Agrawal, D., Tarokh, V., Naguib, A., and Seshadri, N. (1998). Space-time coded OFDM for high data rate wireless communication over wideband channels. *IEEE Veh. Technol. Conf.*, **3**: 2232–2236.

Akay, E. and Ayanoglu, E. (2006). Achieving full frequency and space diversity in wireless systems via BICM, OFDM, STBC, and Viterbi decoding. *IEEE Trans. Commun.*, **54**: 2164–2172.

Aksoy, K. and Aygölü, U. (2007). Super-orthogonal space-time-frequency trellis coded OFDM. *IET Commun.*, **1**(3): 317–324.

Alamouti, S. (1998). A simple transmit diversity scheme for wireless communications. *IEEE J. Sel. Areas Commun.*, **16**(8): 1451–1458.

Bölcskei, H. (2006). MIMO-OFDM wireless systems: Basics, perspectives, and challenges. *IEEE Trans. Wireless Commun.*, **13**: 31–37.

Borgmann, M. and Bölcskei, H. (2005). Noncoherent space-frequency coded MIMO-OFDM. *IEEE J. Sel. Areas Commun.*, **23**(9): 1799–1810.

Diggavi, S. N., Al-Dhahir, N., Stamoulis, A., and Calderbank, A. R. (2004). Great expectations: the value of spatial diversity in wireless networks. *Proceedings of the IEEE*, **92**(2): 217–270.

Disvalar, D. and Simon, M. (1988). Multiple trellis coded modulation (MTCM). *IEEE Trans. Commun.*, **36**: 410–419.

Fazel, F. and Jafarkhani, H. (2008). Quasi-Orthogonal Space-Frequency and Space-Time-Frequency Block Codes for MIMO-OFDM channels. *IEEE Trans. Wireless Commun.*, **7**(1): 184–192.

Foschini, G. J. and Gans, M. J. (1998). On limits of wireless communications in a fading environment when using multiple antennas. *Wireless Personal Communications*, **6**: 311–335.

Glisic, S. G. (2007). *Advanced wireless communications: 4G cognitive broadband technology*. John Wiley and Sons Ltd, 2nd edition.

Gong, Y. and Letaief, K. (2003). An efficient Space-Frequency coded OFDM system for broadband wireless communications. *IEEE Trans. Commun.*, **51**(11): 2019–2029.

Himsoon, T., Su, W., and Liu, K. (2006). Single-block differential transmit scheme for broadband wireless MIMO-OFDM systems. *IEEE Trans. Signal Process.*, **54**(9): 3305–3314.

Hochwald, B. and Sweldens, W. (2000). Differential unitary space-time modulation. *IEEE Trans. Wireless Commun.*, **48**(12): 2041–2052.

Hochwald, B. M. and Marzetta, T. L. (2000). Unitary space-time modulation for multiple-antenna communications in rayleigh flat fading. *IEEE Trans. Inf. Theory*, **46**(2): 543–564.

Hochwald, B. M., Marzetta, T. L., Richardson, T. J., Sweldens, W., and Urbanke, R. (2000). Systematic design of unitary space-time constellation. *IEEE Trans. Inf. Theory*, **46**(6): 1962–1973.

Hong, Z., Thibault, L., and Zhang, L. (2006). Differential space-frequency trellis codes. *IEEE Trans. Wireless Commun.*, **5**(10): 2664–2668.

Hughes, B. L. (2000). Differential space-time modulation. *IEEE Trans. Inf. Theory*, **46**(7): 2567–2578.

Jafarkhani, H. (2001). A quasi-orthogonal space-time block code. *IEEE Trans. Commun.*, **49**: 1–4.

Jafarkhani, H. (2005). *Space-Time Coding: Theory and Practice*. Cambridge University Press.

Jafarkhani, H. and Hassanpour, N. (2005). Super-quasi-orthogonal space-time trellis codes for four transmit antennas. *IEEE Trans. Wireless Commun.*, **4**(1): 215–227.

Jafarkhani, H. and Seshadri, N. (2003). Super-orthogonal space-time trellis codes. *IEEE Trans. Inf. Theory*, **49**(4): 937–950.

Jakes, W. C. (1974). *Microwave Mobile Communications*. IEEE Press.

Jankirman, M. (2004). *Space-time codes and MIMO systems*. Artech House, Inc.

Li, Q., Li, K., and Teh, K. (2008). Noncoherent space-frequency codes for broadband MIMO systems over frequency-selective fading channels. En *VTC Spring*, páginas 554–558. IEEE.

Liu, L. and Jafarkhani, H. (2007). Successive transmit beamforming algorithms for multiple-antenna OFDM systems. *IEEE Trans. Wireless Commun.*, **6**(4): 1512–1522.

Liu, S. and Chong, J. (2004). Improved design criterion for Space-Frequency trellis codes over MIMO-OFDM systems. *ETRI Journal*, **26**(6): 622–634.

Liu, Z. and Giannakis, G. B. (2003). Block differentially encoded OFDM with maximum multipath diversity. *IEEE Trans. Wireless Commun.*, **2**(3): 420–423.

Liu, Z., Xin, Y., and Giannakis, G. (2002). Space-Time-Frequency coded OFDM over frequency-selective fading channels. *IEEE Trans. Signal Process.*, **50**(10): 2465–2476.

Lu, B. and Wang, X. (2003). A Space-Time trellis code design method for OFDM systems. *Wirel. Pers. Commun.*, **24**(3): 403–418.

Lu, B., Wang, X., and Narayanan, K. (2002). LDPC-based space-time coded OFDM systems over correlated fading channels: Performance analysis and receiver design. *IEEE Trans. Commun.*, **50**(1): 74–88.

Ma, Q., Tepedelenlioglu, C., and Liu, Z. (2005). Differential space-time-frequency coded OFDM with maximum multipath diversity. *IEEE Trans. Wireless Commun.*, **4**(5): 2232–2243.

Madhow, U. (2008). *Fundamental of Digital Communication*. Cambridge University Press.

Medbo, J. and Schramm, P. (1998). Channel models for HIPERLAN/2 in different indoor scenarios. *ETSI/BRAN document num. 3ERI085B*.

Proakis, J. (2000). *Digital Communications (4th edition)*. NY: McGraw-Hill.

Rappaport, T. (2002). *Wireless Communications: Principles and Practice (2nd edition)*. Prentice Hall PTR.

Sharma, N. and Papadias, C. B. (2003). Improved quasi-orthogonal codes through constellation rotation. *IEEE Trans. Commun.*, **51**: 332–335.

Stuber, G. (2001). *Principles of Mobile Communications*. Boston, MA: Kluwer.

Su, W. and Liu, K. J. R. (2005). Differential space-frequency modulation via smooth logical channel for broadband wireless communications. *IEEE Trans. Commun.*, **53**: 2024–2028.

Su, W. and Xia, X. (2002). Quasi-orthogonal space-time block codes with full diversity. *Global Telecommunication Conference (Globecom)*, **2**: 1098–1102.

Su, W., Safar, Z., and Liu, K. (2005). Towards maximum achievable diversity in space, time, and frequency: performance analysis and code design. *IEEE Trans. Wireless Commun.*, **4**(4): 1847–1857.

Tan, J. and Stuber, L. (2004). Multicarrier delay diversity modulation for MIMO systems. *IEEE Trans. Wireless Commun.*, **3**: 1756–1763.

Tao, M. (2006). High rate trellis coded differential unitary space-time modulation via super unitarity. *IEEE Trans. Wireless Commun.*, **5**(12): 3350–3354.

Tarokh, V. and Jafarkhani, H. (2000). A differential detection scheme for transmit diveristy. *IEEE J. Sel. Areas Commun.*, **18**(7): 1169–1174.

Tarokh, V. and Jafarkhani, H. (2001). Multiple transmit antenna differential detection from generalized orthogonal designs. *IEEE Trans. on Information Theory*, **47**(6): 2626–2631.

Tarokh, V., Seshadri, N., and Calderbank, A. R. (1998). Space-time codes for high data rate wireless communications: Performance criterion and code construction. *IEEE Trans. Inf. Theory*, **44**(2): 744–765.

Tarokh, V., Jafarkhani, H., and Calderbank, A. R. (1999a). Space-time block codes from orthogonal designs. *IEEE Trans. Inf. Theory*, **45**(5): 1456–1467.

Tarokh, V., Naguib, V., Seshadri, N., and Calderbank, A. R. (1999b). Space-time codes for high data rate wireless communications: performance criteria in the presence of channel estimation errors, mobility and multiple paths. *IEEE Trans. Commun.*, **47**(2): 199–207.

Tirkkonen, O. (2000). Optimizing space-time block codes by constellation rotations. *Finnish Wireless Communications Workshop*, **1**: 1–6.

Tirkkonen, O., Boariu, A., and Hottinen, A. (2000). Minimal non-orthogonality rate 1 space-time block code for 3+ tx antennas. *ISSSTA*, **2**: 429–432.

Ungerboeck, G. (1982). Channel coding for multilevel/phase signals. *IEEE Trans. Inf. Theory*, **28**(1): 55–67.

Wang, D. and Xia, X. (2005). Optimal diversity product rotations for quasi-orthogonal STBC with MPSK symbols. *IEEE Commun. Lett.*, **9**(5): 420–422.

Zhang, W., Xia, X. G., and Ching, P. C. (2007). High-Rate Full-Diversity Space-Time-Frequency Codes for Broadband MIMO Block Fading. *IEEE Trans. Commun.*, **55**: 25–34.

Zhu, Y. and Jafarkhani, H. (2005). Differential modulation based on Quasi-orthogonal codes. *IEEE Trans. Wireless Commun.*, **4**(6): 3018–3030.

Zhu, Y. and Jafarkhani, H. (2006). Differential super-orthogonal space time trellis codes. *IEEE Trans. Wireless Commun.*, **5**(12): 3634–3643.

Appendix A

Notation and Abbreviations

Notation

$\alpha_{i,j}$	Path gain from transmit antenna i to receive antenna j
$\mathbb{C}^{M\times N}$	The set of $M \times N$ matrices over the field of complex numbers
$\mathbb{R}^{M\times N}$	The set of $M \times N$ matrices over the field of real numbers
$(\cdot)^T$	Transpose
$(\cdot)^*$	Complex conjugate
$(\cdot)^H$	Transpose conjugate
$\text{rank}(\cdot)$	The rank of a matrix
$\text{Tr}(\cdot)$	The trace of a matrix
$\det(\cdot)$	The determinant of a matrix
$\|\cdot\|_F$	The Frobenius norm of a matrix
$\circ$	The Hadamard product of two matrices
$\otimes$	The Kronecker product of two matrices
$\Re(\cdot)$	Real part of a complex variable
$\Im(\cdot)$	Imaginary part of a complex variable
$\mathbf{I}_N$	The identity matrix of dimensions $N \times N$
$\mathbf{0}$	The zero matrix
$E[X]$	The expected value of a random variable

Abbreviations

3GPP	3rd Generation Partnership Project
BPSK	Binary Phase-Shift Keying
CFR	Channel Frequency Response
CGD	Coding Gain Distance
CIR	Channel Impulse Response
CSI	Channel State Information
DF	Differential Encoding over the Frequency Domain
DPSK	Differential Phase Shift Keying
DQOSFTC	Differential Quasi-Orthogonal Space-Frequency Trellis Code
DSFTC	Differential Space-Frequency Trellis Code
DT	Differential Encoding over the Time Domain
DUSTM	Differential Unitary Space–Time Modulation
Ex-SOSTFTC	Extended Super-Orthogonal Space-Time-Frequency Trellis Code
FDM	Frequency-Division Multiplexing
FDMA	Frequency Division Multiple Access
FER	Frame Error Rate
FSC	Frequency Selective Channel
ICI	Intercarrier Interference
IFFT	Inverse Fast Fourier Transform

ISI	Inter Symbol Interference
LAN	Local Area Network
LOS	Line-of-sight
LTE	Long Term Evolution
MAN	Metropolitan Area Network
MIMO	Multiple-Input Multiple-Output
ML	Maximum Likelihood
MTCM	Multiple Trellis Coded Modulation
OFDM	Orthogonal Frequency Division Multiplexing
OSTBC	Orthogonal Space-Time Block Code
PAM	Pulse Amplitude Modulation
PAPR	Peak-to-Average Power Ratio
PEP	Pairwise Error Probability
PSK	Phase-Shift Keying
QAM	Quadrature Amplitude Modulation
QOSFTC	Quasi-Orthogonal Space-Frequency Trellis Code
QOSTBC	Quasi-Orthogonal Space-Time Block Code
QOSFBC	Quasi-Orthogonal Space-Frequency Block Code
QOSTFBC	Quasi-Orthogonal Space-Time-Frequency Block Code
QOSTFTC	Quasi-Orthogonal Space-Time-Frequency Trellis Code

QPSK	Quadrature Phase-Shift Keying
RMS	Root mean square
SER	Symbol Error Rate
SF	Space-Frequency
SISO	Single-Input Single-Output
SNR	Signal-to-Noise Ratio
SOSTTC	Super-Orthogonal Space-Time Trellis Code
ST	Space-Time
STBC	Space-Time Block Code
STF	Space-Time-Frequency
STFTC	STF Trellis Code
STTC	Space-Time Trellis Code
TCM	Trellis Coded Modulation
WB	Wideband
WiMAX	Worldwide Interoperability for Microwave Access
ZMCSCG	Zero Mean Circularly Symmetrical Complex Gaussian